Intramembrane proteolysis of ephrin-B2 by γ-secretase regulates podosome dynamics and migration of microglia

Dissertation

zur Erlangung des Doktorgrades (Dr. rer. nat.)

der

Mathematisch-Naturwissenschaftlichen-Fakultät

der

Rheinischen Friedrich-Wilhelms-Universität Bonn

vorgelegt von

Nadja Kemmerling, MSc

aus

Düsseldorf

Bonn, 31.08.2015

Angefertigt mit Genehmigung der Mathematisch-Naturwissenschaftlichen

Fakultät der Rheinischen Friedrich-Wilhelms-Universität Bonn

1. Gutachter: Prof. Dr. rer. nat. Jochen Walter

2. Gutachter: Prof. Dr. rer. nat. Sven Burgdorf

Tag der Abgabe: 31.08.2015

Tag der Promotion: 30.11.2015

Erscheinungsjahr: 2016

An Eides statt versichere ich, dass ich die Dissertation "Intramembrane proteolysis of ephrin-B2 by γ-secretase regulates podosome dynamics and migration of microglia" selbst und ohne jede unerlaubte Hilfe angefertigt habe und dass diese oder eine ähnliche Arbeit noch an keiner anderen Stelle als Dissertation eingereicht worden ist.

Auszüge der ausgewiesenen Arbeit wurden beim Journal Glia eingereicht und die Möglichkeit einer Veröffentlichung dieser wird momentan vom genannten Journal geprüft.

Promotionsordnung vom 17. Juni 2011 _____

Nadja Kemmerling

Dedicated to my mother

and my grandparents Carl & Marianne

Table of Contents

Index

List of figures

List of tables

Abbreviations

aa	Amino acid
Ab	Antibody
AD	Alzheimer´s disease
ADAM	A disintegrin and metalloprotease
APH-1	Anterior pharynx defective-1
APP	Amyloid precursor protein
APS	Ammonium persulfate
Aβ	β-Amyloid
BBB	Blood brain barrier
Bp	base pairs
BSA	Bovine serum albumin
Capn	Calpain
CDS	Coding sequence
CNS	Central nervous system
co-IP	Co-immunoprecipitation
Ct	Cycle threshold
CTF	C-terminal fragment
DAPI	4',6-Diamidin-2-phenylindol
DAPT	*N*-[(3,5-Difluorophenyl)acetyl]-L-alanyl-2-phenyl]glycine-1,1-dimethylethyl ester
dko	Double knock-out
Dlg1	Drosophila disc large tumor suppressor
dNTP	deoxynucleotide triphosphate
DMEM	Dulbecco´s Modified Eagle´s Medium
DMSO	Dimethyl sulfoxide
DN	Dominant negative
DOC	Deoxycholic acid
DTT	Dithiothreitol

ECL	Enhanced chemiluminescence
EDTA	Ethylenediaminetetraacetic acid
EfnB	ephrin-B
EGTA	Ethylene glycol tetra acetic acid
EOAD	Early-onset AD
EphB R	erythropoietin-producing hepatocellular carcinoma cell line B receptor
ESdM	Embryonic stem (ES) cell derived microglia
EtOH	Ethanol
FAD	Familial Alzheimer's' disease
FAK	Focal adhesion kinase (aka PTK2)
FCS	Fetal calf serum
FL	Full-length
GAPDH	Glyceraldehyde 3-phosphate dehydrogenase
GFP	Green fluorescent protein
HBSS	Hank´s balanced salt solution
HSPG	Heparan sulphate proteoglycan
HEK	Human embryonic kidney cells
HEPES	4-(2-hydroxyethyl)-1-piperazineethanesulfonic acid
HRP	Horse radish peroxidase
ICC	Immunocytochemistry
ICD	Intracellular domain
IP	Immunoprecipitation
Kb	Kilobases
LB medium	Lauria-Bertani medium
LDHA	Lactate dehydrogenase A
LOAD	Late-onset AD
MEF	Murine embryonic fibroblast
MMP	Matrix metalloprotease

ms	Mouse
Nct	Nicastrin
NTF	N-terminal fragment
OD	Optical density
PBS	Phosphate buffered saline
PCR	Polymerase chain reaction
Pen-1	Presenilin enhancer 1
PenStrep	Penicillin/Streptomycin solution
PFA	Paraformaldehyde
PI	Proteinase inhibitor
PI3K	Phosphatidylinositol-3 kinase
PS	Presenilin
PSD95	Post synaptic density protein 95
PTK2	Phosphotyrosine kinase 2 (aka FAK)
Pxn	Paxillin
rb	Rabbit
RIP	Regulated intramembrane proteolysis
RPTK	Receptor protein tyrosine kinase
RPTP	Receptor-like protein tyrosine phosphatase
RT	Room temperature/Reverse transcriptase
FAP	Fast alkaline phosphatase
SDS	Sodium dodecyl sulphate
SH2	Src homology-2
SNP	Single nucleotide polymorphism
SOC medium	Super optimal broth with catabolite repression medium
TBS	Tris buffered saline
TCA	Trichloroacetic acid
TEMED	N,N,N´,N´-tetramethylethylenediamine
TIRF	Total internal reflection fluorescence

Tln	Talin
TREM	Triggering receptor expressed on myeloid cells
VEGF	Vascular endothelial growth factor
WB	Western immunoblotting
WT	Wild-type
ZO-1	Zonula occludens-1 protein

Amino acid	3-letter code	1-letter code
Alanine	Ala	A
Arginine	Arg	R
Asparagine	Asn	N
Aspartic acid	Asp	D
Cysteine	Cys	C
Glutamic acid	Glu	E
Glutamine	Gln	Q
Glycine	Gly	G
Histidine	His	H
Isoleucine	Ile	I
Leucine	Leu	L
Lysine	Lys	K
Methionine	Met	M
Phenylalanine	Phe	F
Proline	Pro	P
Serine	Ser	S
Threonine	Thr	T
Tryptophan	Trp	W
Tyrosine	Tyr	Y
Valine	Val	V

1. Introduction

1.1 The Eph-ephrin system

The Eph-ephrin system is involved in many different processes and is ubiquitously expressed throughout the body (Hafner et al., 2004). Of all receptor tyrosine kinase (RTK) families found in the human genome, the Eph receptor family is the largest group. The Eph receptors can be assigned into two groups: EphA (EphA1-8, 10) and EphB (EphB1-4, 6) receptors. Upon ligand binding they are able to transmit signals intracellularly and thereby steer processes critical in embryonic development but also during adulthood (Pasquale, 2008; Pasquale, 2010). These include cell migration and the formation of tissue boundaries and segmentation (Klein, 2012). Eph receptors comprise several different domains (Figure 1) within their N-terminal ectodomain they contain a globular ligand binding domain (LBD), a cysteine rich region containing a sushi and an epidermal growth factor (EGF)-like domain and two fibronectin type III repeats (FN1 and FN2). The FN domains are followed by a transmembrane helix and the intracellular part. The latter part consists of a juxtamembrane region which contains several conserved tyrosine residues, a tyrosine kinase domain, a sterile a-motif (SAM) protein-protein interaction domain and a C-terminal Psd-95, Dlg and zo-1 (PDZ) domain (Pasquale, 2008) (Figure 1). Upon stimulation by ligand binding, the intrinsic tyrosine kinase of the Eph receptor is activated and can subsequently mediate tyrosine phosphorylation of target proteins. These target proteins in turn can regulate small Rho family GTPases, like RhoA, Rac1 and Cdc42 and henceforth modify cytoskeletal dynamics.

The ephrin ligands, which have not been studied as extensively as their receptors, are also classified into ephrin-A and ephrin-B groups. These assignments were made based on their structure, which is significantly different between class A and B ephrins. Ephrin-A proteins (ephrin-A1-5) are attached to the membrane by a glycosylphosphatidylinositol (GPI)-anchor, while ephrin-B proteins (ephrin-B1-B3) are type I transmembrane proteins, which contain a PDZ domain in their short cytoplasmic tail (Figure 1). Both groups possess an N-terminal receptor binding domain. Ephrin-A ligands mainly bind to EphA receptors and ephrin-B ligands mainly bind to EphB receptors. An exception from this rule are the EphA4 receptor which can bind, albeit weaker, to ephrin-B, and the EphB2 receptor which can bind to ephrin-A5 (Pasquale, 2004). Within the A and B groups they bind promiscuitively to each other. It was found that each Eph receptor binds an ephrin ligand, dimerizes with another Eph-ephrin complex, and consecutively two Eph-ephrin dimers join to form a tetramer, in which each ligand interacts with two receptors and each receptor interacts with two ligands (Himanen et al., 2001). Interestingly, the receptors and their ligands not only bind *in trans* (between two neighbouring cells) but also *in cis* (within the same cell) to each other. It is

speculated that these different binding mechanisms might have an activating and an inhibitory effect, respectively (Arvanitis and Davy, 2008). In 1996 Holland et al. studied the influence of the EphB RTK on axon guidance. It had been found that mice lacking EphB RTK showed defects in axon guidance (Henkemeyer et al., 1996; Orioli et al., 1996). Remarkably, when they investigated transgenic mice expressing a catalytically inactive mutant EphB RTK, axon guidance remained intact (Holland et al., 1996). They concluded that the EphB/ephrin-B system cannot only transmit signals towards the receptor holding cell (forward signaling), but that the ligands possess receptor-like functions and are able to induce intracellular signaling cascades in the ligand presenting cell (reverse signaling).

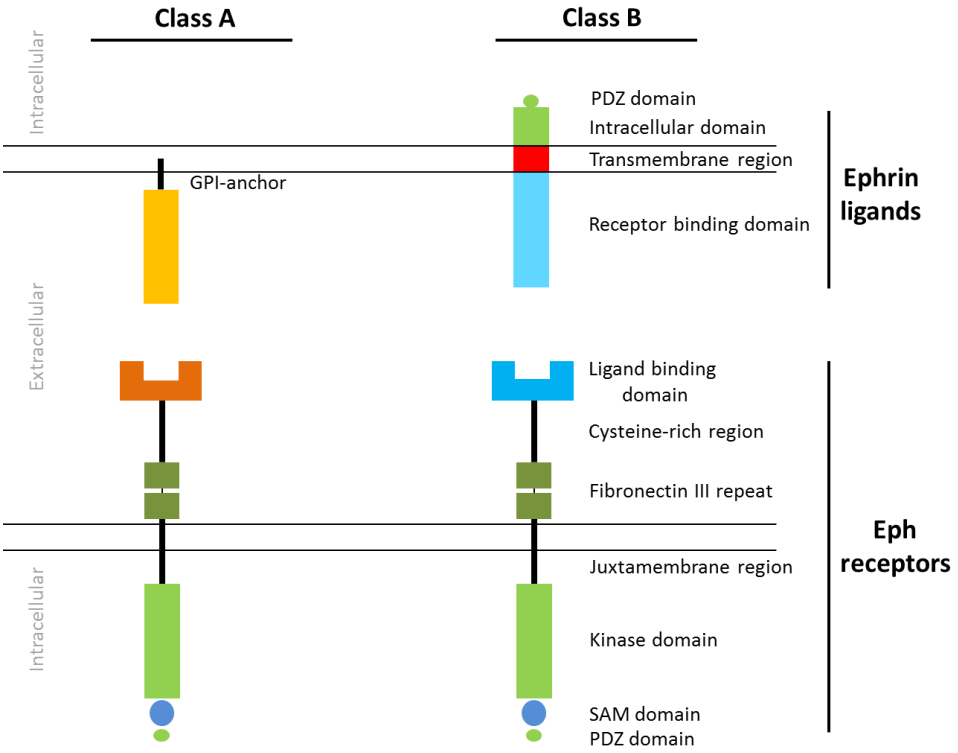

Figure 1: Domain structures of ephrins and Eph receptors.
Class A and B Eph receptors possess similar domains and are primarily discriminated based on their Eph class-specificity loop (Himanen et al., 1998), located within their globular ligand binding domain. Extracellularly, they contain a globular ligand binding domain (LBD) a cysteine rich region and two fibronectin type III repeats (FN1 and FN2). The intracellular part consists of the juxtamembrane region, a tyrosine kinase domain, a sterile a-motif (SAM) protein-protein interaction domain and a PDZ domain. Ephrin ligand classes substantially differ from each other. Ephrin-A ligands are tethered extracellularly to the plasma membrane by a GPI anchor. Ephrin-Bs are transmembrane I proteins and contain a receptor binding domain, a transmembrane domain and an intracellular domain with a PDZ domain. EphA receptors mainly bind ephrin-As, while EphB receptors mainly bind ephrin-Bs. Within their classes, ligands and receptors bind promiscuitively to each other. Scheme deduced from (Boyd et al., 2014).

Indeed, it has been found that ephrin-B also undergoes phosphorylation upon interaction with EphB receptors. This involves for instance Src family kinases (Bruckner et al., 1997; Georgakopoulos et al., 2006) and the fibroblast growth factor receptor (FGFR) (Chong et al., 2000). During ephrin-B reverse signaling its intracellular domain (ICD) becomes phosphorylated upon recruitment of SH2 or PDZ domain containing proteins. Although they do not possess an ICD, ephrin-A proteins have also been found to transmit reverse signals (Holmberg et al., 2005; Knoll and Drescher, 2002), probably by means of co-receptors. The p75 neurotrophin receptor (p75NTR) (Lim et al., 2008) and the TrκB neurotrophin receptor tyrosine kinase (Marler et al., 2008; Marler et al., 2010) have been suggested as potential transmembrane binding partners that can mediate reverse signaling of ephrin-A. Ephrin-A downstream signaling involves stimulation of proteins like ephexin, Vav-2 (Cowan et al., 2005) and Tiam-1(Tanaka et al., 2004). Analogous to ephrin-B, ephrin-A stimulation mainly regulates cell adhesion and migration. Vav-2 activation for example leads to Rac1 activation and thereby to cytoskeletal reorganization (Cowan et al., 2005).

1.1.1 The Eph-ephrin system during CNS development

The expression pattern of the Eph-ephrin system has been well characterized in the developing CNS of mice (Bruckner et al., 1999; Liebl et al., 2003). Murine knock out models indicated its involvement in many developmental processes (Table 1). It is known to regulate many processes ranging from segmentation, neural crest migration, topographic mapping of the CNS, axon guidance, vascular development to neurogenesis during development. In vertebrates, the paraxial mesoderm as well as the hindbrain is segmented. Eph-ephrin signaling is involved in both the initial segmentation and in the subsequent division of somites into anterior and posterior halves. EphA4 is expressed in the anterior half, while ephrin-B2 is localized to the posterior half (Durbin et al., 1998; Tepass et al., 2002). During subsequent hindbrain segmentation, rhombomeres 1 to 7 are transiently formed. These rhombomeres later specify where neural crest cells migrate and nerves originate. In mice, Eph receptors are expressed in rhombomeres 3 and 5, while ephrins are expressed in rhombomeres 2, 4 and 6. In some rhombomeres Eph receptors are expressed together with their ligands, however, at most sites where receptors and ligands interact, mutual cell detachment and formation of rhombomere boundaries occurs (Cooke and Moens, 2002).

The Eph-ephrin system is moreover involved in spatial restriction of neural crest cells, specifically trunk and branchial crest cells. Neural crest cells originate at the dorsal region of the neural tube and continue to migrate in order to ultimately differentiate into many cell types, including neurons and glia of the peripheral CNS, the craniofacial skeleton and many pigment cells. The interaction between the Eph receptors expressed by ventrally migrating

neural crest cells and the ephrin ligands expressed in the posterior sclerotome mediate a repulsive response that restricts the migration of the cells to the anterior half of each somite (Krull et al., 1997; Santiago and Erickson, 2002; Wang and Anderson, 1997). Later during development, the Eph-ephrin system is involved in topographic mapping processes. In the retina and in the midbrain, different gradings of EphAs and ephrin-As control anterior-posterior axon orientation. Axons expressing low EphA but high ephrin-A levels project to posterior regions, while axons with high EphA and low ephrin-A expression project to anterior regions (Wilkinson, 2000). Ephrins and Ephs have also been shown to segregate connections between the thalamus and the neocortex. It was reported that ephrin-A5 knock out mice display limbic-thalamic neurons which form additional aberrant projections to the sensorimotor cortex, again suggesting that ephrin-A5 acts as a guidance cue in order to prevent unrestricted connections to inappropriate neocortical areas (Uziel et al., 2002).

Interestingly, more recent findings have implicated ephrin-B signaling in the human lissencephalic phenotype, which is characterized by insufficient migration of post mitotic neocortical neurons, resulting in an inside-out layering of the cortex and a hypoplastic cerebellum. This phenotype, in mice also known as Reeler phenotype, which has previously been associated with mutations in the extracellular matrix (ECM) glycoprotein reelin (Hong et al., 2000), could be rescued by ephrin-B2/-B3 overexpression. Transgenic mice displaying a triple homozygous knock out for ephrin-B proteins (B1, B2 and B3) in turn, resembled the Reeler phenotype, demonstrating an involvement of ephrin-B in the arrangement of neocortex laminations (Senturk et al., 2011).

An additional prominent function of the Eph-ephrin system in the CNS, but also in the rest of the embryo, constitutes its role in vasculogenesis and angiogenesis. Both EphB4 and ephrin-B2 null mice display embryonic lethality around day E10.0. It was suggested that one of the main reasons for this perinatal lethality is defective early angio- and vasculogenesis (Gerety et al., 1999; Wang et al., 1998). It was discovered that primordial arterial vessels express ephrin-B2, while primordial venous endothelium expresses EphB4, suggesting a role of the two proteins in the differentiation and/or separation of endothelial cells. Transgenic mice lacking the ephrin-B2 ICD resembled the defective angiogenesis of the ephrin-B2 null mice, indicating that ephrin-B2 reverse signaling is a prerequisite for embryonic angio- and vasculogenesis (Adams et al., 2001). Two other studies indicated that ephrin-B2 reverse signaling mediated by its PDZ domain is only crucial for lymphatic and retinal blood vessel development (Makinen et al., 2005; Sawamiphak et al., 2010). These results suggest that ephrin-B2 reverse signaling mediated by the PDZ-binding domain is critically involved in lymphatic and retinal blood vessel development.

TABLE 1: EPH-EPHRIN GENE MANIPULATION IN MICE

Genotype	Phenotype	Reference
EphA1 -/-	Subpopulation kinky tail (80%), subpopulation disruption of hormone induced apoptotic processes (18% of females)	(Duffy et al., 2008)
EphA2 -/-	Kinky tail and ectopic vertebrae due to splitting of the notochord	(Naruse-Nakajima et al., 2001)
EphA3 -/-	75% perinatal lethality, due to cardiac defects	(Stephen et al., 2007)
EphA4 -/-	Kangaroo like hopping gait	(Kullander et al., 2001b)
EphA5 -/-	Retinotectal map abnormalities	(Feldheim et al., 2004)
EphA6 -/-	Involved in learning and memory	(Savelieva et al., 2008)
EphA7 -/-	Reduction of somatosensory cortex, impaired topographic mapping of axons	(Dufour et al., 2003; Miller et al., 2006)
EphA8 -/-	No discernible phenotype, abnormal axon projection	(Park et al., 1997)
EphA10 -/-	Not known	N/A
Ephrin-A1 -/-	Impaired cardiac function, thickened aortic and mitral valves	(Frieden et al., 2010)
Ephrin-A2 -/-	No growth morphological defects, retinal map abnormalities	(Feldheim et al., 2000)
Ephrin-A3 -/-	Abnormal hippocampal spines, decreased learning and memory	(Carmona et al., 2009)
Ephrin-A4 -/-	Not known	N/A
Ephrin-A5 -/-	Subpopulation (17%) midline defect dorsal head, retinal map abnormalities	(Feldheim et al., 2000; Frisen et al., 1998)
EphB1 -/-	Reduced ipsilateral projection and pain behaviour after pain induction	(Henkemeyer et al., 2003)
EphB2 -/-	No discernible phenotype	(Henkemeyer et al., 1996)
EphB3 -/-	Cleft palate, with perinatal lethality anterior commissure, absent corpus callosum	(Orioli et al., 1996)
EphB4 -/-	Embryonic lethal (E9.5), abnormal cardiac looping	(Gerety et al., 1999)
EphB6 -/-	No discernible phenotype	(Shimoyama et al., 2002)
Ephrin-B1 -/-	Perinatal lethality, defects in neural crest derived tissues, abnormal skeletal patterning	(Davy et al., 2004)
Ephrin-B2 -/-	Embryonic lethal (E11), disruption of angiogenesis in yolk sac	(Wang et al., 1998)
Ephrin-B3 -/-	Neo-hopping gait, failure of corticospinal tract (CST) pathfinding	(Kullander et al., 2001a; Yokoyama et al., 2001)

1.1.2 The Eph-ephrin system in the adult brain

All Eph receptors and all ephrin ligands have been shown to be expressed in the human brain with high expression of the Eph receptors EphA4, EphA6, EphA7, EphB1 and EphB6 and of the ephrin ligands ephrin-A5 and ephrin-B2. Ephrin-B3 expression levels are overall low in humans, but the highest expression levels can be detected in the brain (Goldshmit et al., 2006; Hafner et al., 2004).

The Eph-ephrin system has mainly been investigated regarding its role in synaptic plasticity in the adult brain. Binding of EphB to ephrin-B is thought to induce formation of large raft like patches on neuronal cells which contain N-methyl-D-aspartate (NMDA) receptors amongst other synaptic components, indicating a role of the Eph-ephrin system in the assembly of post-synaptic transmission, long-term potentiation (LTP) and long-term depression (LTD) (Calo et al., 2006; Dalva et al., 2000). Additionally, a functional role of Eph receptors in spine morphogenesis was demonstrated. *In vitro* transfection of a catalytically inactive EphB2 variant into hippocampal neurons inhibited their spine morphogenesis (Henkemeyer et al., 2003; Nishimura et al., 2006). The mechanisms by which EphB receptors regulate dendritic spine morphogenesis probably involve interaction with guanine exchange factors (GEF), which in turn regulate the activity of Rho GTPases and thereby control the remodelling of actin filaments (Henkemeyer et al., 2003; Penzes et al., 2003). Besides spine morphogenesis the Eph-ephrin system has also been found to induce growth cone collapse. A study by Murai et al. demonstrated that when EphA4, which has been shown to be expressed on hippocampal neurons, was stimulated by ephrin-A3, which is expressed on astrocytes neuronal growth cones collapsed (Murai et al., 2003). These findings suggest that the system mediates a form of communication between neurons and glial cells, which is important for synaptic plasticity and remodelling.

1.1.3 Signaling of the Eph-ephrin system

Forward signaling

Like previously described, the Eph-ephrin system is capable of bidirectional signaling. Forward signaling, thus signaling toward the receptor holding cell, has been extensively investigated and many proteins involved in downstream cascades have been identified. Upon ephrin-binding, Eph receptors undergo auto- and Src mediated phosphorylation of the Eph ICD. Subsequently, the tyrosine kinase catalytic domain is fully activated (Kalo and Pasquale, 1999) and kinases which contain Src homology 2 (SH2) domains are recruited (Figure 2). Another way of Eph receptor activation is receptor spanning crosstalk. For instance, upon separate activation of fibroblast growth factor receptor (FGFR) or EphA4 both receptors were found to trans-phosphorylate each other and regulate common downstream

pathways (Yokote et al., 2005). Similar mechanisms have also been observed for Ryk, the chemokine receptor CXCR4, integrins, cadherins, claudins (Arvanitis and Davy, 2008).

After SH2 domain containing protein binding to the Eph receptors, downstream effectors are stimulated (Kalo and Pasquale, 1999; Wybenga-Groot et al., 2001). Rho guanine nucleotide exchange factors (GEFs), like Vav2, Tiam, Kalirin and Intersectin, for instance have been shown to be activated by phosphorylated Eph receptors (Cowan et al., 2005; Klein, 2009; Murai and Pasquale, 2005; Sahin et al., 2005). They activate in turn key components of Eph signaling: Rho GTPases, including RhoA, Cdc42 and Rac. These Rho GTPases regulate cell shape and movement by initiating the formation of stress fibers (Rho), lamellipodia (Rac) and filopodia (Cdc42) (Klein, 2009; Ogita et al., 2003; Shamah et al., 2001). But also ubiquitination and degradation of some GEFs, like ephexin5 can be induced by phosphorylated EphB receptors. By this degradational mechanism, ephexin binding to EphB is inhibited, which simultaneously disinhibits RhoA activity (Margolis et al., 2010). The small GTPases of the Ras family are also subject of Eph receptor regulation. H-Ras, which is able to activate the MAP kinase cascade, is one of their targets. Eph receptors are among the few proteins that can negatively regulate H-Ras signaling (Elowe et al., 2001; Tong et al., 2003). Interestingly, downstream of other receptors, like other RTKs or integrins, Eph receptors can stimulate Ras-MAP kinase signaling (Elowe et al., 2001; Kim et al., 2002b; Miao et al., 2001). The MAP kinase cascade is well known for its ability to stimulate cell replication, but also regulates axon guidance, neurite outgrowth and cell migration, by phosphorylating cytoskeletal components (Forcet et al., 2002; Klemke et al., 1997).

Another important downstream forward signaling target is the focal adhesion kinase (FAK). In fibroblasts, ephrin-A1 stimulation resulted in increased phosphotyrosine levels of EphA2, FAK, $p130^{Cas}$ and paxillin. When fibroblasts derived from FAK or $p130^{Cas}$ knock out mice were investigated, phosphorylation as well as migration of cells was inhibited (Carter et al., 2002).

Additionally, in 2009, Shi et al. found that mature dendritic spines could be reversed into an immature filopodial like phenotype in primary hippocampal neurons, when investigating neurons expressing a dominant negative mutant of EphB2. These cells could be rescued by FAK re-expression, but not by re-expression of a FAK Y397 mutant, indicating the significance of FAK Y397 phosphorylation in downstream EphB2 signaling (Shi et al., 2009). Subsequently, FAK was confirmed to be a binding partner of EphB2 in a study in which EphB2 complexes were analyzed via Co-IP and subsequent mass spectrometry analysis after ephrin-B1 stimulation (Darie et al., 2011).

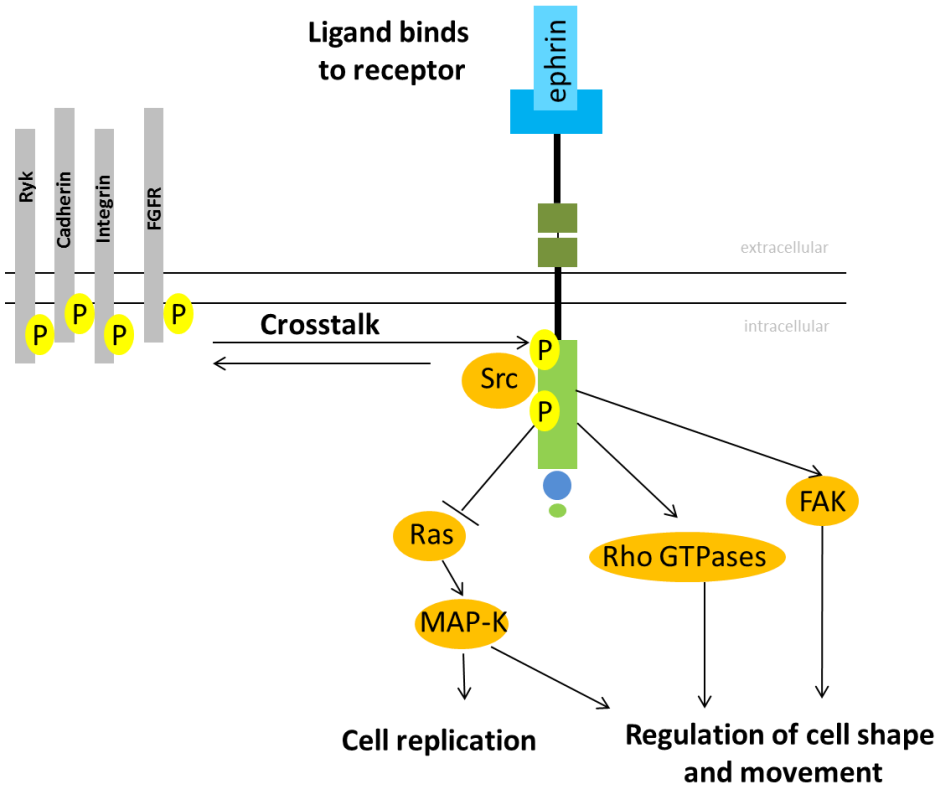

Figure 2: Eph receptor forward signaling.
Upon ligand binding the tyrosine kinase domain of the Eph receptor is auto- or Src phosphorylated. An alternative way of Eph receptor activation occurs via receptor-crosstalk between the Eph receptor and receptors like FGFR, Ryk, cadherin, integrin, and CXCR4. Eph receptors activate multiple downstream cascades, many of which involve small family GTPases like Rho and Ras. Another prominent Eph receptor target is FAK. By stimulation of these downstream effectors mainly processes influencing cellular adhesion and migration are initiated, but also cell replication is affected.

Reverse signaling

The ephrin ligands possess no intrinsic catalytic activity. However, they can bind and induce the activation of intracellular effectors and thereby regulate intracellular signaling pathways. Since the way ephrin-A and ephrin-B ligands are attached to the membrane is fundamentally different, they also rely on different mechanisms to transmit their signals intracellularly (Figure 3). Both ephrin groups are subject to shedding by A disintegrin and metalloproteases (ADAMs) and, in case of ephrin-A1 and ephrin-B1, by matrix metalloproteinases (MMPs) (Beauchamp et al., 2012; Tanaka et al., 2007). As previously mentioned, ephrin-A molecules are tethered to the cellular membrane via GPI-anchors and do therefore not possess an ICD which they could utilize for reverse signaling. However, various studies indicate that ephrin-As are capable of reverse signaling (Cutforth et al., 2003; Davy and Robbins, 2000; Huai and Drescher, 2001; Knoll et al., 2001). In cultured cells, EphA

mediated ephrin-A activation resulted for instance in integrin dependent adhesion (Huai and Drescher, 2001), likely involving MAP kinases and Fyn (Davy et al., 1999; Davy and Robbins, 2000). Ephrin-A reverse signaling furthermore affects cell adhesion and changes in cytoskeletal architecture via the Src family kinase Fyn (Davy et al., 1999; Davy and Robbins, 2000) and has been implicated in the pathfinding of vomeronasal sensory neurons (Knoll et al., 2001) and spinal motor axons (Marquardt et al., 2005). The neurotrophin receptor p75 forms a complex with ephrin-As and Fyn in caveolae and was therefore suggested to be a possible co-receptor candidate for ephrin-A (Lim et al., 2008). These studies also indicated that the Fyn pathway, which is downstream of ephrin-A, is p75 dependent and that ephrin-A associated repellent effects are p75 mediated (Lim et al., 2008). Within the same year, another neurotrophin receptor, namely TrκB receptor was identified as another ephrin-A interaction partner. The TrκB is a receptor for brain derived neurotrophic factor (BDNF), which, when injected into the tectum, increased branching and complexity of retinal axon arbours (Cohen-Cory and Fraser, 1995). Due to their expression in anteroposterior and dorsoventral gradients, the Eph-ephrin-A family members are ideal interaction partners for TrκB receptors, since they contain topographic information for axonal arbour growth. It was demonstrated that ephrin-A proteins suppress axonal branching in the retina by interacting *in cis* with the CC2 domain of TrκB, and thereby activated Akt further downstream (Marler et al., 2008).

Ephrin-B proteins belong to the group of type I transmembrane proteins and possess a short intracellular C-terminal tail. Upon binding of an EphB receptor to an ephrin-B ligand, the ephrin-B proteins are extracellularly shed and/or endocytosed. Ephrin-B3 proteins are cleaved by the human rhomboid family protease 2 (RHBDL2) (Pascall and Brown, 2004). In the case of ephrin-1 and ephrin-B2, shedding induces subsequent cleavage by the γ-secretase, which also releases the intracellular ephrin-B domain from cellular membranes. Georgakopoulos et al. showed that EphB2 binding induces ephrin-B2 shedding and subsequent γ-secretase cleavage. In this study, the resulting ICD was demonstrated to bind the transmembrane I protein PAG/Cbp, which typically forms a complex with the C-terminal Src kinase (Csk) and Src to inhibit the latter. Binding of the ICD caused the release of Src from the complex and subsequent Src autophosphorylation on Y418. Additionally, Src was found to form a complex with the ICD, suggesting not only disinhibition but also activation Src by release of the ephrin-B2 ICD (Georgakopoulos et al., 2011). This ICD, like many other γ-secretase products generated intracellularly, has been shown to translocate to the nucleus, suggesting a gene regulatory function for this protein (Tomita et al., 2006; Waschbusch et al., 2009).

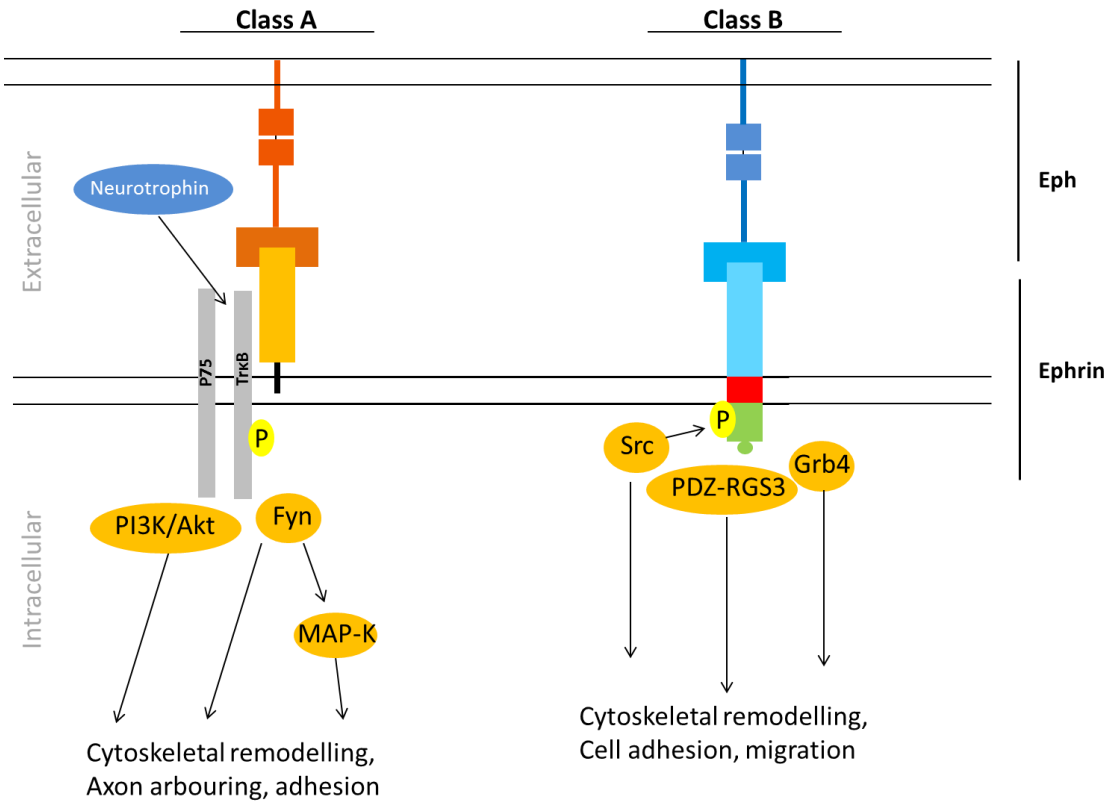

Figure 3: Ephrin-A and ephrin-B reverse signaling.
Ephrin-A reverse signaling is probably initiated by EphA receptor binding and simultaneous binding of p75 or TrκB. It is not clear whether neurotrophin binding to p75 or TrκB can also influence ephrin-A reverse signaling. Intracellular ephrin-A signaling is mediated by p75 or TrκB and can activate downstream effectors like PI3K/Akt, Fyn and the MAP-K cascade. By these cascades in turn, cytoskeletal remodelling, axon arbouring and cell adhesion are thought to be regulated. Ephrin-B reverse signaling is initiated by EphB receptor binding and is followed by intracellular ephrin-B phosphorylation mediated by Src. This phosphorylation recruits further downstream effectors, which can bind to the ephrin-B ICD. Ephrin-B reverse signaling regulates cytoskeletal remodelling, cell adhesion and migration.

Furthermore, Src can also phosphorylate full length membrane bound ephrin-B. The ephrin-B ICD contains four SH2 domains, which have been shown to attract proteins like Grb4 upon tyrosine phosphorylation (Georgakopoulos et al., 2006; Segura et al., 2007). The PDZ domain located in the ICD has been suggested to be important for ephrin-B regulation, since it constitutes the binding site for the protein tyrosine phosphatase (PTP)-BL, which can terminate ephrin-B effector recruitment by SH2 domain dephosphorylation (Palmer et al., 2002). Another protein that is known to bind the ephrin-B PDZ domain is PDZ- regulator of G-protein signaling 3 (RGS3), which was shown to inactivate G-protein signaling (Lu et al., 2001). This study also suggested that downstream pathways of the chemokine stromal cell derived factor-1 (SDF-1) may be regulated by the ephrin-B PDZ domain and the PDZ-RGS3 protein, thereby linking reverse signaling to cellular guidance. Furthermore the previously described

ephrin-B SH2 domain binding protein Grb4 was found to attract the G protein-coupled receptor kinase-interacting protein 1 (GIT 1) (Segura et al., 2007). These two examples indicate a role of ephrin-B reverse signaling in the regulation of processes which are mediated by G proteins.

Proteolytic processing and subcellular trafficking

After high affinity binding between Eph and ephrin proteins the interaction can be terminated by either of two mechanisms: 1) Extracellular shedding or 2) endocytosis. Eph receptors as well as ephrin proteins are substrates of ADAM proteases. Shedding of Eph receptors by ADAM proteases is triggered upon binding of the receptor to its ligand and can, like the binding between Ephs and ephrins, occur *in cis* or *in trans* (Georgakopoulos et al., 2006; Hattori et al., 2000; Janes et al., 2005). In addition to shedding, the interaction between Ephs and ephrins that are localized on different cells i.e. *in trans*, can also be terminated by means of endocytosis. In case of endocytosis the Eph-ephrin complex can be internalized into the receptor holding or the ligand holding cell in order to evoke de-adhesion and repulsion between two cells (Lauterbach and Klein, 2006; Mann et al., 2003; Marston et al., 2003; Zimmer et al., 2003). This process is called *trans*-endocytosis and, interestingly, resulted in the internalization of vesicles containing both full length proteins (Marston et al., 2003; Pitulescu and Adams, 2010; Spacek and Harris, 2004; Zimmer et al., 2003). In a study by Marston et al. for instance, neighbouring fibroblasts were microinjected with either EphB4 or ephrin-B2. At contact sites of the neighbouring cells, trans-endocytosis was observed to take place. Trans-endocytosed vesicles contained full length proteins of the EphB4 as well as the ephrin-B2 ligand. The determinants of the direction of endocytosis are not fully understood. It was however shown that if cells which express EphB2, bind to cells expressing ephrin-B1 variants lacking the ICD, the complex is mostly endocytosed by the EphB2 containing cell. When however EphB2 phosphorylation is defective, the complex is internalized into the ligand holding cell (Zimmer et al., 2003). Thus, the direction of endocytosis seems to be dependent on the direction of signaling. Furthermore, in this process, which so far has not been widely explored, EphB1 was found to be associated with caveolin-1, while ephrin-B1 was found to be associated with clathrin (Vihanto et al., 2006), suggesting involvement of caveolae and a clathrin-dependent mechanism, respectively. Whether the internalized molecules are degraded or recycled and in which way this process could influence the migrational behaviour of cells remains to be resolved and might give interesting information on the regulation of cell repulsion and cell sorting independent of proteinase cleavage.

1.1.4 The Eph-ephrin system in pathological conditions

Since the Eph-ephrin system is ubiquitously expressed throughout the body, it has been implicated in various pathological conditions.

In neural cell repair after injury, the system seems to provide guidance cues to re-establish appropriate connections. Macrophages expressing EphB3 were found to promote axonal sprouting of damaged retinal neurons, which expressed ephrin-B3 (Liu et al., 2006). Other results indicated that the Eph-ephrin system hinders proper axon regrowth through its repulsive signaling (Wu et al., 2007). A study by Yue et al. found for instance that ephrin-A5 stimulation of neurites inhibited outgrowth of EphA4 positive spinal cord neurons (Yue et al., 1999). Similar mechanisms have been shown for cortical neurons in response to ephrin-B3 (Benson et al., 2005; Kullander et al., 2001a).

A disease which is known to be caused by different mutations, or in some cases a deletion of ephrin-B1 is the X-linked developmental disorder craniofrontonasal syndrome (CFNS) (Davy et al., 2006; Wieland et al., 2004). In this disease mosaic-like ephrin-B1 expression causes impaired gap junction communication, and thereby cell sorting abnormalities and inhibition of osteoblast differentiation (Compagni et al., 2003). Ephrin-B1 mutant mice display similar malformations of the axial skeleton like humans, i.e. polydactyly, asymmetric attachment of ribs and lack of joints (Compagni et al., 2003; Henkemeyer et al., 1996; Orioli et al., 1996). The CFNS associated ephrin-B1 mutations T111I and P54L are located in an essential part of the ephrin-B1 receptor binding domain, suggesting impaired ephrin-B1 signaling in CFNS patients. Accordingly, *in vitro* Eph receptor induced ephrin-B1 cluster formation as well as intracellular ephrin-B1 signaling is impaired in cells expressing mutant ephrin-B1 proteins (Makarov et al., 2010). It is not known whether mutations in other Ephs and ephrins may cause related disorders.

Given its prominent role in cell differentiation and signaling the Eph-ephrin system is extensively studied in the field of oncology. Eph-ephrin protein expression is altered in essentially all types of cancer cells (Ireton and Chen, 2005). It is also expressed in tumor vasculature, where it promotes angiogenesis (Brantley-Sieders and Chen, 2004; Heroult et al., 2006). In cancer cells, Eph receptors are mostly upregulated, while ephrin ligands are downregulated. Therefore, despite their high expression levels Eph receptors are mainly inactive in those cells. Although mostly downregulated, ephrin ligands have been reported to promote cell transformation and cancer cell migration/metastasis (Campbell et al., 2006; Meyer et al., 2005; Tanaka et al., 2007). The expression of Eph-ephrin proteins in blood vessels is essential during development as well as in adulthood. In tumor angiogenesis however, it significantly contributes to tumor growth and metastasis and has therefore been targeted in cancer treatment and therapy. Ephrin-B2 for example is widely expressed in the vasculature of many tumors, which is not surprising given the fact that ephrin is found in the embryonic arterial vasculature and its expression in endothelial cells is upregulated by hypoxia and VEGF and is therefore a cancer therapy target (Brantley-Sieders and Chen, 2004; Heroult et al., 2006).

Interestingly, in a genome wide association study (GWAS), Hollingworth et al. showed a correlation between Alzheimer disease and the occurrence of the single nucleotide point (SNP) mutation rs11767557 of the EphA4 receptor (Hollingworth et al., 2011). Recently, Rosenberger et al. found an altered distribution of the EphA4 receptor in hippocampi of AD patients compared to control cases. This was observed at early AD stages, in which synaptic loss is thought to occur. Furthermore in AD patients, the EphA4 receptor colocalized with neuritic plaques. It was therefore suggested that impaired hippocampal EphA4 signaling may lead to the onset of memory decline in AD (Rosenberger et al., 2014). Correspondingly, reduced expression of the EphA4 receptor has previously been linked to cognitive impairment in a transgenic mouse model for AD (Simon et al., 2009).
Two other studies state by contrast that EphA4 signaling is enhanced in transgenic mouse models of AD and mediates synaptic plasticity impairment (Fu et al., 2014; Vargas et al., 2014). They also showed that soluble Aβ oligomers, which also contribute to synaptic loss in AD, induced EphA activation and that inhibition of EphA4 in the CA1 region reversed suppression of long term potentiation in mice (Fu et al., 2014). Due to these controversial findings it would be interesting to investigate whether the different binding partners of EphA4, which range from ephrin-A to ephrin-B proteins might influence the nature of EphA4 effects.

1.2 The γ-secretase complex

As described above, Ephs and ephrin-Bs can undergo proteolytic processing by the γ-secretase. The γ-secretase complex has been and still is of great interest to researchers investigating Alzheimer's disease, since it is responsible for the generation of the β-amyloid peptide, a protein which accumulates in the CNS of patients who suffer from Alzheimer's disease (AD) (Benilova et al., 2012; Murphy and LeVine, 2010). However, being able to cleave more than 90 transmembrane I proteins, this aspartyl protease has been shown to be involved in many more processes surpassing those involved in the etiology of AD. Together with the site-2 protease (S2P), the signal peptide peptidases (SPPs), and the rhomboids, the γ-secretase belongs to the family of intramembrane cleaving proteases, called I-CliPs (Haapasalo and Kovacs, 2011). The γ-secretase complex consists of four critical subunits called presenilin (PS1 or PS2), nicastrin (Nct), Anterior pharynx-defective 1 (Aph-1) and presenilin enhancer 2 (Pen-2) (Figure 4). All four subunits are essential for the functioning of the transmembrane aspartyl protease (Edbauer et al., 2003). Due to the plethora of presenilin mutations that have been found to be associated with early onset familial Alzheimer's disease (EOAD), the PS are the most intensively studied components of the γ-secretase complex. Containing two aspartic acid residues (Asp257 and Asp385) which catalyze substrate cleavage, PS constitutes the active site of the complex. PS comprises a total of 9 transmembrane domains (TMDs) (Laudon et al., 2005; Oh and Turner, 2005; Spasic et al.,

2006). The two aspartic acid residues important for substrate cleavage are located in TMD 6 and 7. During assembly and maturation of the complex, PS undergoes endoproteolysis resulting in the generation of an N- and a C-terminal PS fragment (NTF and CTF, respectively), which form stable heterodimers (Seeger et al., 1997; Yu et al., 1998).

Nct was the secondly discovered γ-secretase subunit (Yu et al., 2000). This large and highly conserved transmembrane I protein was suggested to be the substrate binding unit of the γ-secretase. Specifically, the DYIGS and peptidase (DAP) domain of Nct, which is located in its large extracellular part, was found to form the substrate binding site (Shah et al., 2005). Others found Nct to be important for γ-secretase maturation but not for its activity (Chavez-Gutierrez et al., 2008). The discussion about the Nct function remains controversial.

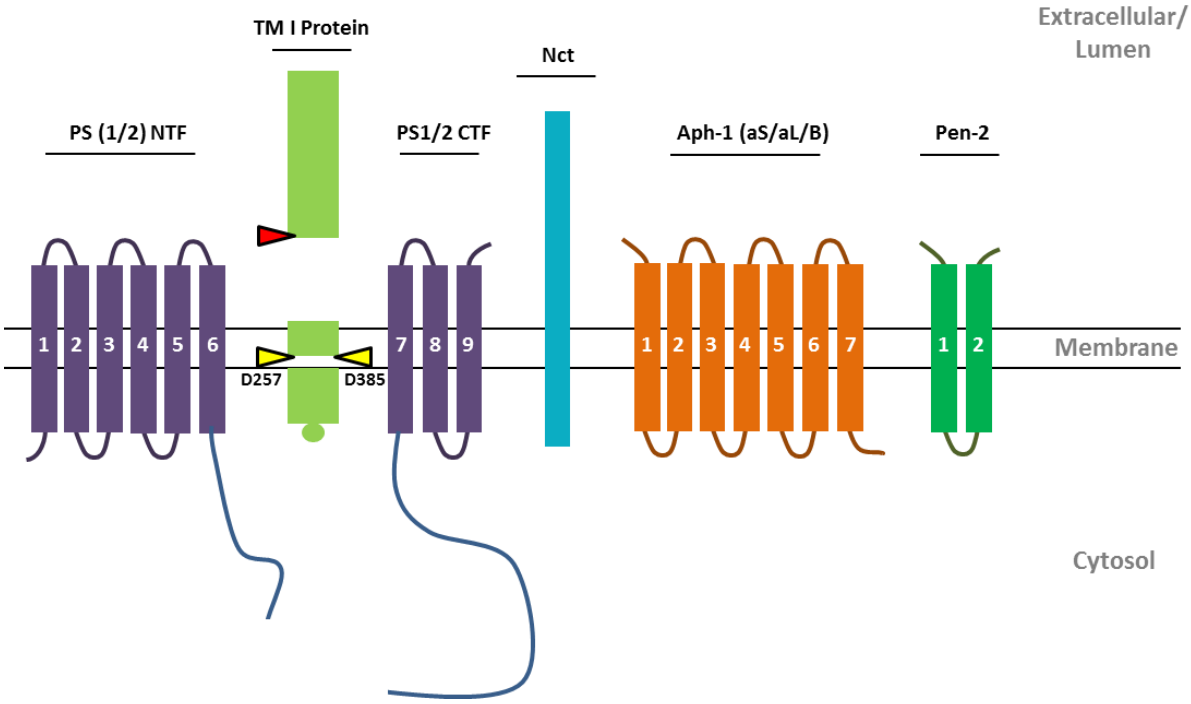

Figure 4: The γ-secretase complex and intramembranous cleavage.
The γ-secretase complex consists of four subunits. Presenilin (PS), Nicastrin (Nct), Anterior pharynx-defective 1 (Aph-1) and the Presenilin enhancer 2 (Pen-2). The γ-secretase complex always exists in a 1:1:1:1 stoichiometry. Two PS genes exist, PS1 and PS2. Aph-1 has two isoforms, Aph-1a and Aph-1b, of which Aph-1a also has two splice variants, called Aph-1aS and Aph-1aL. The γ-secretase mainly cleaves type I transmembrane (TM I) proteins. Ectodomain shedding of the TM I proteins (red arrow) precedes intramembranous γ-secretase cleavage (yellow arrow). Two conserved aspartate residues in the sixth and eighth TMR of PS, namely D257 and D385 respectively, serve as active site residues, defining the γ-secretase as an aspartyl protease. Scheme deduced from (Steiner et al., 2008).

Two years later, an additional component of the γ-secretase complex was found: Aph-1. Upon Aph-1 knock out, a phenotype comparable to that seen in PS and Nct deficient

C.elegans was observed (Francis et al., 2002; Goutte et al., 2002). The 7 TMD protein Aph-1 associates with PS and Nct, regulating the assembly of the γ-secretase complex (Lee et al., 2002). Aph-1 possesses two isoforms, Aph-1 a and Aph1 b, former occurring in two splice variants (Aph-1aS and Aph-1aL) (Shirotani et al., 2004b). Concurrently with Aph-1, the fourth component, Pen-2, was discovered. It contains two TMDs, with a luminal C- and N-terminus. Aph-1 is thought to be necessary for endoproteolytic processing of PS into its N- and C-terminal fragments and for full maturation of nicastrin, thereby facilitating the translocation from the endoplasmatic reticulum (ER) into the Golgi (Francis et al., 2002).

1.2.1 Assembly of the γ-secretase complex

As mentioned previously, presence of all four components of the γ-secretase complex and its proper assembly has been shown to be crucial for its function and its transport out of the ER. It was demonstrated that PS fragment levels strongly decrease upon Nct and Aph-1 RNAi knock down (Edbauer et al., 2002; Shirotani et al., 2004a). Knock down of Pen-2 resulted in accumulation of PS holoproteins, suggesting a regulatory role of Pen-2 in endoproteolytic processing of PS proteins (Prokop et al., 2004). Additionally, knock out of PS decreased Pen-2 levels and, while its expression levels stayed unchanged, Nct accumulated in its immature form indicating that the γ-secretase complex cannot exit the ER in absence of PS (Edbauer et al., 2002). In the ER the four components are not only generated but also assembled into one complex. Essential domains for γ-secretase complex assembly are the PS1 C-terminus (Bergman et al., 2004; Kaether et al., 2004), the TMD of Nct (Capell et al., 2003; Morais et al., 2003), the C-terminus of Pen-2 (Hasegawa et al., 2004; Kim et al., 2004; Prokop et al., 2004) and the TMD 4 of Aph-1 (Edbauer et al., 2004; Lee et al., 2004b). Mature Nct, which underwent glycosylation, can bind Aph-1. This heterodimer then binds the PS holoprotein, forming a heterotrimer, which in turn can bind to Pen-2. Upon Pen-2 binding, PS can undergo endoproteolytic cleavage in the ER, the ER-Golgi intermediate compartment (ERGIC), and/or the Golgi. Some γ-secretase components, like Nct and PS, have a half-life of less than 24 hours when they are not incorporated into the complex and cannot leave the ER due to ER retention signals. Upon full assembly however, ER retention signals in Pen-2 are masked between the proteins and the membrane and the complex can translocate from the ER to the Golgi via the ERGIC (Dries and Yu, 2008; Kaether et al., 2004; Kaether et al., 2007; Spasic et al., 2007). Upon reaching the *trans*-Golgi, Nct is fully matured by further glycosylation. It has further been proposed that the γ-secretase needs a slightly acidic environment for effective substrate cleavage indicating γ-secretase activity in endosomal or lysosomal compartments rather than at the plasma membrane (Pasternak et al., 2003). Others found the γ-secretase to be active at the plasma membrane however (Chyung et al., 2005; Hansson et al., 2005), making this topic a matter of ongoing discussion.

1.2.2 Regulation of γ-secretase activity

The activity of the γ-secretase complex is regulated on multiple levels. Firstly, as previously mentioned, expression of γ-secretase components may be regulated by degradation after their synthesis in the ER. Secondly, presence of all four subunits and proper assembly is needed for the functionality of the γ-secretase (Edbauer et al., 2003). Overexpression of a single component, such as PS, does only lead to a moderate increase of γ-secretase activity, since the amount of endogenous γ-secretase components is rate limiting (Levitan et al., 2001). Furthermore, different isoforms of γ-secretase components can be incorporated into the complex. In the case of PS, either PS1 or PS2, in the case of Aph-1, either Aph-1a or Aph-1b are utilized for complex assembly, and isoforms of one protein do not appear simultaneously within one complex (Lai et al., 2003; Shirotani et al., 2004b). Thus, different combinations of γ-secretase components could affect the activity and specificity of this protease complex.

Differential activity of the PS isoforms is demonstrated by the fact that phenotypic characteristics of PS1 and PS2 deficient systems are distinct. Additionally, isoform-specific expression levels are variable among different tissues (Lai et al., 2003). For Aph-1a, two splice variants (Aph-1aS and Aph-1aL) have been found which increases the number of assembly variants once more (Shirotani et al., 2004b). It was for instance found that if γ-secretase complexes contain different Aph-1 isoforms, they also produce Aβ fragments of different lengths (Serneels et al., 2009). It is still investigated whether product generation is influenced by different cleavage site preferences of the isoforms.

Several proteins, like CD147 (Zhou et al., 2005), TMP21(Chen et al., 2006), calsenilin (Buxbaum et al., 1998), X11/Mint proteins (Borg et al., 1998) and γ-secretase activating protein (GSAP), were suggested to have γ-secretase activity modulating functions. The 16 kDa GSAP fragment, for instance, was shown to form a complex with the γ-secretase and the CTF of the amyloid precursor protein (APP), thereby affecting the production of Aβ and the APP intracellular domain (AICD). When GSAP was knocked out or the GSAP inhibitor Imatinib was administered to the experimental animals, levels of Notch cleavage stayed unaffected, while Aβ generation was selectively decreased (He et al., 2010) (Chu et al., 2014). This study was supported by the finding that the GSAP SNP rs4727380 is correlated with a higher risk of developing AD (Zhu et al., 2014). However, whether GSAP and its inhibitory drug, Imatinib, really play a role in controlling γ-secretase mediated APP cleavage in humans remains controversial. During a phase IV trial, Imatinib was tested as a treatment against chronic myeloid leukaemia (CML), while its effects on Aβ42 levels in the plasma of patients could simultaneously be determined. After a period of 12 months however, no changes in Aβ

production could be detected, challenging previous results (Olsson et al., 2014). Another protein which has been described as a potential regulator of γ-secretase mediated Notch cleavage is the transcription factor hypoxia induced factor-1a (HIF-1a). Since several years, HIF-1a is known for its role in Notch signaling (Gustafsson et al., 2005; Mukherjee et al., 2011), but it has recently been shown to directly bind the γ-secretase, thereby stimulating its Notch cleaving activity (Villa et al., 2014). The study indicates that hypoxia and HIF-1a activation rapidly turn inactive into active γ-secretase complexes.

While the molecular mechanisms that directly regulate the catalytic activity of the γ-secretase are not clear, it is evident that it can only cleave protein substrates with small ectodomains (Struhl and Adachi, 2000). Thus, membrane proteins with larger ectodomains require ectodomain shedding, before regulated intramembrane proteolysis (RIP) by the γ-secretase can occur. When comparing the phenotypes of A disintegrin and metalloproteinase (ADAM) 10 -/- mice and PS double ($PS1^{-/-}$/$PS2^{-/-}$) -/- mice the resemblances are remarkable. Both are embryonic lethal (E9.5), display defective heart and CNS development, vasculogenesis and somitogenesis; and defective Notch signalling (Donoviel et al., 1999; Hartmann et al., 2002; Herreman et al., 1999). Investigating more mechanisms that control the specificity of sheddase activity would therefore also help to understand γ-secretase regulation.

1.2.3 γ-Secretase substrates in cell adhesion and the function of RIP

Since the discovery of the γ-secretase, many substrates for this protease have been identified. Most substrates are single pass type I transmembrane proteins with an average ectodomain length of slightly below 15 amino acids (after shedding) (Struhl and Adachi, 2000). Despite those mostly applicable parameters, there are exceptions. Beta1,6-N-acetylglucosaminyltransferase V (GnT-V) (Nakahara et al., 2006) and CD74 (Becker-Herman et al., 2005), for instance, are type II transmembrane proteins, and the glutamate receptor subunit 3 (GluR3) is a multipass transmembrane protein (Meyer et al., 2003). It has furthermore been shown that γ-secretase cleavage does not exclusively occur within the transmembrane region. γ-Secretase cleavage mostly starts outside the lipid bilayer at the membrane-cytosol interface and then progressively continues its cleavage in a step-wise manner throughout the transmembrane domain (Chandu et al., 2006; Marambaud et al., 2002; Uemura et al., 2006; Zhao et al., 2007). Regarding γ-secretase cleavage specificity, there have been diverse findings. It has been reported that a valine in the ErbB4 receptor tyrosine kinase (Vidal et al., 2005) and the Notch I receptor (Huppert et al., 2000) TMD is required for adjacent γ-secretase cleavage. Although a similar positioned valine has been found in many other γ-secretase substrates it was shown that in other cases this amino acid is

dispensable (Andersson et al., 2005; Lichtenthaler et al., 1999; Taniguchi et al., 2003). Cleavage by the γ-secretase might also be modulated by clustering of protein substrates via TMD interactions (Asundi and Carey, 1995; Huber et al., 1999; Mendrola et al., 2002; Munter et al., 2007; Yonekura et al., 2006), which can occur, for instance, in the case of RTKs upon ligand binding (Fantl et al., 1993). A large number of γ-secretase substrates beside Eph receptors and ephrins are involved in cell-cell interaction, cell adhesion and migration (Table 2).

For instance, deleted in colorectal cancer (DCC), which is a cell surface receptor for netrin-1, regulates axonal outgrowth and cell migration during development (Moore et al., 2007). Together with other co-receptors DCC has been shown to also regulate chemoattraction (Ly et al., 2008). The full-length DCC protein seems to promote axonal outgrowth, while the released DCC intracellular domain has been found to inhibit this process (Parent et al., 2005). Other examples are E-cadherin-β-catenin complexes and the voltage-gated sodium channel β2 subunit ($Na_V\beta2$). The processing of E-cadherin-β-catenin complexes by γ-secretase cleavage results in disassembly of adherens junctions and thereby inhibits cell adhesion (Ito et al., 1999; Marambaud et al., 2002; Parisiadou et al., 2004). Overexpression of the γ-secretase product $Na_V\beta2$ ICD, in CHO and neuroblastoma cells was associated with increased migration in wound healing assays. Inhibition of the γ-secretase in these cells also led to decreased migration (Kim et al., 2005). In summary, the processing of these proteins by γ-secretase could regulate axonal and cell process retraction, inhibition of cell adhesion and stimulation of cellular migration.

For most ICDs produced by γ-secretase cleavage, no signaling function is apparent. Therefore the γ-secretase is sometimes considered as "the proteasome of the membrane" (Kopan and Ilagan, 2004). Several ICDs translocate to the nucleus, some ICDs have already been proven to modulate gene transcription(Haapasalo and Kovacs, 2011). They contain protein-interaction domains (Georgakopoulos et al., 2006), recognition sites for protein modification, transcription activation domains, and enzymatic activities (Haapasalo and Kovacs, 2011; Kopan and Ilagan, 2004). The ICD derived from CD44 for instance can elevate its own expression by activating promoters that contain a 12-*O*-tetradecanoylphorbol-13-acetate (TPA) responsive element (Okamoto et al., 2001). The CD44 ICD can thereby also regulate MMP-9 expression in cancer cells by binding to a consensus DNA sequence of the MMP-9 promoter region (Miletti-Gonzalez et al., 2012). Furthermore, by targeting the transcription co-activator CBP (cAMP-responsive-element binding protein (CREB) binding protein) for degradation, the N-Cadherin ICD has been found to be able to depress the CREB- dependent transcription (Marambaud et al., 2003). Another prominent example is the Notch ICD (NICD). So far at least 13 proteins have been found to interact or be influenced by the NICD in multiple ways (Andersson et al., 2011), among them are HIF-1a which stabilizes

the NICD and synergizes with it to induce transcription of Notch target genes (Bertout et al., 2009; Gustafsson et al., 2005; Sahlgren et al., 2008) and the nuclear factor of kappa light polypeptide gene enhancer in B-cells 1 (NFκB) which is retained longer in the nucleus upon NICD expression and therefore increases transcription of its target genes (Shin et al., 2006).

In summary, a number of the RIP products generated by the γ-secretase seem to have important functions. However, for most of them a physiological or pathophysiological role remains unclear.

TABLE 2: TYPE I PROTEINS CLEAVED BY Y-SECRETASE INVOLVED IN CELL-CELL INTERACTION, ADHESION AND MIGRATION (DEDUCED FROM (HAAPASALO AND KOVACS, 2011)).

Substrate	Function	Cleavage product	Reference
CD43	Cell-Cell interaction	CD43-ICD	(Andersson et al., 2005; Mambole et al., 2008)
CD44	Cell adhesion, hyaloronan receptor	1.CD44-ICD 2. CD44-β	(Cui et al., 2006; Lammich et al., 2002; Murakami et al., 2003; Okamoto et al., 2001; Pelletier et al., 2006)
CXCL16	Transmembrane chemokine, cell adhesion	Smaller MW CTF	(Schulte et al., 2007)
CX3CL1	Transmembrane chemokine, cell adhesion	Smaller MW CTF	(Schulte et al., 2007)
Desmoglein-2	Structural component of desmosomes; formation of intercellular junctions, regulation of tissue morphogenesis	DSG2-ICD	(Hemming et al., 2008)
Dystroglycan	Member of dystrophin-glycoprotein complex; connects ECM with cytoskeleton	DG ICD	(Hemming et al., 2008)
E-Cadherin	Cell adhesion	E-Cad/CTF2	(Ito et al., 1999; Marambaud et al., 2002; Parisiadou et al., 2004)
Ep-CAM	Transmembrane glycoprotein expressed in human malignancies; cell adhesion	EpICD	(Maetzel et al., 2009)
EphA4	RPTK; regulation of dendritic spines	EphA4-ICD	(Inoue et al., 2009)
EphB2	RPTK; axon guidance, cell morphogenesis, tissue patterning, angiogenesis, synapse formation, LTP	EphB2/CTF2	(Litterst et al., 2007)
ephrin-B1	Cell-Cell interaction	ephrin-B1 ICD	(Tomita et al., 2006)

ephrin-B2	Axon guidance	Ephrin-B2 ICD	(Georgakopoulos et al., 2006)
L1	Cell adhesion, neuronal migration, neurite outgrowth	L1-CTF2	(Maretzky et al., 2005)
N-Cadherin	Cell adhesion, synapse formation and maintenance	N-cad/CTF2	(Marambaud et al., 2003; Uemura et al., 2006)
Na_V-β1	Voltage-gated sodium channel subunit; cell adhesion, synaptic transmission	Not known	(Wong et al., 2005)
Na_V-β2	Voltage-gated sodium channel subunit; cell adhesion, synaptic transmission	β2-ICD	(Kim et al., 2007; Kim et al., 2005)
Na_V-β3	Voltage-gated sodium channel subunit; cell adhesion, synaptic transmission	Not known	(Wong et al., 2005)
Na_V-β4	Voltage-gated sodium channel subunit; cell adhesion, synaptic transmission	Not known	(Wong et al., 2005)
Nectin-1α	Formation of adherens junctions and synapses	NE-ICD	(Kim et al., 2002a)
Protocadherin α4	Cell adhesion	α4-CTF2	(Bonn et al., 2007)
Protocadherin γC3	Cell adhesion	Pcdhγ-CTF2	(Haas et al., 2005; Hambsch et al., 2005)
RPTPκ	RPTP; cell adhesion, synapse formation, learning and memory	RPTPκPIC	(Anders et al., 2006)
RPTPμ	RPTP; cell adhesion, synapse formation, learning and memory	RPTPμPIC	(Anders et al., 2006)
Syndecan-1	HSPG; neurite outgrowth, cell migration, learning and memory	Not known	(Hemming et al., 2008)
Syndecan-2	HSPG; neurite outgrowth, cell migration, learning and memory	Not known	(Hemming et al., 2008)
Syndecan-3	HSPG; neurite outgrowth, cell migration, learning and memory	SICD	(Schulz et al., 2003)
VE-Cadherin	Cell adhesion	Not known	(Marambaud et al., 2002)

1.2.4 The γ-secretase in AD

AD is characterized by dementia, cerebral cortical atrophy, and the combined occurrence of extracellular β-amyloid plaques and intraneuronal neurofibrillar tangles (Buckner et al., 2005; Villemagne and Masters, 2014). The greatest known risk factor for Alzheimer's disease (AD) is age. Most AD patients are diagnosed after the age of 65. Only 5 % of AD patients are younger than 65 at the onset of the disease. These patients, who suffer from early onset Alzheimer's disease (EOAD) have in 30-70 % of the cases PS1 gene mutations (Campion et al., 1999; Cruts and Van Broeckhoven, 1998; Rogaeva et al., 2001), in up to 5 % PS2 gene

mutations (Bird et al., 1988; Finckh et al., 2000; Lleo et al., 2004) and in 10-15 % amyloid precursor protein (APP) mutations (Campion et al., 1999). Thus, about 50 % of EOAD cases can be attributed to mutations in these three genes. Many presenilin mutations are clustered within the transmembrane domains and in the large C-terminal loop of the sixth presenilin TMD (Dries and Yu, 2008). Due to the critical role of PS and of course APP itself in Aβ production, one of the dominant theories in the field is the 'amyloid-cascade hypothesis'. It links pathologic amyloid accumulation with neuronal dysfunction and dementia (Hardy and Higgins, 1992).

Commonly, presenilin and APP mutations result in early deposition of aggregated Aβ in the brain. Surprisingly, conditional complete loss of presenilin also results in neurodegeneration without any Aβ present (Saura et al., 2004). As described above, presenilin and APP mutations only cause the disease in a small fraction of AD patients. However, the fact that mutations in these genes can trigger the onset of AD, suggests that these proteins also play an important role in the etiology and/or progress of LOAD patients.

Furthermore, neuroinflammatory processes have been involved in the etiology and/or progression of AD. Neuroinflammation in AD patients is associated with neuronal damage, increased Aβ generation and cognitive impairment. Whether it is a cause or a consequence of the disease has not been determined. Some animal models suggest that the onset of microglial activation takes place before accumulation of amyloid plaques, while other have stated the opposite (Cagnin et al., 2001; Griffin et al., 1989; Heneka et al., 2005; Okello et al., 2009). As possible cause or consequence of AD, neuroinflammation and therefore also microglial behaviour has become increasingly important to study (Heneka et al., 2015).

1.3 Microglia

Microglia, are the only resident immune cells in the CNS and resemble macrophages in the brain. They are relatively uniformly distributed in the brain, with higher densities in areas like the olfactory telencephalon, the dendate gyrus of the hippocampus, the substantia nigra and portions of the basal ganglia (Lawson et al., 1990; Mittelbronn et al., 2001; Sharaf et al., 2013). Microglia comprise 10-15 % of all glial cells in the CNS and display highly ramified processes and a small cell body under physiological conditions. Even in this 'resting state' they constantly scan and surveil their environment. In 1990, time-lapse microscopy of primary rat microglia identified them as highly dynamic cells, that constantly extend and retract their processes to palpate their environment (Thomas, 1990). Microglia are of myeloid origin and invade the CNS from the yolk sac during embryonic development where they are maintained by self-renewal throughout adult life (Ginhoux et al., 2010; Hashimoto et al., 2013). Initially a broad classification into the M1 and M2 phenotype was used for microglia.

Microglia rather contributing to a more cytotoxic and pro-inflammatory environment were classified as M1 phenotype, while the M2 phenotype was attributed to microglia playing a more neuroprotective role. It is now widely accepted that numerous forms of microglia exist, which have not ultimately been characterized (Cherry et al., 2014). However a rather inflammatory phenotype is triggered by pathogen associated molecular patterns (PAMPs), like lipopolysaccharides (LPS) and pro-inflammatory cytokines, produced by Th1 cells, of which IFNγ is the main constituent (Boche et al., 2013; Colton and Wilcock, 2010; Perry and Teeling, 2013). A rather neuroprotective microglial phenotype is triggered, among other factors, by stimulation with glucocorticoids, IL-10 and IL-4. The latter two can be secreted by Th2 cells, eosinophils and basophils (Martinez and Gordon, 2014). Under physiological conditions, main processes that are regulated by microglia are the phagocytosis of dendritic spines and apoptotic cells during development and in adulthood. Microglia probably contribute to brain plasticity for instance. In 2010, Tremblay et al. found that synapses that were previously contacted by microglia, were pruned more often than those without microglial contact (Tremblay et al., 2010). More recently, microglia were directly identified to phagocytose synapses in the juvenile visual cortex, mediated probably by molecules of the complement system (Schafer et al., 2012). Furthermore, phagocytosis of apoptotic cells and cellular debris, and in some cases even viable cells is one of the most important tasks of microglia, especially during development. In certain brain areas in which cells undergo programmed cell death during rat development, microglia were reported to remove up to 100% of the cells present (Dalmau et al., 2003). In mice, microglia were shown to phagocytose 90% of all cells undergoing apoptosis between the age of one to twelve months (Sierra et al., 2010). As previously mentioned, microglia can also phagocytose viable neurons (Fricker et al., 2012; Neher et al., 2011), their progenitors (Neukomm et al., 2011; Reddien et al., 2001) and other viable cells (Kopatz et al., 2013; Neumann et al., 2008). This process was recently termed 'phagoptosis'. In physiology, this mechanism is used by microglia to kill and remove senescent cells. Phagoptosis also occurs under pathological conditions, i.e. to defend the CNS against invading cells during inflammations (Brown and Neher, 2014).

Microglia in pathology

The spectrum of functions and processes influenced and mediated by microglia under pathological conditions is broad. As the only resident immune cells of the CNS they participate in virtually all neurological diseases. An important function under pathological conditions is the phagocytosis of microbes, including bacteria, yeast and fungi. Although microglial pathogen detection, promotion of inflammation and phagocytosis help to protect the CNS, they can also cause CNS damage. A study by Hoffmann et al. showed that

intrathecal treatment of mice with a TLR-2 agonist resulted in meningeal inflammation and neuronal apoptosis. TLR-2 is expressed nearly exclusively on microglial cells compared to other cells residing in the brain. These results indicate that TLR-2 driven neurodegeneration could possibly be caused by microglia (Hoffmann et al., 2007). In the course of Parkinson's disease (PD), microglia also become highly activated, and produce proinflammatory cytokines, chemokines and reactive oxygen species (ROS)(McGeer et al., 1988) and have been found to engulf degenerating dopaminergic neurons (Barcia et al., 2012), a mechanism which worsens progression of the disease.

On the other hand PD is characterized by loss of dopaminergic neurons in the substantia nigra pars compacta and neuronal accumulation of a-synuclein in cytoplasmic inclusions (Lewy bodies)(Beitz, 2014). The exact contribution of microglia to the progression of the disease is not clear yet, since the CNS of Parkinson's patients may be infiltrated with T-cells (Brochard et al., 2009; Mosley et al., 2012). Microglia may however, scavenge accumulating a-synuclein protein and thereby promote neuronal viability. It was reported that microglial TLR-4 deficiency impaired clearance of a-synuclein in a multiple system atrophy (MSA) mouse model. This clearance deficiency resulted in neuronal cell death, motor dysfunction and increased pro-inflammatory cytokine release (Stefanova et al., 2011), indicating a decelerating effect of microglial function on PD progression.

In Alzheimer's disease (AD) microglial cells are localized around Aβ plaques, which are one of the main neuropathological hallmarks of AD. So far, like in the case for other CNS diseases involving microglia, there is dissension whether microglia play a protective or a destructive role in the Alzheimer's brain. In the early stages of the disease they might phagocytose aggregated Aβ molecules effectively and thereby slow down its harmful consequences. However, at later stages activated microglia can participate in a form of chronic neuroinflammation, in which they constantly secrete cytokines, neurotoxins and proteases which induce or at least contribute to neurodegenerative changes in the Alzheimer's brain (Akiyama et al., 2000; McGeer and McGeer, 2004). It has been suggested that ageing and/or this chronic neuroinflammatory environment may alter the microglial state of activation. Apart from age dependent microglial changes, the numerous forms of activated microglia that exist remain to be characterized in more detail (Minghetti, 2005; Streit et al., 2008). Hence, their significance in the etiology and their targeting for a possible treatment of AD, remains debatable (Streit, 2004).

In 2013, a genome wide association study published by Guerreiro et al. demonstrated a genetic correlation between the occurrence of LOAD and the R47H mutation of the triggering receptor expressed on myeloid cells 2 (Trem2) (Guerreiro et al., 2013; Jonsson et al., 2013). There are still various findings about Trem2 expression patterns. However many publications state that Trem2 is expressed on microglia under physiological and/or under

pathological conditions (Hickman et al., 2013; Jay et al., 2015; Lue et al., 2015; Sessa et al., 2004; Thrash et al., 2009). Interestingly, loss of function mutations of Trem2 and its co-receptor DAP12, result in a phagocytic system disease, termed Nasu-Hakola or polycystic lipomembranous osteodysplasia with sclerosing leukoencephalopathy (PLOSL) (Paloneva et al., 2002), in which patients display dementia (Bianchin et al., 2004). These results support the hypothesis that microglia play an important role in the etiology of LOAD.

1.3.1 Microglial migration

In 1999, Dailey et al. observed that microglia were capable of phagocytosing dead cells on hippocampal slice cultures. They saw that these microglia transformed from highly ramified cells into an amoeboid cell type, first retracting their processes and then extending dynamic protrusions, followed by cellular movement (Dailey and Waite, 1999; Stence et al., 2001). When brain tissue is damaged, degenerated neurons release several signaling molecules, like cytokines, nucleotides and chemokines, to recruit microglia. The microglial stages of activation can be assigned into 'find-me' and 'eat-me' signals (Ravichandran, 2011). Lipid lysophosphatidylcholine (LPC) (Lauber et al., 2003), sphingosine 1-phosphate (S1P) (Gude et al., 2008), the fractalkine CX3CL1 (Truman et al., 2008), and the nucleotides ATP and UTP (Elliott et al., 2009), are well known find-me signals. Microglia possess several purinergic receptors, like P2Y6, P2Y12 and P2X4, which, upon activation, can stimulate microglial process extension, migration and phagocytosis. Inhibiting those receptors also negatively affects microglial migration.

The fractalkine CX3CL1 can be released by neurons as a soluble 60 kDa fragment, in a caspase dependent manner. This fragment can act as a chemoattractant for microglia, which in comparison to other CNS cell types almost exclusively express the CX3CL1 receptor (CX3CR1) (Cardona et al., 2006; Lee et al., 2010). Therefore, it is not surprising that CX3CR1 knock out mice produce microglia and macrophages which display dysfunctional migration (Truman et al., 2008) and that in animal models of neurodegenerative diseases the CX3CR1 knock out induces neuronal cell death (Cardona et al., 2006; Pabon et al., 2011). It was also reported that neurons generate interleukin-34 (IL-34) in order to communicate with microglia and stimulate their migration (Mizuno et al., 2011). The IL-34 receptor, termed colony-stimulating factor 1 receptor (CSF1R), is primarily expressed by microglia. These examples indicate how crosstalk between neurons and microglia is established and shows the importance of find-me signals in the brain. Once the phagocytes have followed the 'find-me' signal and are in proximity of a non-viable and/or damaged cell, they recognize it by 'eat-me' signals. Eat me signals are localized on the outer leaflet of the apoptotic cell and include high amounts of phosphatidylserine (PtdSer), alteration of intercellular adhesion

molecule-1 (ICAM-1) epitopes, changes in charge and glycosylation patterns on the cell surface and exposure of the endoplasmatic reticulum (ER)-resident protein calreticulin (Ravichandran, 2011).

Notably, γ-secretase also has been implicated in microglial function. Although for other cells PS1 has been shown to be the predominantly occurring catalytical variant in the γ-secretase complex, Jayadef et al. and Farfara et al. showed that loss of PS2 rather than loss of PS1 activity impairs microglial function. In those studies PS2 knock out led to increased cytokine secretion and decreased migratory behaviour during microglial responses (Farfara et al., 2011; Jayadev et al., 2010).

Key components of microglial migration: podosomes

In order to adhere to a substrate or to move its body, a cell needs to transfer intracellular forces to the ECM. This occurs via transmembrane proteins, such as integrins, which can extracellularly connect to the ECM and intracellularly to adapter proteins and the cytoskeleton. Depending on the cellular function and cell type, these connections can be differently assembled. Under physiological conditions many cell types express structures termed focal complexes and adhesion sites (FAS), which have a dash-like appearance and are enriched in proteins such as talin, paxillin and vinculin (Zamir and Geiger, 2001). Some cells, like osteoclasts (Zambonin-Zallone et al., 1988), macrophages (Lehto et al., 1982; Linder et al., 1999), dendritic cells (Burns et al., 2001) and endothelial cells (Burgstaller and Gimona, 2005), however, express podosomes instead. These structures are also called invadopodia in cells associated with pathological conditions, due to their invasive properties, for example when being expressed by invasive human cancer cell lines. Podosomes are dot-like contacts that have an F-actin core that is surrounded by a ring structure consisting of adhesion and scaffolding proteins, like talin and vinculin (Linder and Aepfelbacher, 2003) (Figure 5). Despite the different shape and size, the composition of FAS and podosomes seems to be largely similar, with a few exceptions (Block et al., 2008; Wernimont et al., 2008). Moreover, these structures contain multiple proteinases, like MMP-2 (Osiak et al., 2005) and MMP-9 (Sato et al., 1997), which can modulate the ECM, enabling podosome containing cells to move through dense tissue (Linder and Kopp, 2005). Proteins that have been identified in podosomal structures, include actin nucleators (Arp2/3, formins), polymerization activators (cortactin, coronin, WIP and Wiskott-Aldrich Syndrome proteins WASp and N-WASp), actin binders (tropomyosin, coronin), filament crosslinkers (a-actinin, caldesmon), adhesion molecules (vinculin, zyxin) and kinases (Abl, Src, Pyk2/FAK) (Gimona et al., 2008). A signaling cascade involving Cdc42, (neural) Wiskott–Aldrich syndrome protein ((N-)WASP) and the Arp2/3 complex plays a crucial role in the formation of podosomes and actin filaments (Linder and Aepfelbacher, 2003).

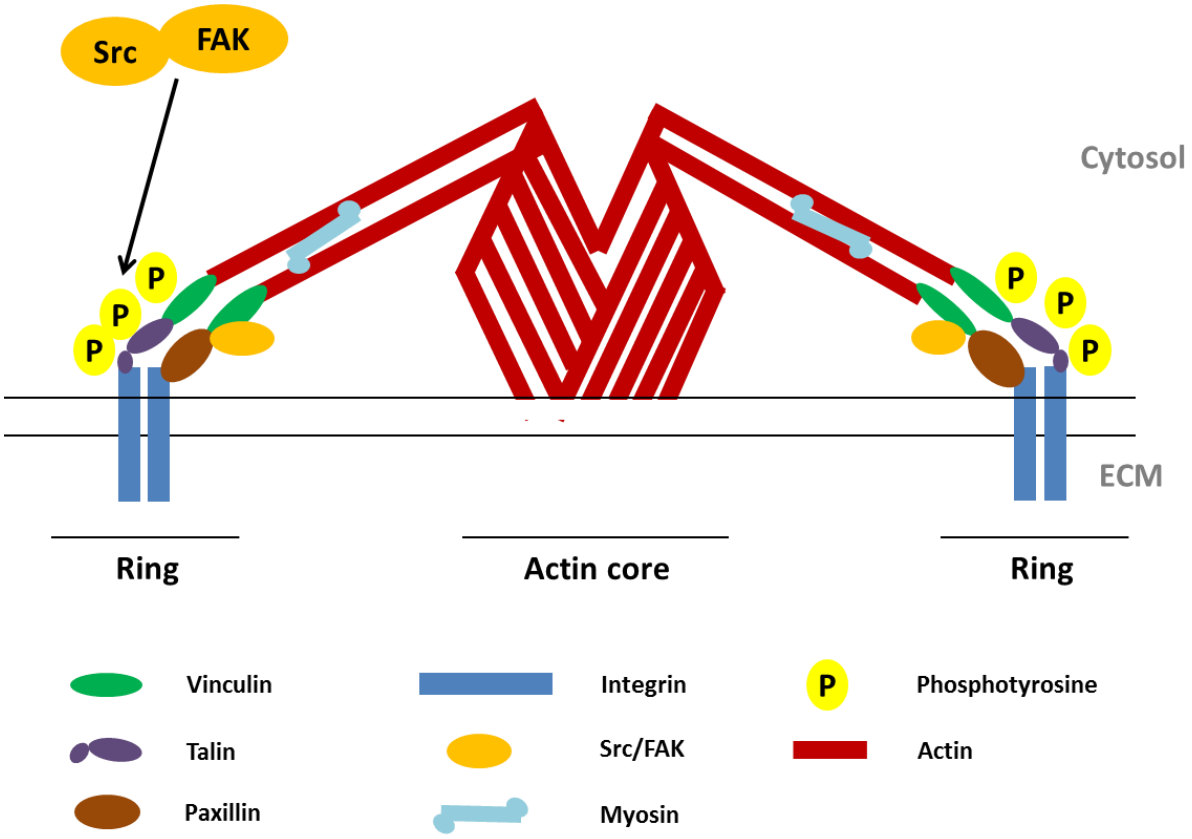

Figure 5: Podosomal structure and components.
Podosomes consist of an F-actin core surrounded by a ring structure, consisting of highly tyrosine phosphorylated adhesion and scaffolding proteins. The ring structure is connected to the ECM by transmembrane receptors like the integrin heterodimers. Src and FAK, which can also integrate into the podosomal ring structure, are known as the main kinases which phosphorylate tyrosine residues of podosomal proteins. Scheme deduced from (van den Dries et al., 2013).

Assembly of podosomes involves tyrosine phosphorylation of most podosomal proteins. The main kinases responsible for the phosphorylation in podosomes are Src and FAK (also known as Pyk2). Interestingly, it has been reported that the mere presence but not the activity of these kinases is sufficient for podosome assembly. Their activity rather seems to be crucial for podosomal disassembly. Inactive FAK and Src leads to strong adhesion and thus, low motility of cells (Ilic et al., 1995; Kaplan et al., 1994). Upon kinase activation they initiate podosomal remodelling, which is a prerequisite for cell migration. Calpain, which is another important player of podosomal disassembly, cleaves podosomal components, such as WASP, FAK and Talin1 (Calle et al., 2006; Chan et al., 2010; Franco et al., 2004) and thereby also promotes cell movement.

1.4 Rationale and aim of the study

The Eph-ephrin system is known to play important roles during development and adulthood. It is associated with the regulation of cellular adhesion and migration. So far, mainly regulation and effects of Eph forward signaling have been investigated. Although downstream targets of ephrin-B reverse signaling have been less investigated, it is known that reverse signaling can stimulate proteins like Src and Grb4 and thereby endothelial sprouting and cell repulsion (Georgakopoulos et al., 2006). In previous studies, the γ-secretase complex was revealed to be involved in ephrin-B1 as well as ephrin-B2 processing in MEF and HEK293 cells (Georgakopoulos et al., 2006; Tomita et al., 2006). Additionally, deletion of PS1 and/or a PS1/2 double knock out was demonstrated to disrupt FAS in fibroblasts. Interestingly, they could be rescued by overexpressing the γ-secretase product ephrin-B2 ICD (Waschbusch et al., 2009).

The interest in microglia has increased in recent years, due to the fact that many diseases, including AD, are believed to be strongly affected by neuroinflammation. Therefore, the overall goal of this project was to characterize the role of γ-secretase and ephrin-B in microglial migration.

To this end, we aimed to generate a microglial cell model, expressing different PS and ephrin-B2 constructs. Embryonic stem cell derived microglial precursor cells (ESdM) were used for most of our analyses. These cells stably proliferate, have not been oncogenically transformed and have most characteristics of primary microglia (Napoli et al., 2009). For stable target gene expression, a lentiviral transduction system was established. The influence of γ-secretase inhibition on ephrin-B2 signaling was investigated by a pharmacological as well as a genetic approach. Moreover, intracellular ephrin-B2 dependent signaling pathways were analyzed and characterized. An additional important objective was to assess the functional relevance of γ-secretase and ephrin-B2 by structural analysis of cell adhesion and migration assays.

2. Materials and Methods

Chemicals used in the following experiments were purchased in purity grade "per analysi" from Sigma-Aldrich (Steinheim, Germany), LifeTechnologies (Frankfurt, Germany) Roche (Basel, Switzerland), Roth (Karlsruhe, Germany), Applichem (Darmstadt, Germany), Tocris/R&D Systems (Wiesbaden-Nordenstadt, Germany), Cayman Chemicals (Ann Arbor, USA) or SantaCruz Biotechnology (SantaCruz, USA). Cell culture media and buffers were purchased from LifeTechnologies (Frankfurt, Germany). Exceptions are stated in the respective experiment descriptions. For a list of used equipment see Table 3.

TABLE 3: LABORATORY EQUIPMENT

Equipment	Company
-80°C Freezer	Thermo Scientific
37°C CO2 Incubator	Binder
Cell culture clean bench	Thermo Scientific
Centrifuge (5804)	Eppendorf
Water bath	Medigen
SDS PAGE chamber	Höfer
Xcell SureLock Mini-Cell	Life technologies
Xcell 4 SureLock MidiCell	Life technolgies
Western Blotting chamber	Höfer
Cooling System (E100)	Lauda
Chemiluminescence Imager (ChemiDoc XRS) with Analysis Software Quantity One	Bio-Rad
Licor Infrared Imager (Odyssey CLx) with Analysis Software Image Studio 3.1	LiCor
PCR Cycler	Eppendorf
DNA-electrophoresis chamber	Amersham
7300 Real-Time PCR System	Applied Biosystems
TransUV illuminator (GVM 20)	Syngene

Implen Nano-Spectrophotometer P-class	Implen
Microcentrifuge (5415R)	Eppendorf
Centrifuge (5804R)	Eppendorf
Centrifuge (5804)	Eppendorf
Autoclave	H+P
Heating block	Stuard Scientific
Thermomixer (compact)	Eppendorf
Magnetic stirrer	Velp Scientifica
pH meter (MP225)	Mettler Toledo
Photometer (Genesis)	Thermo Scientific
Vortex (MS2 Minishaker)	IKA
Analytical Balance (Labstyle 204)	Mettler Toledo
Microtiterplate Reader (Multiskan RC)	Thermo Scientific
Fluorescence microscope (AxioVert 200) with ZEN 2 analysis Software	Zeiss
Nikon eclipse Ti with NIS-elements Software	Nikon

2.1 Molecular biological techniques

2.1.1 Polymerase chain reaction (PCR)

Template DNA encoding ephrin-B2 sequences used for this project, were a kind gift of Dr. Bernd Hoffmann. In order to subclone the constructs into lentiviral vectors, they were first amplified by PCR (Table 4, Table 5). For this, a master mix containing the following components was used:

10x Pfu buffer + 20 mM MgSO4	5 µl
dNTP mix, 10 mM each	1 µl
Forward Primer	0.5-1 µM
Reverse Primer	0.5-1 µM
Template DNA	10-100 ng
Pfu Polymerase	1 µl
H2O	to 50 µl

During the PCR program, DNA strands were denatured, primers were annealed at temperatures indicated in Table 5, and finally, elongated (Table 4, 2 minutes /kilo base), to create a new DNA strand. Then, program steps 2-4 were repeated 29 times until step 5 was started.

1. Initial denaturation of DNA	95°C, 5 minutes
2. Denaturation of DNA	95°C, 0.5 minutes
3. Annealing of primers	varying °C, 0.5 minutes
4. Elongation of primers	72°C, 2 minutes/kilo base
5. Final elongation	72°C, 5 minutes

TABLE 4: SPECIFICATION OF CONSTRUCTS USED FOR LENTIVIRAL TRANSDUCTION

Name of construct	NCBI accession number	CDS bp position (beginning-end)	Length of insert (bp)
Ephrin-B2 ICD myc	NM_004093.3	825-1075	264
Ephrin-B2 CTF myc	NM_004093.3	703-1075	372
Ephrin-B2 FL myc	NM_004093.3	1-1075	1041

TABLE 5: CLONING PRIMERS

Name	Primer Sequence	Annealing temp (Tm)
Ephrin-B2 ICD myc	**Fw:** ttt gga tcc atg aag tac cgg agg aga cac agg **Rv:** ccg acg cgt tca cag atc ctc ttc tga gat gag ttt ttg ttc gac ctt gta gta aat gtt	58°C
Ephrin-B2 CTF myc	**Fw:** ttt gcg gcc gc taa tac gac tca cta tag gg **Rv:** ccg acg cgt tca cag atc ctc ttc tga gat gag ttt ttg ttc gac ctt gta gta aat gtt	55°C
Ephrin-B2 FL myc	**Fw:** ttt gga tcc atg gct gtg aga agg gac tcc gtg tgg **Rv:** ccg acg cgt tca cag atc ctc ttc tga gat gag ttt ttg ttc gac ctt gta gta aat gtt	60°C

2.1.2 Separation and purification of DNA fragments

In order to separate the amplified DNA fragments from the template vectors, the PCR reaction mix was supplemented with OrangeG loading dye, and loaded on a gel consisting of 1 % agarose in TBE buffer, containing 2 µl GelRed/100 mL. The gel was run at 120 V, for 45 minutes in TBE buffer. Thereafter, DNA bands were visualized via UV light, cut out of the gel and DNA was purified using the Wizard®SV Gel and PCR Clean up system (Promega) and dissolved in H_2O.

TBE buffer
9 mM Tris-Borate, 2 mM EDTA, dH_2O, pH 8.0
6x OrangeG loading dye
60 % Glycerin, 0.15 % Orange G, 60 mM EDTA, 10 mM Tris, dH_2O, pH 7.6
GelRed (Biotium Inc.)
1:10.000

2.1.3 DNA restriction and dephosphorylation

Purified DNA fragment inserts and the lentiviral plasmid (pLVX-EF1a) were digested by the appropriate restriction enzymes (Table 6) for 3 h at 37°C. The lentiviral vector pLVX-EF1a, which contains a puromycin resistance gene, allows for selective culturing of cells. The vector furthermore contains an EF1a promoter and therefore constitutively overexpresses inserted genes. After digestion the linearized DNA was dephosphorylated by adding 1 U of FastAP thermosensitive alkaline phosphatase for 20 minutes at 37°C to the restriction mixture.

TABLE 6: ENZYMES USED FOR RESTRICTION DIGESTION (THERMO SCIENTIFIC)

DNA	Restriction enzymes	Restriction buffer
Ephrin-B2 ICD myc	BamHI, MluI	BamHI buffer
Ephrin-B2 CTF myc	NotI, MluI	Orange buffer
Ephrin-B2 FL myc	BamHI, MluI	BamHI buffer
pLVX-EF1a	BamHI, MluI	BamHI buffer
pLVX-EF1a	NotI, MluI	Orange buffer

2.1.4 DNA ligation

Linearized and dephosphorylated DNA plasmids and inserts were separated and purified like previously described in 2.1.2. Consecutively, backbone and insert were mixed in a 1:3 molar ratio and the bacteriophage T4 ligase and its buffer were added. After 1 h incubation of the ligation mix at room temperature, T4 ligase was inactivated at 65°C for 10 minutes.

2.1.5 Generation of chemically competent *E.coli* (Top 10)

For generation of chemically competent *E. coli*, 5 mL LB medium were inoculated with Top 10 *E.coli* and grown overnight at a rotation speed of 210 rpm at 37°C. On the next day, the preculture was used to inoculate 200 mL of LB medium with an optical density (OD) of 0.1 (measured at 600 nm). The culture was grown until it reached an OD of 0.5 and was then chilled at 4°C for 15 minutes. Then, the culture was centrifuged for 10 minutes at 4000xg at 4°C, the supernatant was discarded and the bacteria pellet was resuspended in 80 mL TfBI

on ice. After 15 minutes, bacteria were pelleted again, resuspended in 8 mL TfBII and again incubated on ice for 15 minutes. Subsequently, they were aliquoted, shock frozen in liquid nitrogen, and stored at -80°C.

Transformation buffer I (TFB I)
100 mM RbCl, 50 mM $MnCl_2$, 30 mM potassium acetate, 10 mM $CaCl_2$, 15 % Glycerol, pH 5.8
Transformation buffer II (TFB II)
10 mM MOPS, 10 mM RbCl, 75 mM $CaCl_2$, 15 % Glycerol, pH 6.8
Low salt Lauria-Bertani (LB) medium
1 % tryptone, 0.5 % yeast extract, 0.5 % NaCl, dH_2O, pH 7.0 (autoclaved)

2.1.6 Transformation of *E.coli* (Top10) and *E.coli* colony screen

In order to transform the chemically competent *E.coli*, bacteria were thawed and then incubated with the pre-cooled lentiviral DNA vectors on ice for 20 minutes. For DNA uptake, a 45 second heat shock at 42°C was performed. After incubation on ice for 2 minutes, 1 mL Soc medium was added and bacteria were rotated at 750 rpm for 1 h at 37°C. Then, bacteria were pelleted, resuspended in 50 µl Soc medium, and were then plated onto an agar plate containing ampicillin over night at 37 °C. Following overnight incubation, the different colonies were screened for positive clones. For this, wells of a 96 well plate were filled with 200 µl Soc medium with ampicillin. Then colonies were picked and each well was inoculated with a different colony and incubated at 37 °C for 3 h. In order to identify positive clones, 0.5 µl of bacteria containing Soc medium was used as template for an ephrin-B2 PCR (2.1.1). Positive clones were sequenced by an external company to control for mutations.

Super optimal broth with catabolite repression (SOC) medium
0.5 % yeast extract, 2 % tryptone, 10 mM NaCl, 2.5 mM KCl, 20 mM $MgSO_4$, 20 mM glucose
LB agar plates
1 % tryptone, 0.5% yeast extract, 0.5% NaCl, 15 g/l agar, dH_2O, pH 7.0 (autoclaved); before pouring the plates the antibiotics were added to the warm (~ 40-50 °C) solution.
Selection antibiotics
Ampicillin: 100 µg/ml (Stock: 100 mg/ml, dH_2O)

2.1.7 Cryo conservation of transformed *E.coli*

Overnight grown bacterial suspensions were mixed with sterile glycerol and frozen at -80°C. For re-usage, a sterile tip was used to scratch off 1 µl of the glycerol stock, which was then grown overnight in 4 mL antibiotic containing LB medium at a rotational speed of 210 rpm at 37°C.

Conservation medium
25 %: Glycerol, dH_2O (sterile filtered, pore size: 0.2 µm), 75 %: bacterial suspension

2.1.8 Purification of plasmid DNA from *E.coli*

For purification of DNA from *E.coli* bacterial cultures of 50-250 mL, the NucleobondExtra Midi Kit (Macherey&Nagel) was used. For DNA purification of up to 5 mL cultures the NucleoSpin Plasmid Kit (Macherey & Nagel) was used. Briefly, cells were pelleted, resuspended and incubated with a lysis and a neutralization buffer. Then, then suspension was cleared from cell debris by centrifugation and DNA containing supernatant was loaded to a DNA binding column. After washing the DNA it was precipitated by isopropanol and washed with 70 % ethanol. The ethanol was removed and the pellet was air dried, and finally dissolved in DNase free H_2O.

2.1.9 RNA isolation from eukaryotic cells

Prior to RNA isolation, cells were washed with Phosphate buffered saline (PBS), pelleted and stored on ice until further use. For RNA isolation from ≤ $3x10^5$ cells the RNeasy Micro Kit was used; for ≥ $4x\ 10^5$ cells the RNeasy Mini Kit was used. Briefly, cells were disrupted by adding a lysis buffer containing RNase inhibitors, were consecutively homogenized by passing the lysate 5 times through a 20 Gauge needle, and were finally loaded onto an RNA binding column. After the RNA binding, the column was washed and RNA was finally eluted in RNase free H_2O. Until further use, RNA was stored at -80°C.

2.1.10 DNA digestion and reverse transcription (RT)-PCR

In order to remove endogenous DNA from the eluted RNA (2.2.9), the RNA was incubated with DNase I and the respective buffer (New England BioLabs) for 20 minutes at 37°C. DNase I heat inactivation was done at 75°C for 10 minutes. Next, cDNA was transcribed from isolated RNA by using the RevertAid First Strand cDNA Synthesis Kit (Thermo Scientific). For this purpose, the RNA was incubated with hexameric primers, an RNase inhibitor, mixed dNTPs, the reverse transcriptase and its buffer for 1 h at 42°C. The mixture was inactivated at 70 °C for 15 minutes. In case of storage cDNA was kept at -80°C.

2.1.11 Photometric determination of DNA concentration

In order to determine concentration and purity of the dissolved nucleic acids, 0.5-2 µl of sample were loaded onto the Nanophotometer 330 (Implen). Nucleic acids were measured at 260 nm. By determining the 260/280 ratio, protein contamination of the samples was assessed. In case of RNA, this value had to be ≥ 2.0, in case of DNA ≥ 1.8. Furthermore the 260/230 ratio was assessed to control for impurities caused by buffer salts. Both RNA and DNA values had to be ≥ 2.0 for further use.

2.1.12 Analysis of gene expression by qPCR

Gene expression of cells was analyzed by qPCR using a 7300 Real-Time PCR System (Applied Biosystems). Firstly, a primer master mix containing primers (Table 7) as well as the Sybr Green PCR Master Mix (Applied Biosystems) was prepared. Secondly, a cDNA template master mix, containing the cDNA (2.1.9 and 2.1.10) and DNase free H_2O was prepared. Sybr Green is an asymmetric cyanine dye, which binds to double stranded DNA. The DNA-dye complex emits light at ~520 nm, which can be detected by the Real time PCR system. To control for volume fluctuations between wells, the Rox reference dye was used. It stays unaffected during the qPCR and is a measure for the amount of master mix that was initially added to each well. In order to analyze the amount of DNA generated during the reaction, a cycle threshold (C_t) was set automatically. The C_t is the threshold at which the fluorescence passes a certain level, above baseline and below exponential growth. If a gene displays a comparatively low C_t, only a relatively small number of cycles was necessary to generate enough DNA to pass the fluorescence threshold, meaning that the initial cDNA template concentration and cellular mRNA expression was relatively high. To calculate the relative gene expression, the C_t values of the target genes were normalized to two reference genes (LDH and GAPDH, Table 7) and relative expression ($2^{-\Delta\Delta C_t}$) was calculated.

TABLE 7: LIST OF Q-PCR PRIMERS USED

Gene	Ref number (Qiagen)	Amplicon length
Mm_Capn1_1	QT00112168	76 bp
Mm_Capn2_1	QT00106876	88 bp
Mm_Ptk2_1	QT01059891	98 bp
Mm_Pxn_1	QT01070041	129 bp
Mm_Tln1_1	QT00142107	112 bp
Mm_Tln2_2	QT01057091	74 bp
Mm_GAPDH	QT01658692	144 bp
Mm_LDHA	QT02325414	88 bp
Mm_EfnB1	QT00251244	138 bp
Mm_EfnB2	QT00139202	124 bp
Mm_EfnB3	QT01659112	143 bp

2.2 Cell biological techniques

2.2.1 Cell Culture

HEK293FT cells were kind gift of Prof. Oliver Brüstle (Bonn university). Cells were maintained in Dulbecco´s Modified Eagle´s Medium (DMEM) GlutamaxTM containing 4.5 g/l D-glucose supplemented with 10 % fetal bovine serum (FCS, PAN) and 1 % Penicillin/Streptomycin solution (100 U/ml Penicillin, 100 µg/ml Streptomycin, ThermoFisher Scientific).

ESdM cells were maintained in DMEM F-12 containing 1× N2 supplement, 0.48 mM L-glutamine, 5.3 µg ml−1 D-glucose, HEPES and 1 % Penicillin/Streptomycin solution (100 U/ml Penicillin, 100 µg/ml Streptomycin) [29] at 37°C, 95 %. For passaging, cells were scraped manually and collected with a cell scraper.

Murine primary microglia

Microglia were isolated from C57BL/6 mice and kindly provided by Prof. Michael Heneka (University of Bonn). Following co-cultivation with primary astrocytes, microglia were maintained in Dulbecco´s Modified Eagle´s Medium (DMEM) GlutamaxTM containing 4.5 g/l D-glucose supplemented with 10 % Fetal bovine serum (FCS, PAN) and 1 % Penicillin Streptomycin solution (100 U/ml Penicillin, 100 µg/ml Streptomycin).

2.2.2 Generation of lentiviral particles

2-2.5 x 10^6 HEK 293 FT cells were split onto 15 cm dishes coated with poly-Ornithine and cultured for 16 h. Conditioned medium was replaced by fresh DMEM +/+ and cells were incubated with 25 µM Chloroquine (Sigma-Aldrich) for 5 minutes. Then, HEK293FT cells were co-transfected with the lentiviral plasmid encoding the respective gene, the packaging plasmid Pax2 and the envelope plasmid pMD2.G using 0.25 M CaCl2 and 2x HBS buffer as transfection reagent. After 10-16 hours of incubation, cells were washed with medium and fresh medium was added to the cells. After 24 h medium was renewed and the old medium was kept at 4°C until centrifugation. 24 h cell incubation and medium collection was repeated once and the cells were discarded. The collected supernatants were combined and centrifuged at 4000xg for 5 minutes at 4°C before being filtered through a sterile SFCA membrane (pore size: 0.45 µm, Corning Inc.). After that a polyethylene glycol 6000 (PEG 6000) buffer was prepared according to Kutner et al. (Kutner et al., 2009). The suspension was incubated for 1.5 h at 4°C and was mixed every 20 minutes. It was then centrifuged for 30 minutes at 4000xg. After removing the supernatant the pellet was resuspended in virus freezing medium and was kept at -80°C until further use.

2x HBS buffer
280 mM NaCl, 10 mM KCl, 1.5 mM Na2HPO4, 50 mM Hepes, 12 mM Glucose; pH 7.00
PEG 6000 buffer
68.4% filtered viral supernatant, 8.5% PEG 6000, 0.3 M sodium chloride and 7.76 % PBS
Virus freezing medium
2x HBS buffer, 1 % bovine serum albumine

2.2.3 Transduction of cells with lentiviral particles and selection

To transduce cells, viral particles were applied to a 3.5 cm dish with 1.6 x 10^5 ESdM cells. ESdM cells were incubated 14-16 h with the lentiviral particles. Thereafter, cells were washed twice with DMEM F-12 and fresh medium was added to the cells. Cells were selected in DMEM F-12 containing 2 µg Puromycin for ~9 days. Overexpression of the transduced constructs was tested by immunocytochemical stainings and Western immunoblotting.

2.2.4 Transfection of cells with siRNA

EfnB2 siRNA (100 pmol in water, Flexitube SI00990535, Qiagen) or control siRNA (100 pmol in water, Flexitube , Qiagen) were pipetted into wells of a 24 well plate. To each well 5 µl HiPerFect (Qiagen) and 95 µl Optimem (Life Technologies) were added and incubated for 5-10 minutes. 5.5 x 10^4 cells in 200 µl DMEM F-12 were added to each well. The cells and transfection reagents were incubated for 3 h, followed by addition of 200 µl of DMEM F-12 (see 2.2.1). After incubation over night the medium was changed and cells were cultured for further 72 h before further analysis.

2.2.5 In-Cell Western Assay

Cells were seeded at 80% confluence and cultured overnight in a 96 well dish under previously described conditions (see 2.2.1). Cells were either treated with DMSO (Roth) or 10 µM DAPT for 24 h. 16 h prior to receptor treatment, cells were cultivated in DMEM F-12 without supplements. Then, two master mixes were prepared containing either Optimem with Ctrl Fc (23.53 nM, 110-HG-100, R&D Systems) or containing EphB1 receptor (23.53 nM, 1596-B1-200, R&D Systems). 50 µl of each solution were pipetted in triplicates into the wells for indicated times. Treatment was terminated by addition of 50 µl 4% paraformaldehyde (PFA) solution. All steps following were performed at RT. Cells were permeabilzed for 10 minutes, incubated with blocking solution for 1 h and then with primary antibodies for 1 h (Table 9). Following antibody incubation, cells were washed 3 times and incubated with secondary antibodies (Table 10) for 1 h. After 3 additional washing steps, TBS without additives was added to the wells for detection. Plate images were taken using the Odyssey CLx (Licor) and Image studio software with the following settings:

Resolution : 169 µm

Quality: High Quality

Focus: 4 mm

4 % Paraformaldehyde (PFA) solution
4% PFA, Tris buffered saline (TBS)
Permeabilization solution
0.25 % Triton-X 100 (Roth), TBS
Blocking solution
Licor blocking solution, TBS (1:1)
Antibody solution
Blocking solution: TBS (1:5), primary antibodies
Washing solution
0.125% Triton-X 100, TBS

2.2.6 Immunocytochemistry and Total Internal Reflection Fluorescence (TIRF) microscopy

For fluorescent imaging, cells were seeded onto 35 mm µ-dishes (Ibidi treat, Ibidi) at 40 % confluence at least 16 h prior to staining procedure. All following steps were performed at room temperature. Next, cells were washed once with PBS and were then incubated with 4 % PFA in TBS for 10 minutes. Thereafter, cells were permeabilized for 10 minutes and then incubated with blocking solution for 1 h. Following blocking, cells were incubated with the primary antibody solution (Table 9) for 1 h, washed 3 times and consecutively incubated with secondary antibodies (Table 10), Fluoresceinyl-aminomethyldithiolano-phalloidin (Phalloidin) and 4',6-Diamidin-2-phenylindol (DAPI) for 1 h. After three additional washing steps, TBS without additives was added to the dish for TIRF imaging. The TIRF technique allows to image ≤ 200 nm thin layers at the specimen surface and is therefore highly suitable for the analysis of protein complexes located at the plasma membrane, like podosomes. By an evanescent wave, which is able to excite fluorophores which are adjacent to a glass-water interface, a very specific region can be imaged, without interference of background signals. The evanescent wave is generated when the incident light is totally internally reflected at the glass water interface. For this study, a Nikon eclipse Ti fluorescence microscope with a x 100 apochromat objective and an EM-CCD camera iXon DU879 (Andor, Oxford) was used. Software: NIS-elements.

Blocking solution
5 % Bovine serum albumin (BSA) (Roth), PhosSTOP (Roche), in washing solution (2.2.4)
Antibody solution
1 % Bovine serum albumin (BSA) (Roth), Washing solution (2.2.4), primary/secondary antibodies

2.3 Protein biochemical techniques

2.3.1 Preparation of cell lysates

To obtain whole cell lysates, cells were grown to a confluence of 70-80 %. They were scraped off the dish, pelleted, washed with PBS, pelleted again, and were frozen at -80°C until further use. For protein extraction, they were thawed and incubated 15 minutes with STEN lysis buffer containing protease inhibitor (PI) and 1 mM dithiothreitol (dTT) on ice. Lysates were homogenized by passing cells 20 times through a 20 Gauge needle. Then, lysates were centrifuged for 15 minutes at 16100xg at 4°C. The supernatant was used for further analysis.

Phosphate Buffered Saline (PBS)
140 mM NaCl, 10 mM Na_2HPO_4, 1.75 mM KH_2PO_4, dH_2O, pH 7.4
Hypoton buffer:
10 mM Tris, 1 mM EDTA, 1 mM EGTA, dH_2O, pH 7.6
STEN lysis buffer:
50 mM Tris, 150 mM NaCl, 2 mM EDTA, 1 % NP40 (Sigma-Aldrich), 1 % Triton X-100 (Sigma-Aldrich), dH_2O, pH 7.4
25 x Protease inhibitor (PI) cocktail
1 Complete (Roche) tablet, 1 mL dH_2O

2.3.2 Cell fractionation

To separate membrane, cytosolic and nuclear fractions, cells were washed with PBS, and pelleted by centrifugation. 50 µl of hypotonic buffer containing PI and 1 mM dTT were added to the pellet. All steps hereafter were performed at 0-4°C, all buffers contained PI and 1 mM dTT. After 15 minutes of incubation, cells were homogenized by passing them 20 times through a 20 Gauge needle and centrifuged for 5 minutes at 2000xg. The resultant supernatant 1 contained cellular membranes and cytosol, whilst the pellet 1 contained the nuclear fraction.

The supernatant 1 was further centrifuged for 1 h at 16100xg, the pellet 1 containing nuclear proteins was resuspended in 30 µl buffer C and incubated for 15 minutes. It was then centrifuged for 15 minutes at 16100xg. The nuclear protein supernatant was used for nuclear protein analysis.

After separation of membrane and cytosolic proteins out of the supernatant 1, the cytosolic proteins in the supernatant 2 were used for analysis. The membrane proteins contained in the pellet 2 were resuspended and incubated in 30 µl STEN lysis buffer for 15 minutes, in order to separate them from lipids. After that, this fraction was centrifuged at 16100xg for 15 minutes, and the supernatant contained the membrane proteins.

Hypotonic buffer
10 mM Tris (pH 7.5), 10 mM NaCl, 0.1 mM EGTA
STEN-lysis buffer
(2.3.1)
Buffer C
25 % Glycerol, 20 mM HEPES (pH 7.9), 0.5 M NaCl, 1 mM EGTA, 1 mM EDTA (pH 8.0), 25 mM β-Glycerophosphate

2.3.3 Protein estimation

For protein estimation, two different methods were used, depending on the buffer composition used for cell lysis.

Bicinchoninic acid (BCA) protein assay

To prepare the samples for measurement protein extracts were diluted in a sample/water ratio of 1:10-1:20 and pipetted into a 96-well plate. Consecutively, the reagents were added according to the manufacturer's instructions (Thermo Scientific). The 96-well plate was incubated for 30 min at 37°C. Samples were measured at 562 nm using an imager and protein concentration of the samples was determined by means of a BSA standard curve.

Bradford method

In this method basic and aromatic protein side chains react with Coomassie G-250, which is part of the Bradford reagent (Bio-Rad), shifting its absorption maximum to 595 nm. For estimation protein extracts in different dilutions were mixed 1:5 with Bradford reagent, incubated for 5 min at RT and absorption measured at 595 nm. The protein concentration was finally calculated by means of a standard curve.

BCA protein assay kit (Thermo Scientific)

Bradford reagent (Bio-Rad)

2.3.4 Deglycosylation of proteins

Purified cellular membranes (see 2.3.2) were pelleted and resuspended in denaturing buffer (New England Biolabs) and incubated for 10 minutes at 100°C. Samples were chilled on ice and briefly centrifuged at 6000xg. Subsequently, samples were either incubated with Glycobuffer (New England Biolabs), water and the deglycosylation enzymes, or with water only (control) over night at 37°C. Two different deglycosylation enzymes were used: EndoH and PNGaseF (New England Biolabs). After the deglycosylation reaction, samples were incubated with loading dye for 5 min at 95°C and subjected to SDS-PAGE (see 2.3.5).

2.3.5 Sodium dodecyl sulphate polyacrylamide gel electrophoresis (SDS-PAGE)/NuPAGE

To separate proteins according to their molecular weight, SDS-PAGE was used. Depending on the molecular weight of the proteins of interest, solutions containing an appropriate Acrylamide/Bisacrylamide concentration were mixed (Table 8). The separation gel solution was cast into a cassette, with a layer of 70 % ethanol on top it, to prevent dehydration. Then, after removal of previously added ethanol, stacking gel solutions were cast onto the separation gel. Plastic combs were slided into the stacking gel to create wells for sample loading, while still being liquid. Following complete polymerization of the gel, combs were removed, the cassette was inserted into a gel electrophoresis chamber and running buffer was added to the chamber. Protein samples were denatured by addition of SDS loading dye and boiling for 5 minutes at 95°C. Appropriate amounts of protein samples (~20 µg) as well as the molecular weight standard PageRuler (Thermo Scientific) were loaded into individual wells. Electrophoresis was performed at 30 mA and a maximum of 150 Volt. Alternatively, especially in order to detect small molecular proteins, pre-cast Bis-Tris NuPAGE 4-12 % gradient gels (Life Technologies) were used. Protein samples were prepared according to manufacturer's instruction. As molecular weight standard the LDS See Blue ladder (Life Technologies) was used.

TABLE 8: COMPOSITION OF SDS- PAGE GELS FOR DIFFERENT PROTEIN SIZES

	Separation gel			Stacking gel
	12 %	**10 %**	**7 %**	**4 %**
Protein size (kDa)	≤ 70	20-100	30-200	-
dH2O	7 mL	8.3 mL	10.3 mL	6.2 mL
Acrylamide/Bisacrylamide	8 mL	6.7 mL	4.7 mL	1.3 mL
Lower-TRIS	5 mL	5 mL	5 mL	-
Upper-TRIS	-	-	-	2.5 mL
APS	50 µl	50 µl	50 µl	25 µl
TEMED	50 µl	50 µl	50 µl	25 µl
Total	20 mL	20 mL	20 mL	10 mL

Stacking gel buffer (4 x) (Upper-Tris)
500 mM Tris, 0.4 % SDS, dH2O, pH 6.8
Separation gel buffer (4 x) (Lower TRIS)
1.5 M Tris, 0.4 % SDS, dH2O, pH 8.8 SDS loading dye (5 x) 50 % Glycerin, 7.5 % SDS, 0.1 M DTT,
Ammonium persulfate (APS, Sigma)
10 % Ammonium persulfate, dH2O

N,N,N´,N´-Tetramethylethylenediamine (TEMED, Roth)
Running buffer
25 mM Tris, 200 mM Glycine, 0.1 % SDS, dH2O Acrylamide/Bisacrylamide solution 30 % Acrylamide/Bisacrylamide in the ratio of 37.5:1
SDS Loading dye (5 x)
25 % Upper Tris, 0.34 M SDS, 0.1 M dTT, 50% glycerol, bromphenol blue, dH2O to 10 mL
PageRuler™ prestained protein ladder (Thermo Scientific)
SeeBlue® prestained standard (Life Technologies)

2.3.6 Western Immunoblotting (WB) and ECL imaging

TABLE 9: PRIMARY ANTIBODIES

Name	Company	Species	WB	ICC
Ephrin-B2 C-term (316)	Sigma Aldrich	Rabbit	1:1000	
Ephrin-B2 N-term	Santa Cruz	Rabbit	1:500	
pSrc (Y418)	Life Technologies	Rabbit	1:500	1:300
Src	Millipore	Mouse	1:1000	1:300
pFAK (Y397)	Cell Signaling Technology	Rabbit	1:500	1:300
FAK	Millipore	Mouse	1:1000	1:300
β-actin	Sigma Aldrich	Mouse	1:5000	
Talin-1	Sigma Aldrich	Mouse	1:1000	
Vinculin	Sigma Aldrich	Mouse	1:1000	
Presenilin C-loop	Eurogentec	Rabbit	1:1000	
pAkt (S473)	Cell Signaling Technology	Rabbit	1:1000	
Akt1/PKB	Cell Signaling Technology	Rabbit	1:1000	
MEK 1/2	Cell Signaling Technology	Rabbit	1:1000	
AIF	Cell Signaling Technology	Rabbit	1:1000	
Vimentin	Cell Signaling Technology	Rabbit	1:1000	
pTyrosine	Millipore	Mouse		1:300

TABLE 10: SECONDARY ANTIBODIES

Antibody	Company	WB	ICC	-conjugated
a-ms HRP	Sigma Aldrich	1:25.000		HRP
a-rb HRP	Sigma Aldrich	1:25.000		HRP
a-ms IRDye 680RD	Licor		1:300	IRDye 680
a-rb IRDye 800CW	Licor		1:300	IRDye 800
a-ms Alexa Fluor 647	Life Technologies		1:1000	Alexa 647
a-rb Alexa Fluor 488	Life Technologies		1:1000	Alexa 488

Gels containing separated proteins, were put onto a nitrocellulose membrane (pore size 0.2 µm. Gel and membrane were put between two papers and two sponge layers on each side. After clamping all layers together, the sandwich was submerged in transfer buffer and proteins were blotted onto the membrane at 180 V and 400 mA in 1.5 h. To monitor protein transfer, blotted membranes were washed with TBS-T and incubated for 2 minutes in Ponceau red solution. However, this was not done in case of subsequent phosphoprotein detection. After three more washing steps, blots were incubated 1 h with PBS-T blocking solution at RT, or in the case of phosphoprotein detection, with TBS-T blocking solution at 4°C. Then, blots were incubated with primary antibody solution overnight at 4°C containing appropriate concentration of antibody (Table 9). After washing the membranes 4 times 5 minutes with TBS-T, they were incubated in a solution containing horse radish peroxidase (HRP) coupled secondary antibodies for 1 h at RT (Table 10).

After 4 more washing steps, blots were briefly incubated with ECL solution in order to detect target proteins. Light emission was captured by an ECL imager (BioRad). Occasionally, membrane signals were enhanced by incubation with ECL advanced (GE healthcare). ECL signals were quantified with ImageJ software (Analyze->Gels).

Transfer buffer
5 mM Tris, 200 mM Glycine, 10 % methanol, dH2O
Ponceau Red
3 % (w/v) Ponceau S, 3 % trichloroacetic acid, dH2O
TBS-T
10 mM Tris, 150 mM NaCl, 0.1 % Tween20, dH2O, pH 7.5
TBS-T blocking solution
TBS-T, 5 %, BSA (Roth), PhosSTOP (Roche)
PBS-T blocking solution
PBS-T, 5 % skimmed milk powder (Roth)

Primary antibody solutions
TBS-T blocking solution/PBS-T blocking solution, specific antibody (for dilution see Table)
Secondary antibody solutions
TBS-T/PBS-T, IgG HRP conjugate secondary antibodies (Thermo Scientific)
ECL
(1:1 mix of W1 and W2)
W1: 0.1 M Tris pH 8.5, 0.4 mM cumaric acid, 0.25 mM luminol, dH2O
W2: 0.1 M Tris pH 8.5, 0.018 % H2O2, dH2O

2.3.7 Co-Immunoprecipitation (Co-IP)

To detect protein-protein interactions co-immunoprecipitation (Co-IP) was used. For Co-IP of FAK and ephrin-B2 the previously described hypotonic buffer, supplemented with proteinase inhibitor but without dTT was used. After cell lysis, the protein concentration of the different samples was measured and equal amounts of protein (1 mg/vial) were aliquoted into 1.5 mL vials and PBS was added to 800 µl. Then, samples were incubated with 30 µl of uncoupled Sepharose A beads (against rabbit IgG, Invitrogen) under constant rotation for 1 h at 4°C to remove proteins that bind to the resin unspecifically. Next, the lysate was centrifuged for 2 minutes at 8000xg at 4°C to remove the beads. After centrifugation, the supernatant was transferred into a new vial. 20 µl of the supernatant were separated and kept at -20°C overnight until further analysis. The rest of the supernatant was incubated with 2 µg FAK Ab (see Table 9) and 30 µl of Sepharose A slurry overnight under constant rotation at 4°C. Subsequently, the beads were collected by centrifugation and the supernatant was transferred into a separate vial. The beads were then washed with STEN NaCl and twice with STEN buffer. Washing solution was removed (using a syringe and a 0.4 mm needle). Then, 20 µl of sup after pre-clearing, the beads coupled with FAK antibody and 20 µl of the sup after Co-IP were incubated with 2x loading dye. The samples were then boiled at 95°C and were subjected to protein separation by SDS-PAGE (see 2.3.5).

STEN-NaCl
50 mM Tris, 500 mM NaCl, 2 mM EDTA, 0.2 % NP40 (Sigma-Aldrich), dH2O, pH 7.6

2.3.8 Protein precipitation with trichloroacetic acid (TCA)

Cell culture supernatants were collected and cleared from cellular debris by centrifugation for 5 minutes at 300xg. Sodium desoxycholic acid was added to a final concentration of 0.02 % and incubated for 15 min. TCA solution was then added to a final concentration of 10 %. Then, samples were incubated for 1 h at RT. Precipitates were pelleted by centrifugation for 15 minutes at 16,000xg at 4 °C, and washed twice with ice-cold acetone. The washed pellets were air-dried, resuspended in 10 µl of Tris-SDS buffer and incubated for 10 min at 50 °C.

Finally, 5 µl 2x LDS-sample buffer was added, and samples were subjected to separation by NuPAGE (Life Technologies).

DOC solution
2 % Sodium deoxycholic acid
Trichloroacetic acid (TCA)
100 % TCA, dH2O
Tris/SDS Buffer
50 mM Tris, 1 % SDS, dH2O

2.4 Analysis of cell migration

For migration assays, 15 ng/mL CX3CL1 fractalkine (R&D Systems) containing serum free medium was pipetted into the two filling reservoirs of a µ-slide chemotaxis 3D channel (Ibidi) device. 3x 10^6 ESdM cells were seeded into the channel and all filling ports were sealed by plugs provided by manufacturer in order to prevent evaporation or movement of fluid during imaging. The µ-slide was kept at 37°C and cells were imaged for 8 h (1 frame/5 min) with a fluorescence microscope (AxioVert 200, Zeiss) with ZEN software. Image sequences were manually analyzed (Manual Tracking plug in, ImageJ) and tracks were subsequently plotted (Chemotaxis and Migration tool, Ibidi). The accumulated distance of the 10 fastest migrating cells in each group per day was statistically analyzed.

2.5 Statistical analysis

Analysis of data sets from two sample groups was done by Student's t-test (unpaired, two-sided). For comparison of the mean of more than two groups a One Way ANOVA (with Tukey's post hoc test) was used. For analyzing more than one parameter between groups a Two Way ANOVA (with Sidak's post hoc test) was applied. Confidence level: 95 %. All graphs display mean of data ±SD. Definition of significant P-values used: * ≤ 0.05, ** ≤ 0.01, *** ≤ 0.001, **** ≤ 0.0001.

3. Results

3.1 Ephrin-B expression and processing in microglial cells

3.1.1 Endogenous expression of ephrin-B in primary microglia and ESdM

For this study, embryonic stem cell derived microglia (ESdM) were used. These cells closely resemble primary microglia and can be cultured at a large scale more easily, thereby allowing for biochemical and cell culture analyses (Beutner et al., 2013). Endogenous ephrin-B family member 1-3 expression in primary microglia as well as ESdM was analyzed by qRT-PCR expression analysis.

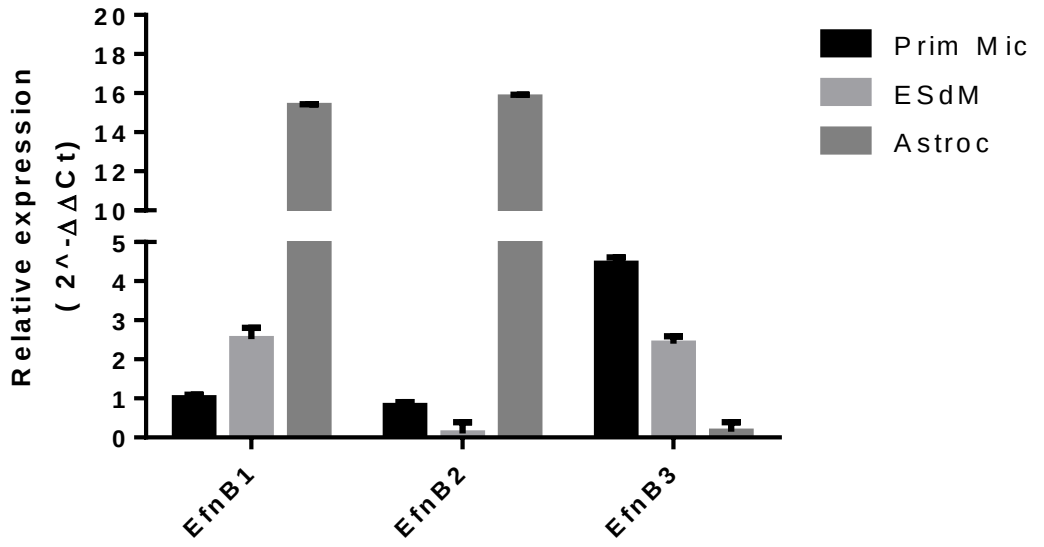

Figure 6: Expression of endogenous ephrin-B (1-3) in primary microglia, ESdM and primary astrocytes.
All three ephrin-B family members are expressed in ESdM as well as primary microglia (n=1, replicate samples=3). Like ESdM, primary microglia were isolated from C57BL/6 mice. Prior to primary microglia harvesting, primary microglia and astrocytes were co-cultured. Therefore primary microglia qRT-PCR samples were controlled for contamination with primary astrocytes by including primary astrocyte samples in the ephrin-B expression analysis. After isolation of mRNA and reverse transcription, cDNA of all three cell types was compared regarding ephrin-B expression. Expression levels were normalized to the reference genes GAPDH and LDHA. Values represent fold expression levels of all three ephrin-Bs relative to ephrin-B1 expression in primary microglia. Ephrin-B expression is low in comparison to reference gene expression (GAPDH/ephrin-B fold expression in ESdM: (B1) 1/ 0.00106222, (B2) 1/0.00004365, (B3) 1/0.00101592).

Despite low ephrin-B expression in comparison to GAPDH and LDHA reference gene expression, the experiment shows that all ephrin-Bs are expressed in both primary and ES-derived microglia (Figure 6). Data indicate no contamination of primary microglia with primary astrocyte mRNA, since ephrin-B1 and –B2 levels are substantially higher in primary astrocytes as compared to the primary microglia.

3.1.2 Generation of ephrin-B2 overexpressing ESdM

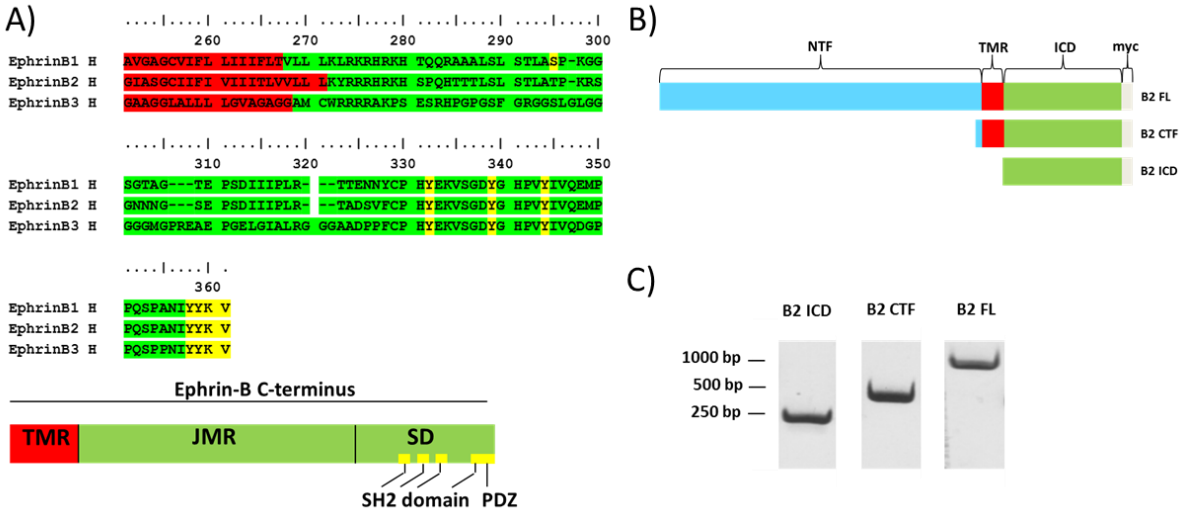

Figure 7: Subcloning of ephrin-B2 constructs.
A) AA sequence comparison and schematic view of the C-terminal fragment of human ephrin-B members. The signalling domain (AA329-361) is 100 % homologous between all ephrin-B family members. Ephrin-B1 contains an additional phosphoserine domain in the juxtamembrane region (indicated in AA sequence by yellow colour). TMR: Transmembrane region (red), JMR: Juxtamembrane region (green), SD: signaling domain (green), SH2 (Src homology 2) and PDZ domain (yellow). **B)** Schematic view of ephrin-B2 full length (FL), ephrin-B2 C-terminal fragment (B2 CTF), an ephrin-B2 intracellular domain (ICD) used for overexpression. NTF: N-terminal fragment, myc: myc-tag. **C)** To identify bacterial clones, which were successfully transformed with constructs containing the target insert, plasmids of several colonies were screened by PCR. Agarose gel shows bands of three positive bacterial clones, which are either positive for ephrin-B2 FL, ephrin-B2 CTF, or ephrin-B2 ICD (ephrin-B2 FL_myc=1031 bp, CTF_myc=402 bp, ICD_myc=249 bp).

Since overall ephrin-B gene expression levels of all three family members were very low in microglial cells, it was decided to overexpress one of the three ephrin-Bs. Ephrin-B1 knock out mice die perinatally and show defects in neural crest tissues (Davy et al., 2004). Ephrin-B3 knock out mice display a characteristic hopping gait due to a defect in corticospinal pathfinding (Kullander et al., 2001a; Yokoyama et al., 2001). Ephrin-B2 knock out mice display lethality at embryonic day 11 (E11) and therefore show the most severe phenotype in comparison to ephrin-B1 and ephrin-B3 knock out phenotypes (Wang et al., 1998). This demonstrates a crucial function of ephrin-B2 in murine development and identified ephrin-B2

as the most promising candidate for exogenous expression in ESdM. Furthermore, this study aimed at analyzing ephrin-B reverse signaling, which is transmitted via the intracellular domain (ICD) of ephrin-Bs. The signaling domain within the ephrin-B ICD is 100% homologous (AA 329-361) (Figure 7A). Ephrin-B2 is furthermore highly conserved in humans and mice showing 97% amino acid (AA) homology. Our own experience and experiments of others have shown that microglial cell lines are difficult to transfect (Balcaitis et al., 2005; Smolny et al., 2014). Therefore ESdM were transduced with lentiviral constructs encoding either human ephrin-B2 FL, CTF or ICD (Figure 7B). The different ephrin-B2 cDNAs were subcloned into a lentiviral vector. After production and purification of lentiviral particles, ESdM cells were transduced with the different ephrin-B2 fragments. To remove non-transduced cells from the population, ESdM were cultivated in 2 µg/ml puromycin. After the selection procedure ephrin-B2 expression of ESdM was tested via Western immunoblotting (also see Figure 8 and Figure 9).

3.1.3 Proteolytic processing of ephrin-B2

It has previously been shown for fibroblasts and other cell types, that binding of the EphB receptor to ephrin-B family members induces shedding of the extracellular domains by ADAM's and MMP's (Janes et al., 2005; Tanaka et al., 2007). This has been reported to be followed by intramembranous cleavage by the γ-secretase in the case of ephrin-B1 and ephrin-B2 (Georgakopoulos et al., 2006; Tomita et al., 2006). Therefore, it was tested whether ephrin-B processing is similar in ESdM. Cells transduced with either a control (Ctrl) vector or an ephrin-B2 full length (FL) vector were investigated (Figure 8A).

Firstly, endogenous ephrin-B expression and processing was tested in Ctrl vector transduced cells. As mentioned previously, the signaling domain of all ephrin-B family members is homologous. For detection, an ephrin-B antibody, which binds to this homologous epitope of the C-terminus of ephrin-B, was used. The endogenously expressed ephrin-B FL and its C-terminal fragment (CTF) were only weakly detectable, while the intracellular domain (ICD) was not detectable at all in the Ctrl vector cells (Figure 6A). To test EphB stimulated ephrin-B processing, both cell lines were treated with a control Fc (Ctrl Fc) or a soluble EphB1-Fc fusion protein. Treatment of the Ctrl cells with a soluble EphB1 receptor resulted in a significantly stronger ephrin-B N-terminal fragment (NTF) accumulation in the medium as compared to the Ctrl Fc treated cells (Figure 8A, B).

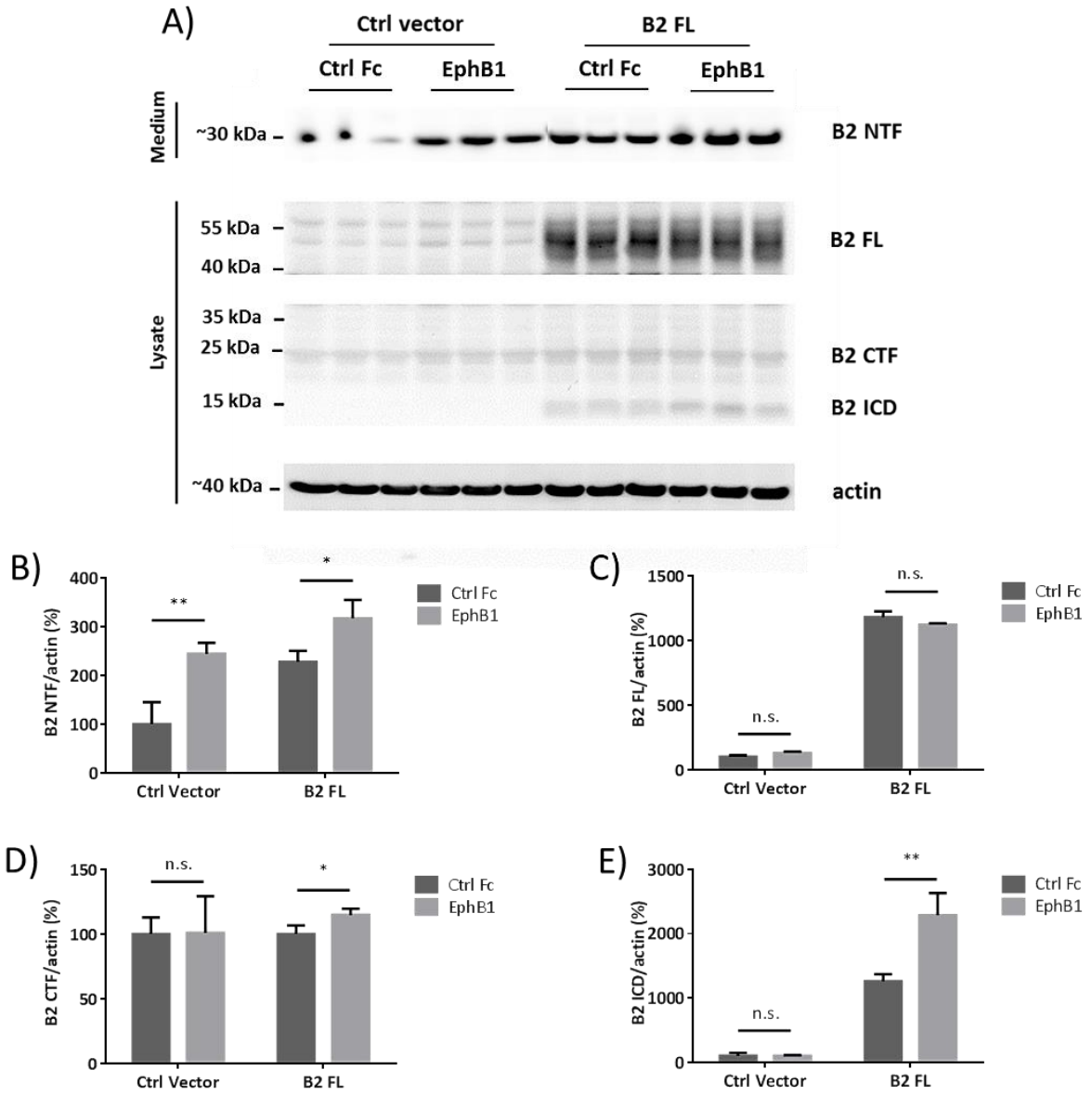

Figure 8: Ephrin-B is shed upon stimulation with EphB1 and is subsequently cleaved.
A) Western blot shows different ephrin-B fragments in ESdM transduced with Ctrl vector or ephrin-B2 FL construct. Ctrl and ephrin-B2 FL cells were additionally treated with a Ctrl Fc or a soluble EphB1-Fc fusion protein for 30 min. **B)** In comparison to the Ctrl Fc treatment, EphB1 receptor stimulation markedly increases endogenous ephrin-B (1-3) (n=3) and overexpressed ephrin-B2 (n=3) shedding, resulting in elevated ephrin-B NTF levels in both cell types. **C)** No significant differences between ephrin-B2 FL levels were observed in Ctrl or ephrin-B2 FL cells, treated with the different receptors (n=3). **D)** Cells transduced with ephrin-B2 FL show a significant increase of ephrin-B2 CTF levels between Ctrl and soluble EphB1 receptor treatment (n=3). **E)** Endogenous ephrin-B ICD is not detectable. Ephrin-B2 FL overexpressing cells show strongly increased ephrin-B2 ICD levels after EphB1 receptor stimulation (n=3). Statistical analysis was done using a two-sided unpaired student's t-test. All data are represented as means ±SD.

The quantification of ephrin-B in cells showed no difference of ephrin-B FL or ephrin-B CTF levels upon treatment with EphB1-Fc (Figure 8A, C, D).

ESdM transduced with an ephrin-B2 full length (B2 FL) construct (described in Figure 7) also showed a marked increase in ephrin-B NTF production upon stimulation with the soluble EphB1 receptor in comparison to the Ctrl Fc treated cells (Figure 8A, B). Ephrin-B2 CTF and ICD levels in these cells rose significantly upon EphB1 treatment (Figure 8A, D, E), whereas ephrin-B2 FL levels showed no difference (Figure 8A, C).

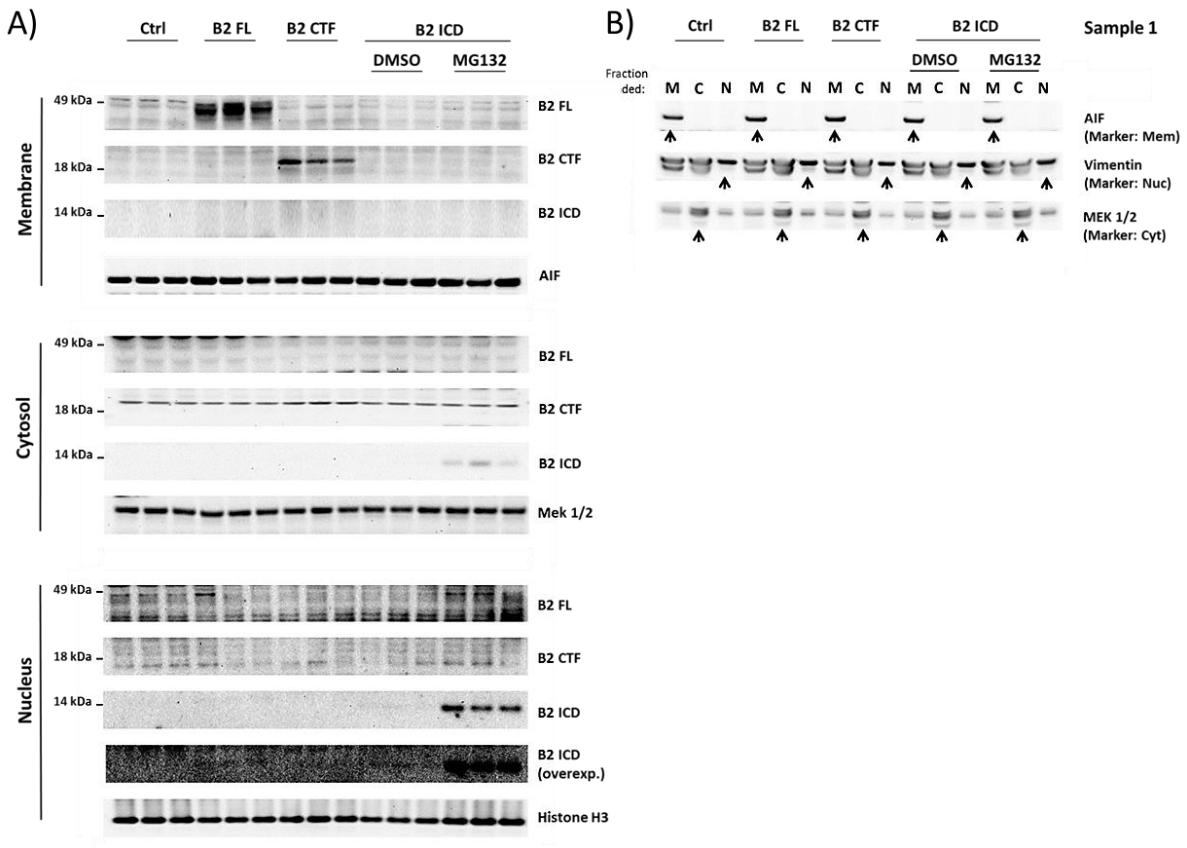

Figure 9: Subcellular localization of different ephrin-B2 fragments.
A) Western blot showing cell fractionation of cells transduced with a control vector or overexpressing either of the three ephrin-B2 constructs in ESdM (B2 FL, B2 CTF or B2 ICD). For cell fractionation, cells were lysed and the different fractions were isolated by use of appropriate buffers and centrifugation, as described in the methods section 2.3.2. The analysis shows that ephrin-B2 FL and CTF are membrane associated, while the ephrin-B2 ICD localizes to cytosol and nucleus. The experiment indicates that the ephrin-B2 ICD is subject to proteasomal degradation, since MG132 treatment (1µM, 4 h) of ephrin-B2 ICD overexpressing cells stabilizes the ephrin-B2 fragment. **B)** Representative cell fractionation control for the first sample of each biological triplicate for each construct shown in A). Detection of marker proteins shows successful separation of the membrane (M), cytosolic (C) and nuclear (N) fraction. AIF: apoptosis inducing factor (membrane marker), vimentin (cytoskeletal/nuclear marker), MEK 1/2: mitogen-activated protein kinase kinase (cytosolic marker).

It was previously described that the ephrin-B1 and –B2 ICD translocate to the nucleus in fibroblasts (Tomita et al., 2006; Waschbusch et al., 2009). To assess the subcellular distribution of ephrin-B2 and its processing products in our microglial model, membrane, cytosol and nuclear fractions were analyzed by Western immunoblotting (Figure 9A). The fractionation control furthermore showed that membrane, cytosol and nuclear fractions were separated successfully (Figure 9B). The overexpressed ephrin-B2 constructs ephrin-B2 FL, CTF and ICD migrated at an apparent molecular weight of ~45 kDa, ~20 kDa and ~14 kDa, respectively. Ephrin-B2 FL and CTF were mainly present in the membranous fraction. The ICD was detectable in the cytosolic as well as the nuclear fraction. Treatment of the ephrin-B2 ICD overexpressing cells with the proteasomal inhibitor MG132 was found to stabilize the intracellular ephrin-B2 ICD levels, indicating proteasomal degradation of the fragment. These findings resemble those previously made in fibroblasts and suggest that the ephrin-B2 ICD also translocates to the nucleus in ESdM.

3.1.4 Maturation of ephrin-B2 FL overexpressed in BV-2

To confirm previous findings in a different microglial cell line, BV-2 were used in the following experiments (Figure 10, Figure 11). BV-2 are, as opposed to ESdM, immortalized cells, which were generated by Blasi et al. by transduction of murine microglial cultures with a retrovirus (J2) carrying a c-raf/c-myc oncogene (Blasi et al., 1990). BV-2 were either transduced with a control vector or the previously described human ephrin-B2 FL construct (Figure 7). Since it has been reported that ephrin-B2 is cleaved by the γ-secretase, cells were treated with the γ-secretase inhibitor DAPT, to stabilize the ephrin-B2 CTF. Furthermore, since we observed rapid proteasomal degradation of the ephrin-B2 ICD in ESdM, cells were additionally treated with the proteasomal inhibitor MG132. Upon treatment with DAPT, the ephrin-B2 CTF accumulated, confirming γ-secretase mediated ephrin-B2 cleavage in BV-2. Cell fractionation showed that ephrin-B2 FL and CTF are present in the membrane fraction. The ephrin-B2 ICD is present in the cytosolic and the nuclear fractions, but can, similar to that in ESdM, be poorly detected without proteasomal inhibition (Figure 10). In the ESdM as well as in the BV-2, migration of full length ephrin-B2 did not fully correspond to its predicted size of ~37 kDa but rather to a size of ~45 kDa. However, ephrin-B2 is predicted to be glycosylated, with its potential glycosylation sites located at Asparagine 36 and 139 within the N-terminal extracellular domain of the protein.

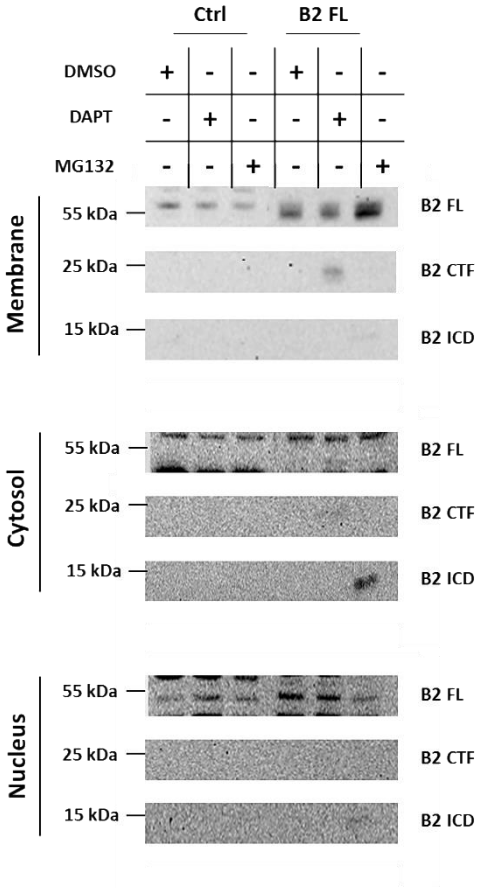

Figure 10: Ephrin-B2 fragments localize to similar fractions in ESdM and BV-2.
Western immunoblot showing cell fractionation of control vector transduced or ephrin-B2 FL overexpressing BV-2, which were incubated with the γ-secretase inhibitor DAPT (10 µM, 24 h), the proteasomal inhibitor MG132 (1 µM, 4 h) or control solvent (DMSO). Only slight differences were detectable in the control vector transduced cells. The ephrin-B2 FL overexpressing cells, however, show ephrin-B2 CTF accumulation upon DAPT treatment in the membrane fraction, as well as accumulation of ephrin-B2 FL upon MG132 treatment. In the cytosolic and nuclear fraction the ephrin-B2 ICD accumulates after proteasomal inhibition with MG132. In order to visualize the ephrin-B2 ICD in the cytosolic and membrane fraction, a higher exposure time than for the membrane fraction was chosen for these images. This probably also resulted in the detection of unspecific bands at 60 and 50 kDa. Furthermore, ephrin-B2 FL was not only detected in the membrane fraction but also in the nuclear fraction, likely due to incomplete separation of the membrane from the nuclear fraction.

Although some functions of glycosylation remain unclear, it is known that one or more N-linked oligosaccharides are present on most proteins transported through the endoplasmatic reticulum (ER) and Golgi apparatus. They are suspected to aid protein transport, folding and act as protection from proteases (Bruce Alberts, 2002).

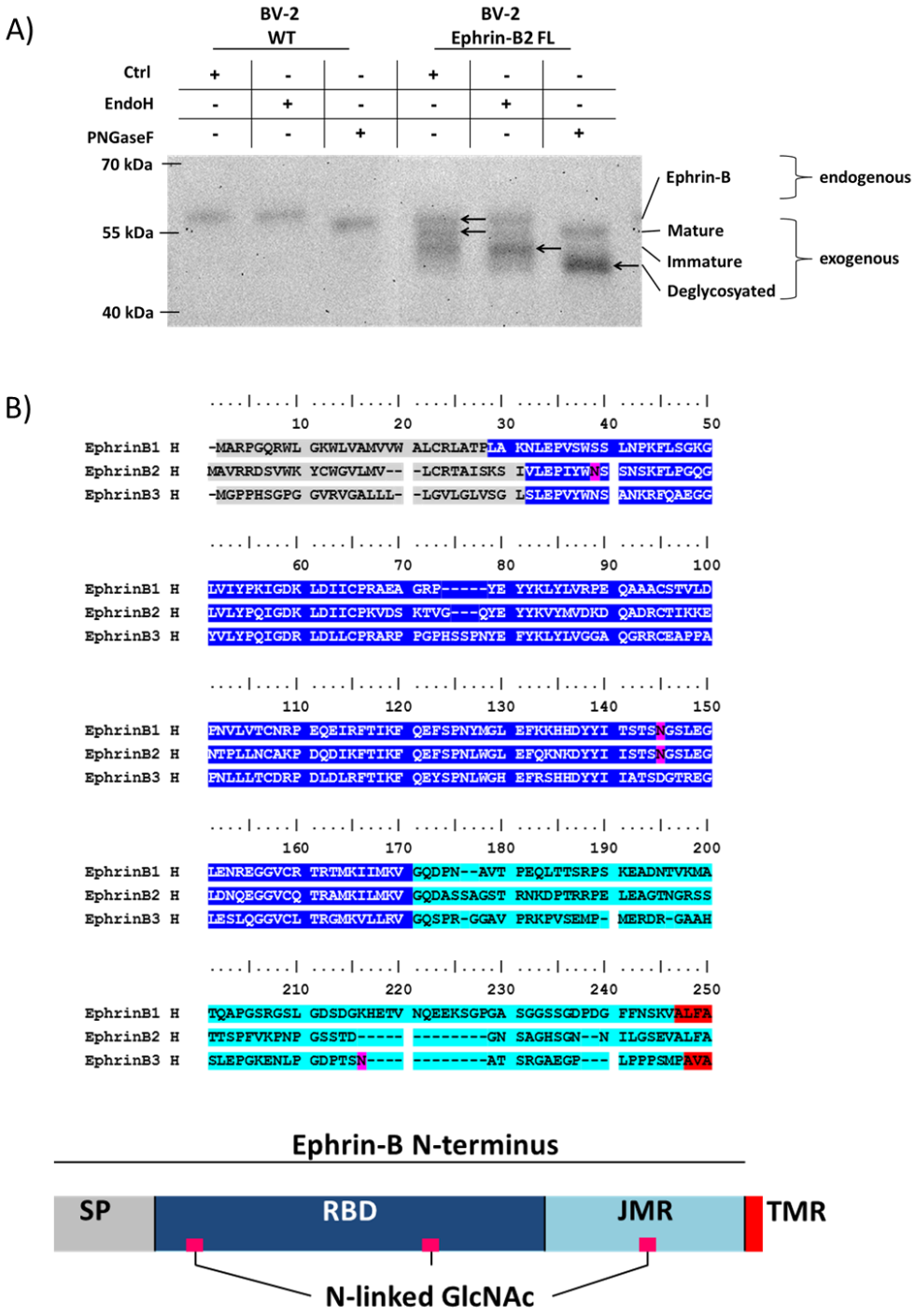

Figure 11: Glycosylation of ephrin-B2 in BV-2.
A) Western immunoblot showing ephrin-B2 in isolated membranes of BV-2 WT or ephrin-B2 FL overexpressing cells. Membranes were incubated with an appropriate buffer and then either treated with the enzyme Endoglycosidase H (EndoH), the enzyme Peptide N-glycosidase F (PNGaseF) or with water. BV-2 WT cells show a single band which is affected by PNGase F treatment only and may represent endogenous ephrin-B. Ephrin-B2 FL overexpressing BV-2 show effective deglycosylation of ephrin-B2 upon EndoH and PNGaseF treatment. Complete deglycosylation reduces the ephrin-B2 mass by ~5-7 kDa. **B)** AA sequence and schematic view of the N-terminus of human ephrin-B family members. Ephrin-B1, 2 and 3 display different predicted glycosylation sites (ephrin-B1: Asp139, ephrin-B2: Asp36, Asp139, ephrin-B3: Asp 36, Asp210). SP: Signal peptide, RBD: Receptor binding domain, JMR: Juxtamembrane region, TMR: Transmembrane region.

Next, it was tested in BV-2 cells whether oligosaccharide modifications contribute to the discrepancy between predicted and apparent molecular mass of ephrin-B2. Endoglycosidase H (EndoH) removes only high mannose and some hybrid types of N-linked carbohydrates, while Peptide N-glycosidase F (PNGaseF) removes all types of N-linked carbohydrates independent of their structure and composition.

The untreated Ctrl sample of the ephrin-B2 FL overexpressing BV-2 in Figure 11A displays three distinct bands. They represent from top to bottom a putative endogenous ephrin-B band, a mature and an immature form of the overexpressed ephrin-B2 protein. The EndoH processed sample contains proteins which do not possess N-linked mannose rich carbohydrates, eliminating the glycosylated mature form. Proteins treated with PNGase F represent completely deglycosylated proteins and migrate at ~40 kDa, demonstrating that glycosylation of ephrin-B2 constitutes 5-7 kDa of the total protein mass. The largest detected proteins in the BV2 WT as well as in the ephrin-B2 FL overexpressing cell samples are not affected by the EndoH treatment but only by the PNGaseF treated samples. It is likely that the upper bands represent the endogenously expressed ephrin-B proteins. Although the glycosylation sites are conserved between humans and mice (Figure 11B), human and murine ephrin-B might migrate differently.

3.2 γ-Secretase mediates reverse signaling of ephrin-B2

To investigate whether EphB1 induces γ-secretase dependent ephrin-B2 cleavage, ephrin-B2 FL overexpressing ESdM were treated with the γ-secretase inhibitor DAPT or a control solvent (DMSO). Upon treatment of those cells with Ctrl Fc or soluble EphB1, ephrin-B2 NTF and ICD generation was measured (Figure 12A). In cell culture media of DMSO as well as DAPT treated cells, ephrin-B2 NTF levels were significantly higher after incubation with soluble EphB1-Fc receptor in comparison to Ctrl Fc treatment. It was therefore concluded that γ-secretase inhibition has no or only a minor effect on ephrin-B2 shedding (Figure 12B). However, when comparing the cellular ephrin-B2 ICD levels after EphB1 stimulation in the Ctrl and DAPT treated cells a significant decrease was measured (Figure 12C), indicating γ-secretase dependent intramembranous cleavage of ephrin-B2 upon EphB1 binding. To validate these findings, ESdM overexpressing ephrin-B2 FL were treated with either DMSO or DAPT and were compared with PSdKO ESdM, which also overexpressed ephrin-B2 FL (Figure 12D). Upon pharmacological γ-secretase inhibition, ephrin-B2 CTF accumulated, while ICD levels decreased (Figure 12D, E, F). PSdKO ESdM completely lacking γ-secretase activity show strong ephrin-B2 CTF and a decrease of the ephrin-B2 ICD levels below the detection limit (Figure 12D, E, F), further confirming that intramembranous cleavage of ephrin-B2 is dependent on γ-secretase.

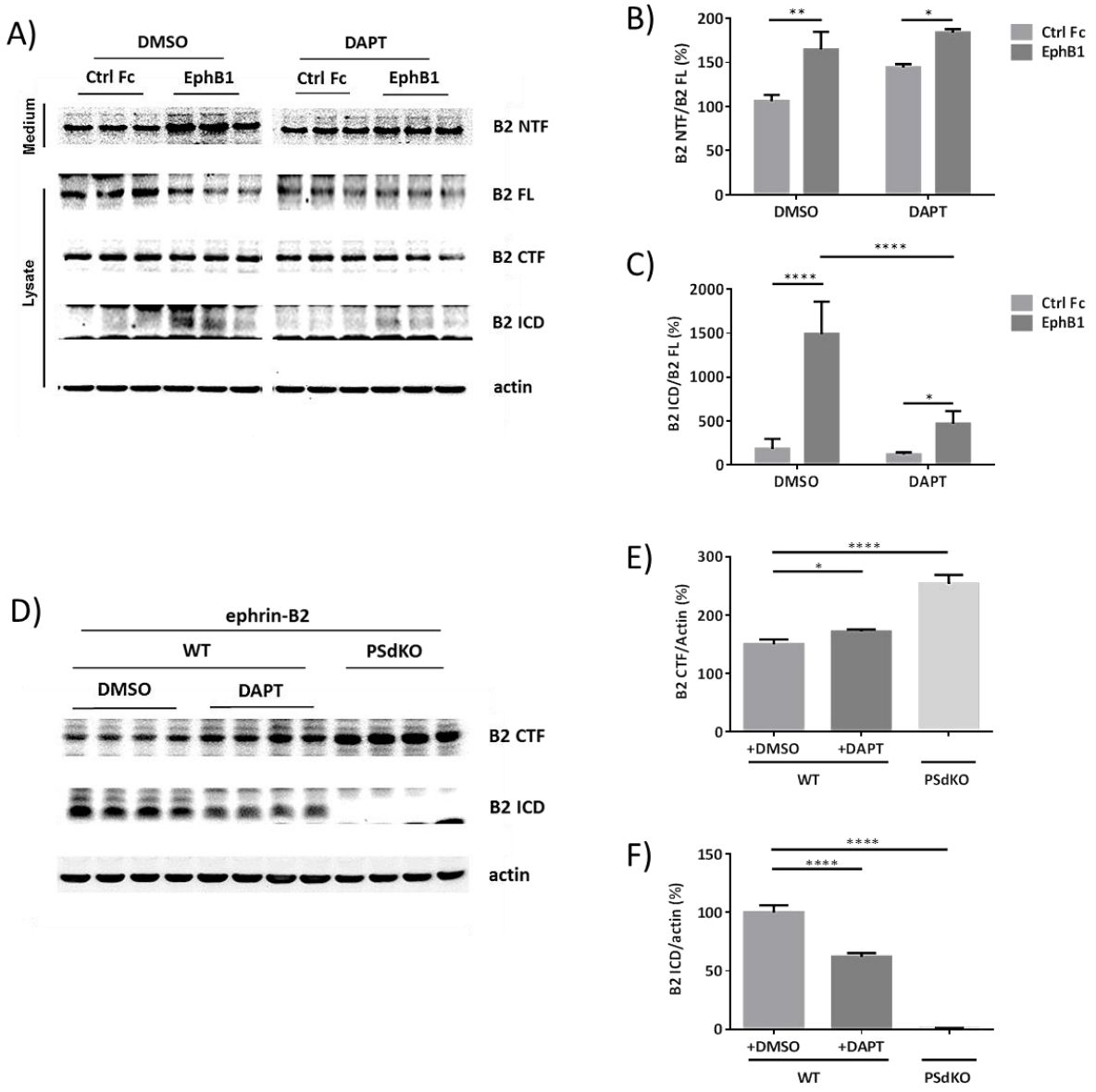

Figure 12: Cleavage of ephrin-B2 is mediated by γ-secretase.
A) Ephrin-B2 FL overexpressing cells were treated with DMSO (Ctrl) or DAPT (10 µM)for 24 h. Cells were then treated with Ctrl Fc or soluble EphB1 (2 µg/mL) receptor for 40 min. **B)** EphB1 induced extracellular shedding can be evoked in DAPT as well as DMSO treated cells. Protein from cell culture medium was TCA precipitated (n=3, Two way ANOVA with Tukey post hoc). **C)** DAPT treated cells show significantly less ICD production as compared to DMSO treated cells (n=3, Two way ANOVA with Tukey post hoc). **D)** Western blot shows effects of pharmacological (DAPT) and genetic (PSdKO) γ-secretase inhibition in ephrin-B2 FL cells on ephrin-B2 CTF and ICD generation. **E)** Quantification demonstrates significant accumulation of ephrin-B2 CTFs after both pharmacological and genetic inhibition of γ-secretase (n=4, One way ANOVA with Tukey post hoc). **F)** Ephrin-B2 ICD markedly decreases after pharmacological inhibition with DAPT and is not detectable in PS deficient cells (n=4, One way ANOVA with Tukey post hoc). All data are represented as means ±SD.

3.2.1 EphB1 stimulates phosphorylation of Src and FAK

EphB1 induced ephrin-B2 reverse signaling has previously been reported to stimulate Src phosphorylation in fibroblasts (Georgakopoulos et al., 2006; Georgakopoulos et al., 2011). Therefore, the effect of EphB1 stimulation on microglia cells overexpressing ephrin-B2 FL was investigated in a time dependent manner (Figure 13A).

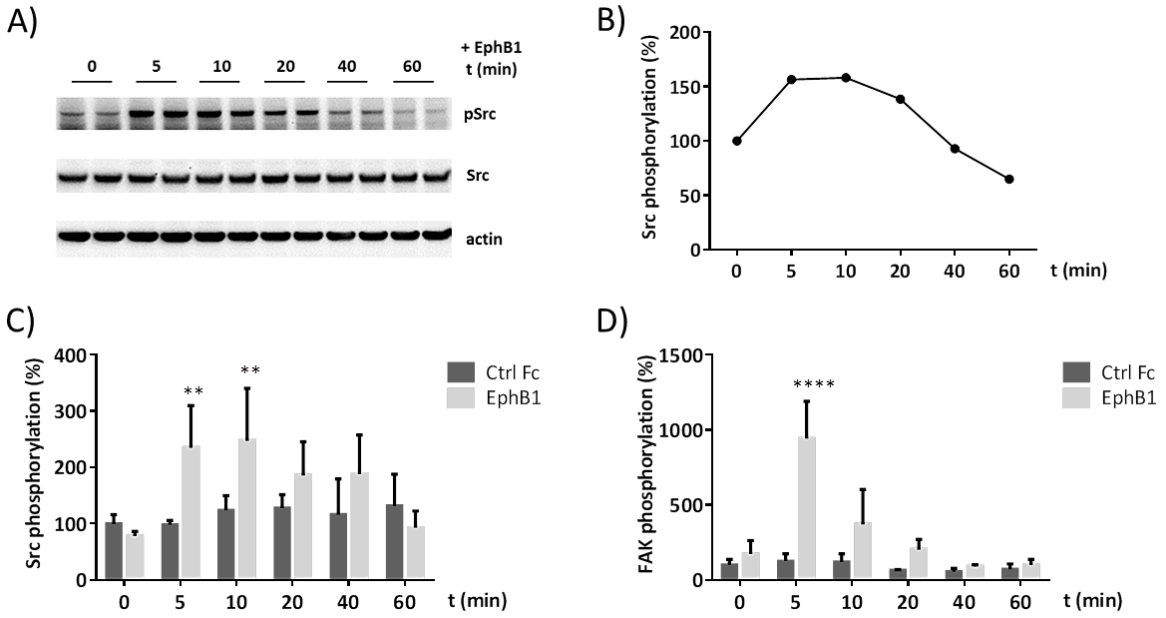

Figure 13: Soluble EphB1 treatment stimulates phosphorylation of Src and FAK.
A) Time dependent stimulation of Src phosphorylation upon EphB1 treatment (2 µg/mL) in ephrin-B2 FL overexpressing cells. **B)** Quantification of Western immunoblotting, shows rapid increase of pSrc after 5 min and a decrease after 20-40 min (n=2, normalized to Src levels, no statistical analysis). **C)** Quantification of In-Cell Western, corresponds to findings in B) and shows significantly increased pSrc, 5 min after EphB1 stimulation in ephrin-B2 FL cells (n=3, normalized to Src levels, Two way ANOVA with Dunnett's post hoc). **D)** In-Cell Western analysis shows significant increase of FAK phosphorylation in ephrin-B2 FL cells 5 min after EphB1 stimulation (n=3, normalized to FAK levels, Two way ANOVA with Dunnett's post hoc). All data are represented as means ± SD.

Quantification of Western immunoblotting shows a strong increase of pSrc within 5-10 min and a rapid decrease of pSrc levels after 20-40 min (Figure 13B). To validate this experiment by a different method, EphB1 induced pSrc stimulation was analyzed in an In-Cell Western assay. The In-Cell Western analysis closely resembled the results found by Western immunoblotting (Figure 13C). Since Src is known to phosphorylate FAK, an important kinase which regulates podosomal turn-over, FAK phosphorylation upon EphB1 receptor stimulation was tested. Interestingly, comparable to Src, FAK phosphorylation also peaked at 5 min (Figure 13D), suggesting simultaneous activation of Src and FAK and possible cross-

phosphorylation of the kinases. Moreover, after EphB1 stimulation, levels of phosphorylated Src rose 2.5 fold, while FAK phosphorylation increased 10 fold. Since signal amplification is typical for signal transduction cascades this indicates that FAK is downstream of Src.

3.2.2 EphB1 induced phosphorylation of Src is dependent on γ-secretase

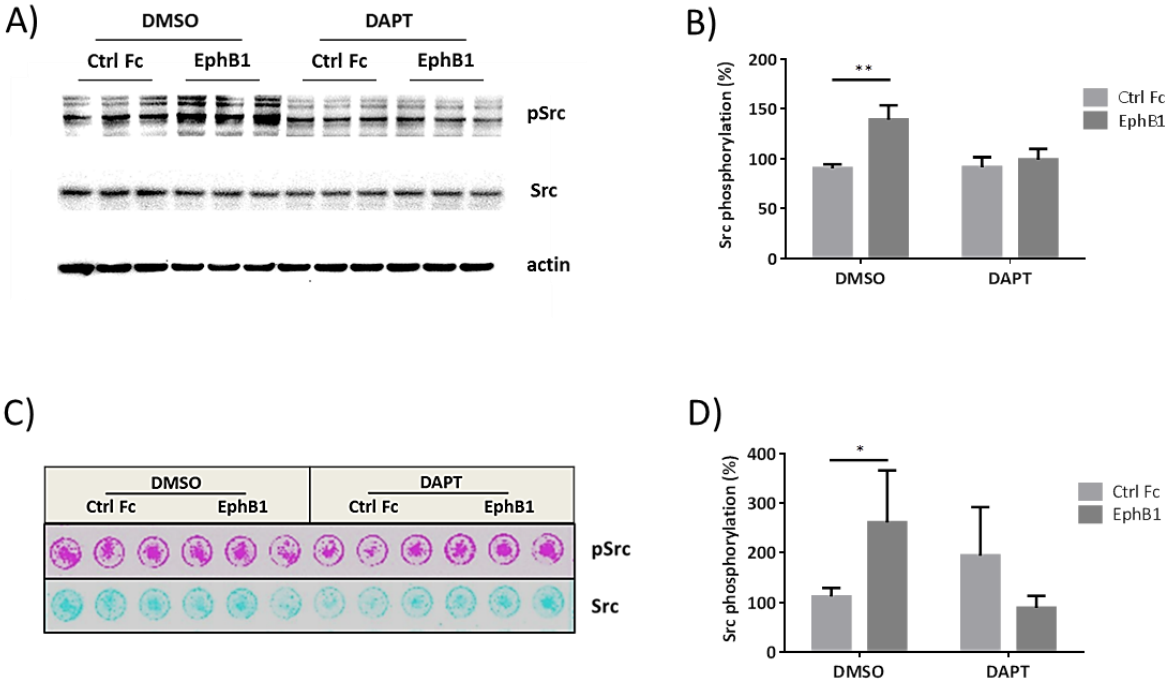

Figure 14: EphB1 induced stimulation of Src phosphorylation is dependent on γ-secretase. **A)** ESdM expressing ephrin-B2 FL were pre-treated with either DMSO or DAPT (10 µM, 24 h), followed by a 5 min treatment with Ctrl Fc or soluble EphB1 receptor (2 µg/mL). **B)** Quantification of DMSO treated cells shows an EphB1 induced pSrc increase, which is inhibited by prior DAPT treatment (n=3, normalized to Src levels, Two-way ANOVA with Tukey post hoc). **C)** In-Cell Western, showing DMSO or DAPT (10 µM, 24 h) treated primary microglia, that were stimulated with Ctrl Fc or soluble EphB1 receptor (2 µg/mL) for 10 min. **D)** Statistical analysis of fluorescence values obtained in C) reveals significant differences in DMSO treated cells, which were stimulated by EphB1, but not in DAPT treated cells (n=3, normalized to Src levels, Two-way ANOVA with Tukey post hoc).
All data are represented as means ± SD.

Next, it was tested whether stimulation of Src phosphorylation by soluble EphB1 occurs in a γ-secretase dependent fashion. Ephrin-B2 overexpressing ESdM were pre-treated with DAPT or DMSO. Then, according to the previous finding that Src activation had its peak at 5-10 min, cells were either treated with Ctrl Fc or soluble EphB1-Fc for 10 min (Figure 14A). Consistent

with earlier observations, EphB1 treatment significantly increased pSrc levels in DMSO treated cells (Figure 14B). Treatment with DAPT prevented EphB1 induced phosphorylation of Src, demonstrating γ-secretase dependence of this cascade (Figure 14B). To validate these findings, these experiments were repeated in primary microglia. Primary microglia were analyzed using an In-Cell Western approach (Figure 14C), since, as compared to biochemical analyses, only low cell numbers are needed to perform this assay. Similar to the results obtained with ESdM cells, soluble EphB1 receptor significantly increased the phosphorylation of Src within 10 min (Figure 14D). Again, prior DAPT treatment prevented stimulation, demonstrating that EphB1 receptor induced pSrc stimulation is also γ-secretase dependent in primary microglia.

3.2.3 Eph receptor stimulated phosphorylation of Src and FAK is dependent on ephrin-B2 ICD generation

To specifically assess the role of the intracellular domain of ephrin-B2 in γ-secretase dependent signaling we sought to establish a genetic model. Firstly, ESdM PSdKO cells were stably transduced with functional PS1 WT or non-functional PS1 (PS1 DN; Mutation: D385N) constructs. Thus, different cell lines with a homogenous genetic background were created. PS1 WT is endoproteolytically cleaved into an N-terminal and a C-terminal fragment. These two fragments form a stable heterodimer together with other proteins (also see chapter 1.2) to efficiently cleave γ-secretase substrates. The PS1 DN variant carries a single amino acid substitution in the catalytic site which completely prevents γ-secretase activity (Figure 15A) (Nyabi et al., 2003; Steiner et al., 1998). Secondly, the cells expressing PS1 DN were additionally transduced with an ephrin-B2 ICD construct. Western immunoblotting revealed expression of PS WT and PS1 DN in PSdKO ESdM. Functional PS is readily endoproteolytically cleaved into a C-and an N-terminal fragment. Therefore, PS1 WT expressing cells show a strong signal for the C-terminal fragment, while the full-length protein can only poorly be detected. The PS1 DN cells by contrast show accumulation of the full-length PS, and only a weak PS CTF signal since endoproteolytic cleavage of PS is strongly impaired in these cells (Figure 15A). The ephrin-B2 ICD was selectively detected after treatment with the proteasomal inhibitor MG132, indicating efficient degradation of this fragment by the proteasome (Figure 15B). This is consistent with the findings on the ICD derived from full-length ephrin-B2 (see Figure 9, Figure 10).

Previous experiments in this study revealed that cell stimulation with EphB1 increased Src and FAK phosphorylation as well as the generation of ephrin-B2 ICD in a γ-secretase dependent manner.

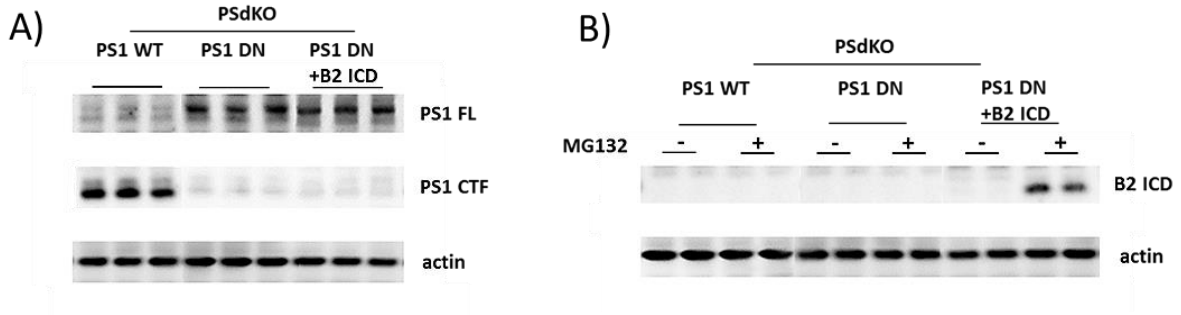

Figure 15: Stable overexpression of PS1 WT and PS1 DN in PSdKO ESdM with or without co-expression of the ephrin-B2 ICD.
A) Western immunoblot probed with a C-terminal presenilin antibody shows PSdKO cells overexpressing either PS1 WT or PS1 DN. Impaired endoproteolytic cleavage of PS1 causes characteristic accumulation of PS1 FL and low levels of PS1 CTFs in PS1 DN cells. PS1 FL panel displays longer exposure than PS1 CTF panel. **B)** Treatment with the proteasomal inhibitor MG132 (1 µM, 4 h) reveals stable overexpression of the ephrin-B2 ICD in PSdKO PS1 DN cells.

To investigate the direct role of the ephrin-B2 ICD on Src phosphorylation, cell lysates of PSdKO PS1 WT, PS1 DN, and PS1 DN with ephrin-B2 ICD overexpression were analyzed by Western immunoblotting with phosphorylation state specific antibodies for Src (Figure 16A).Densitometric analysis showed significantly decreased pSrc levels in cells overexpressing inactive PS1 (PS1 DN) in comparison to PS1 WT overexpressing cells. Interestingly, this discrepancy could be fully compensated by overexpression of the ephrin-B2 ICD in cells expressing inactive PS1 (PS1 DN+B2 ICD) (Figure 16B). In earlier studies it has been shown that autophosphorylation of FAK at Y397 creates a binding site for the SH2 domain of Src, thereby promoting complex formation of both kinases (Schaller et al., 1994). Upon recruitment to Y397-phosphorylated FAK, Src can further phosphorylate other tyrosine residues of FAK (located at positions 407, 576, 577, 861, and 925 (Calalb et al., 1995; Calalb et al., 1996; Schlaepfer et al., 1994; Schlaepfer and Hunter, 1996)) to promote maximal FAK activation. pFAK levels in PS1 DN ESdM were significantly decreased in comparison to PS1 WT cells, showing γ-secretase dependent FAK phosphorylation (Figure 16C). Notably, re-expression of the ephrin-B2 ICD in cells with non-functional PS1 normalized pFAK levels to those of PS1 WT cells, demonstrating that FAK phosphorylation can be induced by the ephrin-B2 ICD (Figure 16D).

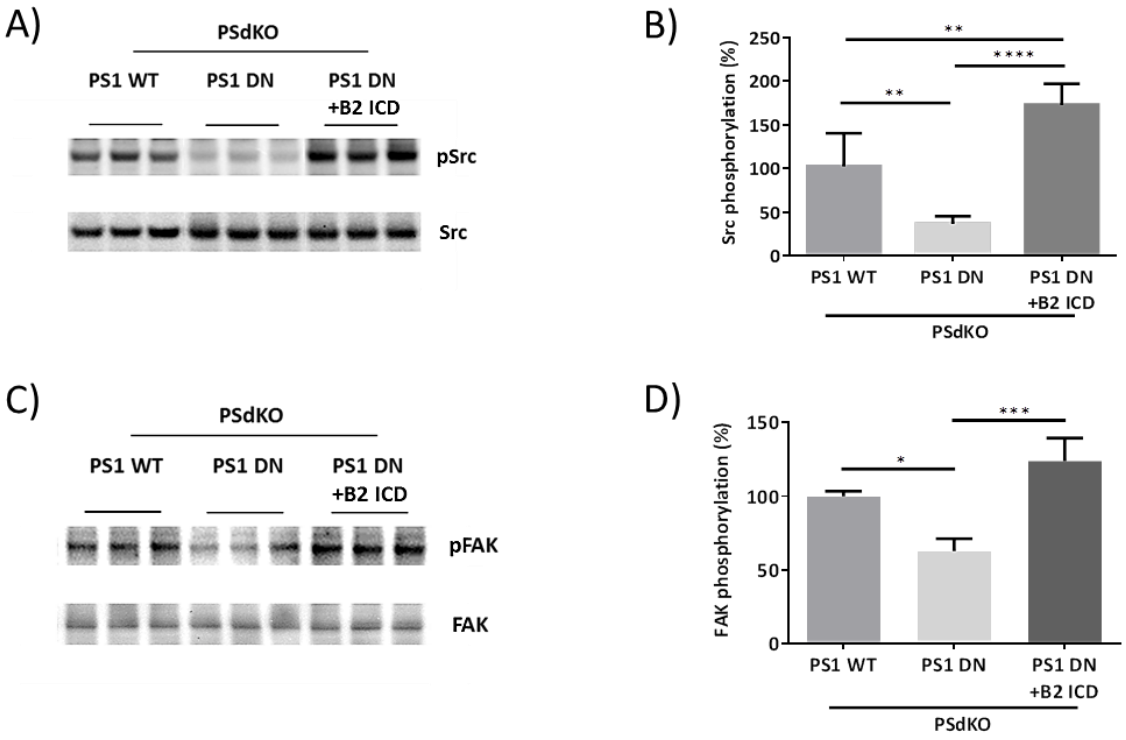

Figure 16: Src and FAK phosphorylation is mediated by ephrin-B2 ICD.
A) Western immunoblotting analysis of pSrc levels in PSdKO PS1 WT and PS1 DN with or without ephrin-B2 ICD overexpression. **B)** pSrc levels are significantly decreased in PS1 DN cells compared to PS1 WT cells. By re-expression of ephrin-B2 ICD in PS1 DN cells, pSrc levels are rescued (n=6, normalized to Src levels, One-way ANOVA with Tukey post hoc). **C)** Western immunoblotting of pFAK in previously described cell lines. **D)** Quantification shows significantly decreased pFAK levels in PS1 DN cells, which can be rescued by additional ephrin-B2 ICD overexpression (n=3, normalized to FAK levels, One-way ANOVA with Tukey post hoc). All values are represented as means ± SD.

It was previously demonstrated that Src directly binds to the ephrin-B2 ICD (Georgakopoulos et al., 2006). The above described data showed that the ephrin-B2 ICD could rescue levels of phosphorylated FAK in cells expressing non-functional PS1. Therefore, it was tested whether ephrin-B2 FL or ephrin-B2 fragments also bind to FAK (Figure 17). However, co-immunoprecipitation did not reveal direct interaction between FAK and ephrin-B2 (Figure 17).

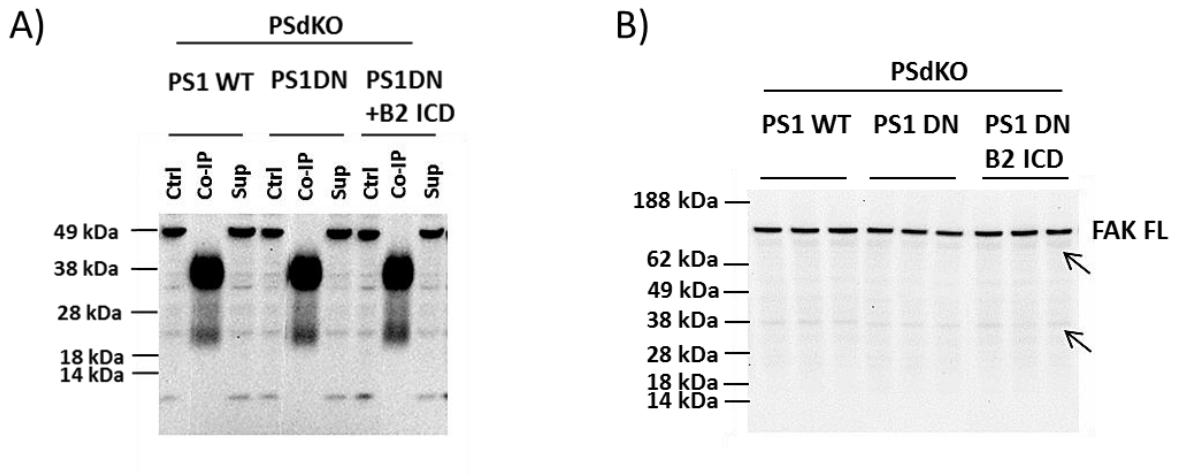

Figure 17: Ephrin B2 does not directly bind to FAK.
A) Whole cell lysates of indicated cell types were lysed using a hypotonic buffer. After pre-clearing of the lysates, they were incubated with 2 µg/ml FAK antibody and G-Sepharose overnight under rotation at 4°C. Western immunoblot shows no co-precipitation of ephrin-B2. Only heavy and light chains of the anti-FAK antibody were detected. Ctrl: Lysate before Co-IP, Co-IP: Beads coupled with FAK Ab, Sup: Lysate after Co-IP. Ctrl and supernatant (Sup) samples show similar bands in all three cell types. This indicates no direct interaction between FAK and ephrin-B2 in neither of the cell types. **B)** Demonstration of specificity of the anti-FAK antibody in whole cell lysates. Besides FAK FL protein, FAK cleavage products can weakly be detected (arrows).

3.2.4 Effects of the ephrin-B2 ICD on Akt phosphorylation

Src and FAK promote cell migration by activating multiple signaling pathways involving not only these two proteins but also phosphatidylinositol (PI) 3-kinase, p130CAS and paxillin (Cary et al., 1998; Gu et al., 1999; Richardson et al., 1997; Sieg et al., 2000). The PI3 kinase/Akt/Protein kinase B (PKB) pathway is highly conserved. PI3K activation leads to the conversion of phosphatidylinositol (3,4)-bisphosphate (PIP2) phospholipids to phosphatidylinositol (3,4,5)-trisphosphate (PIP3). PIP3 in turn can activate Akt/PKB at the plasma membrane by binding to it. Since phosphorylation of Src and FAK was decreased in non-functional PS1 expressing cells, it was investigated whether this may also affect Akt/PKB phosphorylation levels. In order to stimulate Akt/PKB phosphorylation, PS1 WT and PS1 DN cells with or without ephrin-B2 ICD overexpression were treated with insulin (Figure 18A). As opposed to PS1 WT cells, cells overexpressing non-functional PS1 showed no elevation of pAkt levels upon stimulation with insulin. Upon re-expression of the ephrin-B2 ICD in cells with inactive PS1, insulin efficiently stimulated phosphorylation of Akt (Figure 18B). These results indicate that the stimulation of phosphorylation of Akt/PKB by insulin is dependent on γ-secretase activity and that ephrin-B2 reverse signaling evokes activation of Akt/PKB.

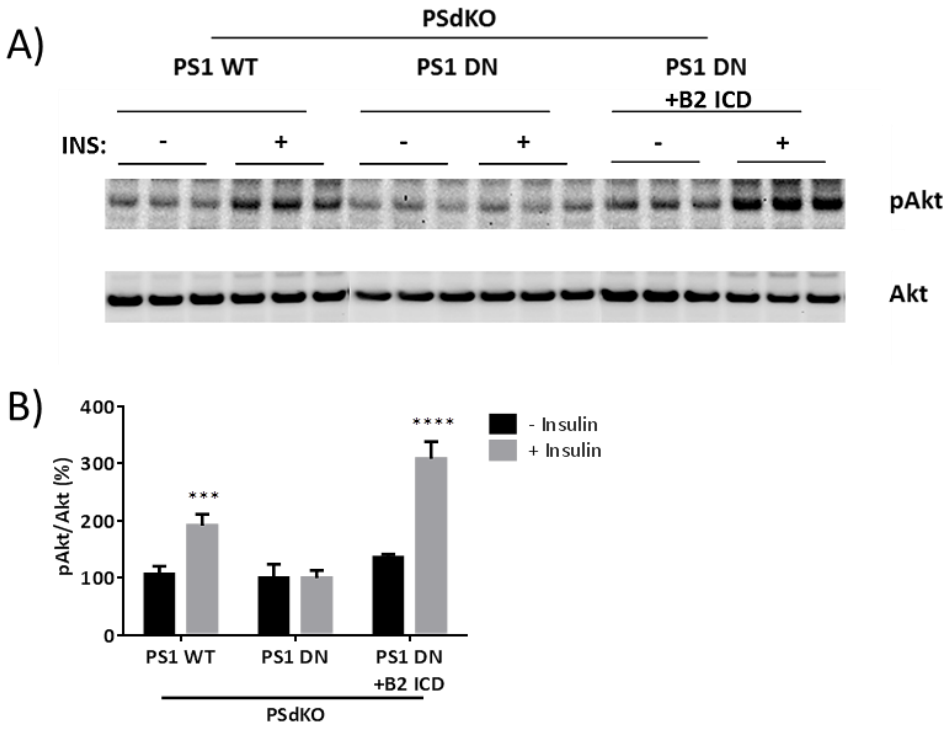

Figure 18: γ-secretase regulates ephrin-B2 induced Akt/PKB phosphorylation.
A) ESdM were treated with 100 nM insulin (INS) for 5 min. Then, pAkt levels in the different PSdKO cell lines were detected by Western immunoblot. **B)** Quantification shows a significant increase in pAkt levels in PSdKO PS1 WT cells after insulin stimulation. In cells expressing non-functional PS1, phosphorylation of Akt/PKB was not stimulated by insulin treatment. Overexpression of the ephrin-B2 ICD restored phosphorylation of Akt/PKB after insulin stimulation (n=3, normalized to Akt, Two-way ANOVA with Sidak post hoc). All data are represented as mean ± SD.

3.3 Functional effects of γ-secretase/ephrin-B2 signaling

3.3.1 Inhibition of γ-secretase affects podosomal surface

Src and FAK are known to be important modulators of podosome and FAK assembly and disassembly. Previous findings in this study showed that FAK as well as Src phosphorylation levels are decreased in cells expressing inactive PS1 (PSdKO PS1 DN). Therefore it was investigated whether these altered phosphorylation levels influence the shape or other characteristics of podosomes. Podosomes constitute a polarized pattern in the cells that predetermines the direction of migration. They are recruited to the leading edge (Figure 19A), which makes it a suitable cellular location to analyze podosomal changes. To visualize podosomes, ESdM were co-stained with the filamentous actin (F-actin) marker phalloidin (displayed in green) and a phosphotyrosine (pTyr) antibody (displayed in red) (Figure 19B).

The cells were imaged using total internal reflection fluorescence (TIRF) microscopy, which is optimal to image cellular structures located at the basal plasma membrane (also see 2.2.7).

Figure 19A illustrates the position of the image sections displayed in Figure 19B, related to the cell body. Podosomes contain an F-actin core, which is surrounded by a ring structure consisting of highly tyrosine-phosphorylated scaffold proteins (Linder and Kopp, 2005). Actin molecules therefore indicate the amount and location of podosomal structures and proteins. Figure 19C shows significantly increased actin levels per area in the leading edge of cells expressing inactive PS1 when compared to cells expressing functional PS1. Interestingly, PS1 DN cells with re-introduced ephrin-B2 ICD displayed similar actin brightness values as the PS1 WT cells. Very similar results were obtained for pTyr (Figure 19D). Since cells expressing inactive PS1 were earlier shown to possess decreased Src and FAK phosphorylation levels this finding was surprising. However, podosomes consist of highly tyrosine phosphorylated proteins and the podosomal size (represented by actin brightness) seemed to be increased. Therefore, the correlation between the increase in tyrosine phosphorylation and actin levels was determined. It was found that the increase in pTyr levels in all three cell types was similar to the size of podosomal surface (represented by actin values) (Figure 19E).

These results indicated an enlargement of the total podosomal surface in the leading edge of cells expressing inactive PS1. Since the higher brightness per area in cells with inactive PS1 might results from a similar amount of proteins concentrated on a smaller surface, it was important to analyze the size of delineated leading edges in the different cell variants. It was found that the average size of the delineated leading edge area was even larger in cells expressing inactive PS1 compared to PS1 WT cells or the rescue cells additionally expressing the ephrin-B2 ICD or PS1 WT cells (Figure 19F). The results thus show that cells expressing inactive PS1 have a brighter podosomal actin staining per area, while displaying on average larger leading edges, suggesting that these cells possess a larger podosomal surface in their leading edge. PS1 DN cells overexpressing the ephrin-B2 ICD, by contrast, display an actin staining intensity and an average leading edge size corresponding to that of the PSdKO PS1 WT cells. This indicates that γ-secretase mediated ephrin-B2 reverse signaling could regulate podosomal assembly and disassembly in the leading edge of microglial cells.

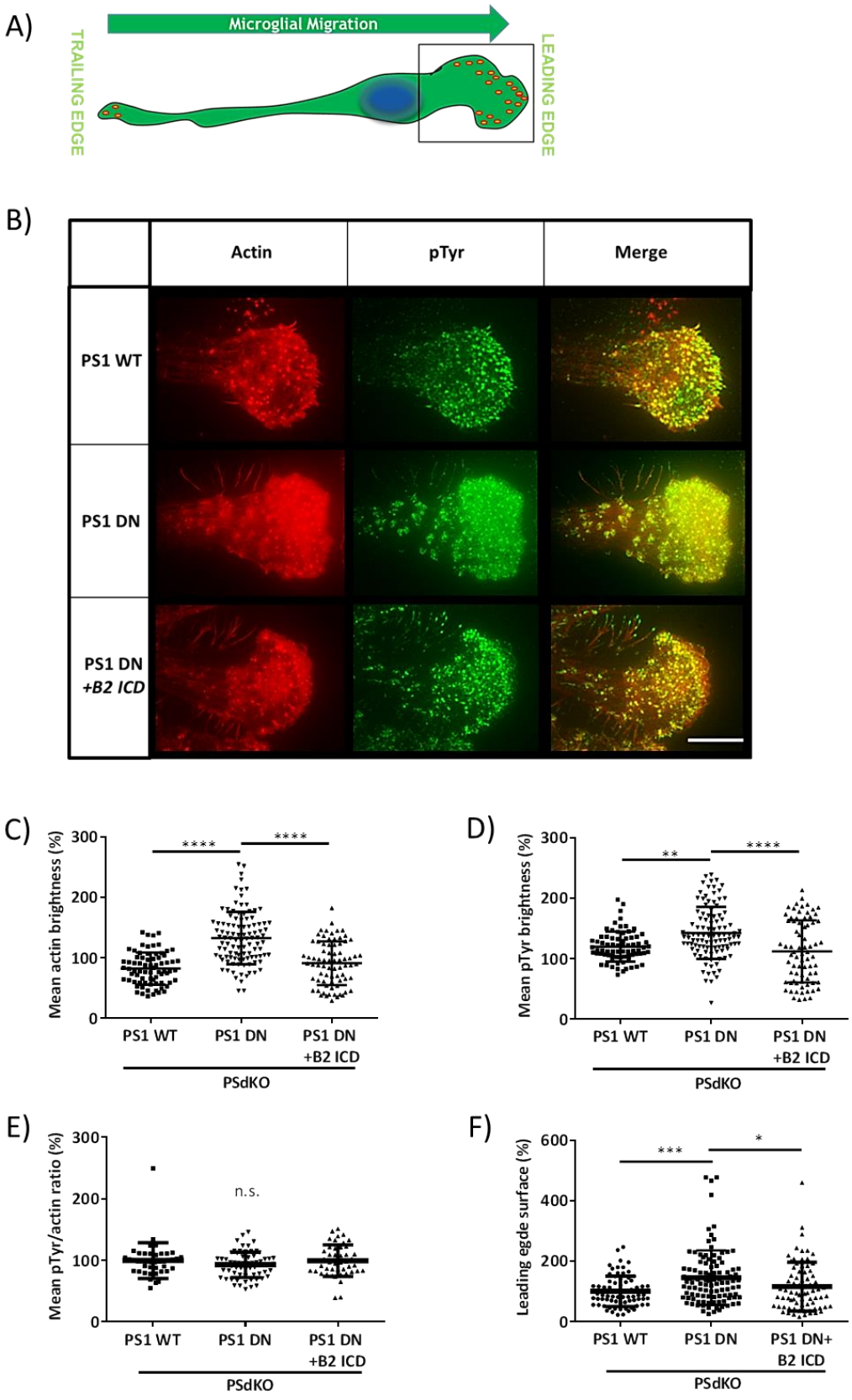

Figure 19: Podosomal surface is enlarged in cells with non-functional PS1.

Figure legend continued on page 78.

3.3.2 Involvement of γ-secretase activity in motility of microglia

Podosomal remodelling is a prerequisite for cell migration and increased podosomal and FAS surface is associated with impaired cellular motility (Ilic et al., 1995; Kaplan et al., 1994). The finding that non-functional γ-secretase causes podosomal changes in ESdM (Figure 19), led to the idea that these changes may also translate to a functional impairment of microglial motility. Therefore, random migration was assessed in cells expressing the different PS variants and the ephrin-B2 ICD. For this purpose, the cells were treated with the fractalkine CX3CL1, which has been shown to effectively stimulate migratory behaviour in ESdM (Napoli et al., 2009) and were imaged by live cell microscopy. The accumulated distance randomly travelled by the different ESdM was analyzed (Figure 20A). The motility of cells expressing inactive presenilin was significantly lower than the motility observed in PS1 WT cells. Interestingly, overexpression of ephrin-B2 ICD normalized random migration of these cells (Figure 20B).

Figure legend (Figure 19) continued from page 77.

A) Schematic view of ESdM. The leading edge is characterized by many podosomes (displayed in red) located next to each other. The position of the leading edge indicates the direction of microglial migration. Box drawn around the lamellipodium including the leading edge depicts which section of the cell is displayed in B). **B)** Representative images from total internal reflection fluorescence (TIRF) microscopy of lamellipodia in the different cell types. The bright actin and pTyr staining at the front of the lamellipodium represents the leading edge. Actin is displayed in green; phosphotyrosine (pTyr) is displayed in red. Scale bar: 10 µm. **C)** Leading edges were manually delineated and actin staining brightness per area was compared between cell lines. Quantification shows significantly increased podosomal actin levels in PS1 DN cells, overexpression of ephrin-B2 ICD in these cells leads to normalization of actin levels. **D)** pTyr levels are also increased in PS1 DN cells, but not in PS1 DN+ephrin-B2 ICD cells. **E)** Calculation of the ratio between pTyr and actin shows no difference, demonstrating that protein phosphorylation positively correlates to podosomal surface. **F)** Comparison of delineated areas in the previously analyzed cell lines shows enlarged leading edge surface area in PS1 DN in comparison to PS1 WT and PS1 DN+ ephrin-B2 ICD cells. Each group contains a minimum of 74 cells. Data was collected in two independent experiments. All data were statistically analyzed by a One-way ANOVA with Tukey post hoc and are represented as mean ± SD.

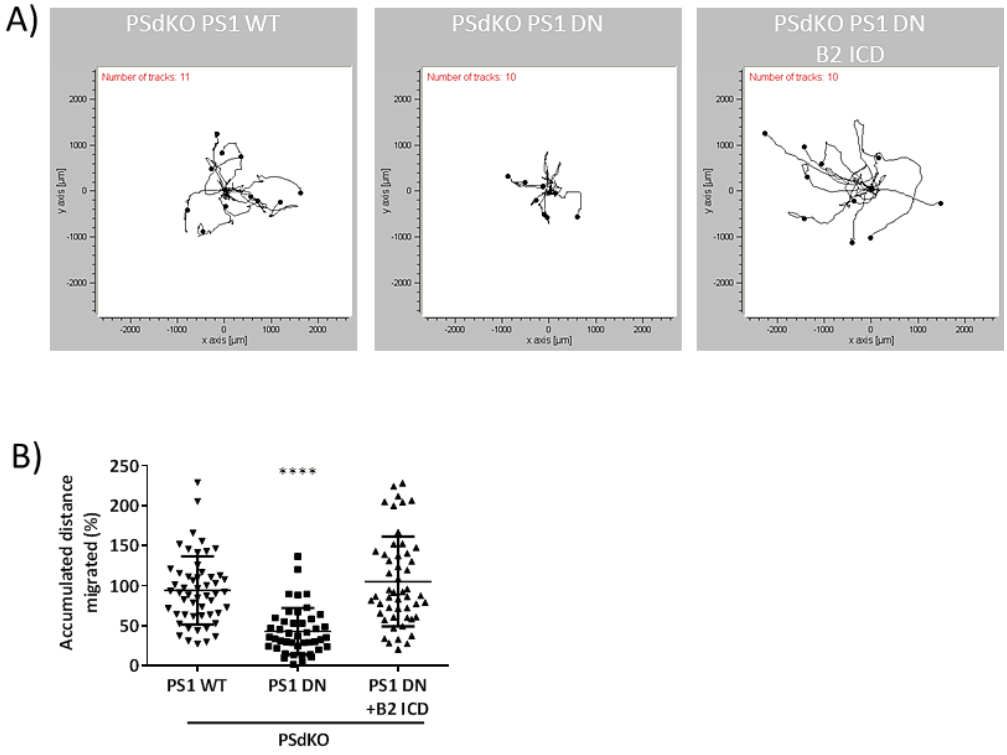

Figure 20: Involvement of functional γ-secretase and ephrin-B2 ICD in microglial migration. **A)** Representative plot of time lapse microscopy with the three different cell types. Cells were cultured in serum free medium for 16 h. Then, shortly before imaging, they were stimulated with CX3CL1 (15 ng/mL). Cells were imaged for a total of 8 h, taking one frame every 5 minutes. **B)** After manual pathway tracking, the accumulated distance travelled by the cells was analyzed. Cells expressing inactive PS1 were significantly less motile in comparison to PS1 WT cells. Decreased motility of the PS1 DN cells could be rescued by re-introduction of the ephrin-B2 ICD. Due to strong differences in migratory states of microglia, only the 10 fastest cells were analyzed per day and group. Data were collected from three independent experiments. Manual tracking was done using ImageJ (Manual tracking plug-in). Plots as well as statistical data were obtained using the Ibidi chemotaxis and migration tool. All data are represented as means ±SD and were statistically analyzed by One-way ANOVA with Tukey post hoc.

To further test the importance of ephrin-B2 during random migration of cells, with a different approach, ephrin-B2 (name of gene: EfnB2) expression was suppressed by siRNA. Figure 21A shows a qRT-PCR analysis in which ephrin-B2 mRNA levels could not be detected in cells transfected with ephrin-B2 siRNA, indicating successful knock down of ephrin-B2. The migration pathways of control and ephrin-B2 knock down cells were plotted (Figure 21B) and the accumulated distance migrated by the cells was determined. Statistical analysis between the two types of knock down cells, however, showed no difference (Figure 21C).

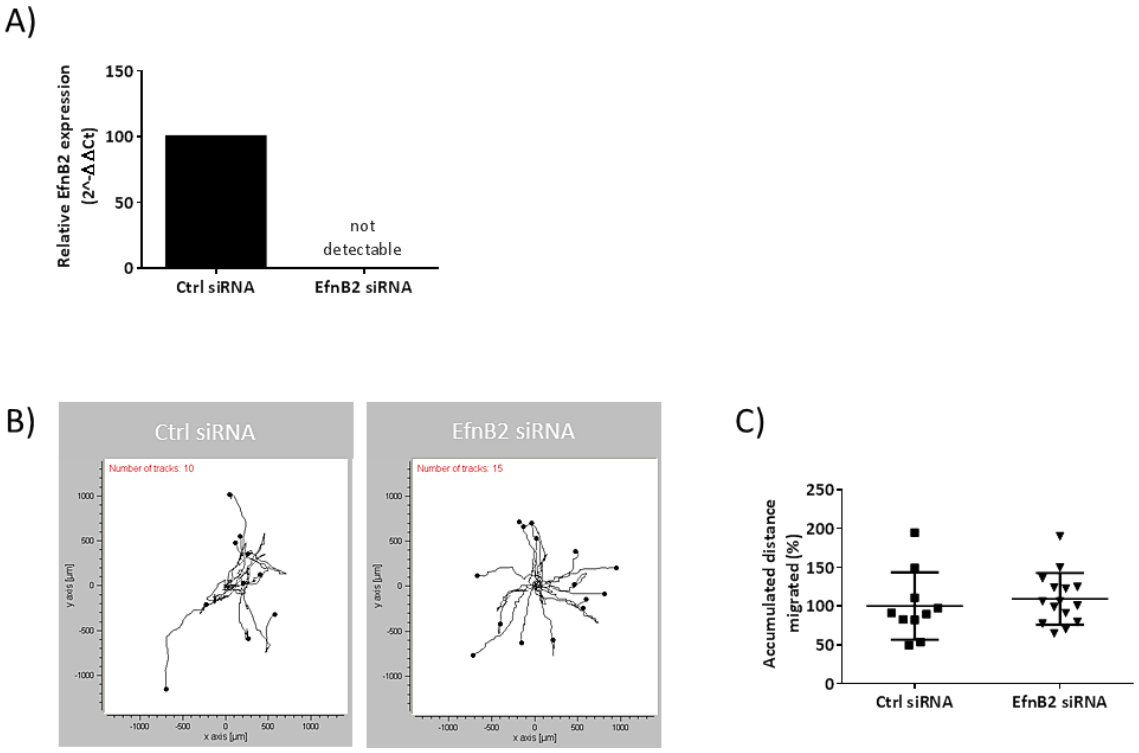

Figure 21: Ephrin-B2 is dispensable for random migration of ESdM.
A) ESdM were transfected with either control siRNA or ephrin-B2 (EfnB2) siRNA. qRT-PCR of transfected cells shows no detectable ephrin-B2 mRNA expression in EfnB2 siRNA transfected cells as compared to Ctrl siRNA transfected cells. GAPDH reference gene expression levels were similar in control and EfnB2 knock down cells (Ct value of GAPDH in Ctrl siRNA cells: 10.86, Ct value of GAPDH in B2 siRNA cells: 10.42; n=1, replicate samples=3).**B)** Random migration plots of siRNA transfected cells, which were stimulated with CX3CL1. The migration assay was performed 72 h after siRNA transfection. **C)** Statistical analysis shows unchanged accumulated random migration of ephrin-B2 knock down cells compared to Ctrl siRNA transfected cells (n=1, Student's t-test, minimum number of cells/group analyzed = 10). All data are represented as means ± SD.

3.3.3 Altered cleavage of FAK in cells without γ-secretase activity

FAK comprises three functional domains. Firstly, the protein 4.1, ezrin, radixin and moesin homology (FERM) domain, which allows FAK to interact with, for instance, the epidermal growth factor (EGF) receptor and the platelet derived growth factor (PDGF) receptor (Frame et al., 2010). Secondly, the tyrosine kinase domain, and thirdly the focal adhesion targeting (FAT) domain, which recruits FAK to focal contacts, and binds to integrin-associated proteins, such as talin and paxillin (Schaller, 2010; Schlaepfer et al., 2004).

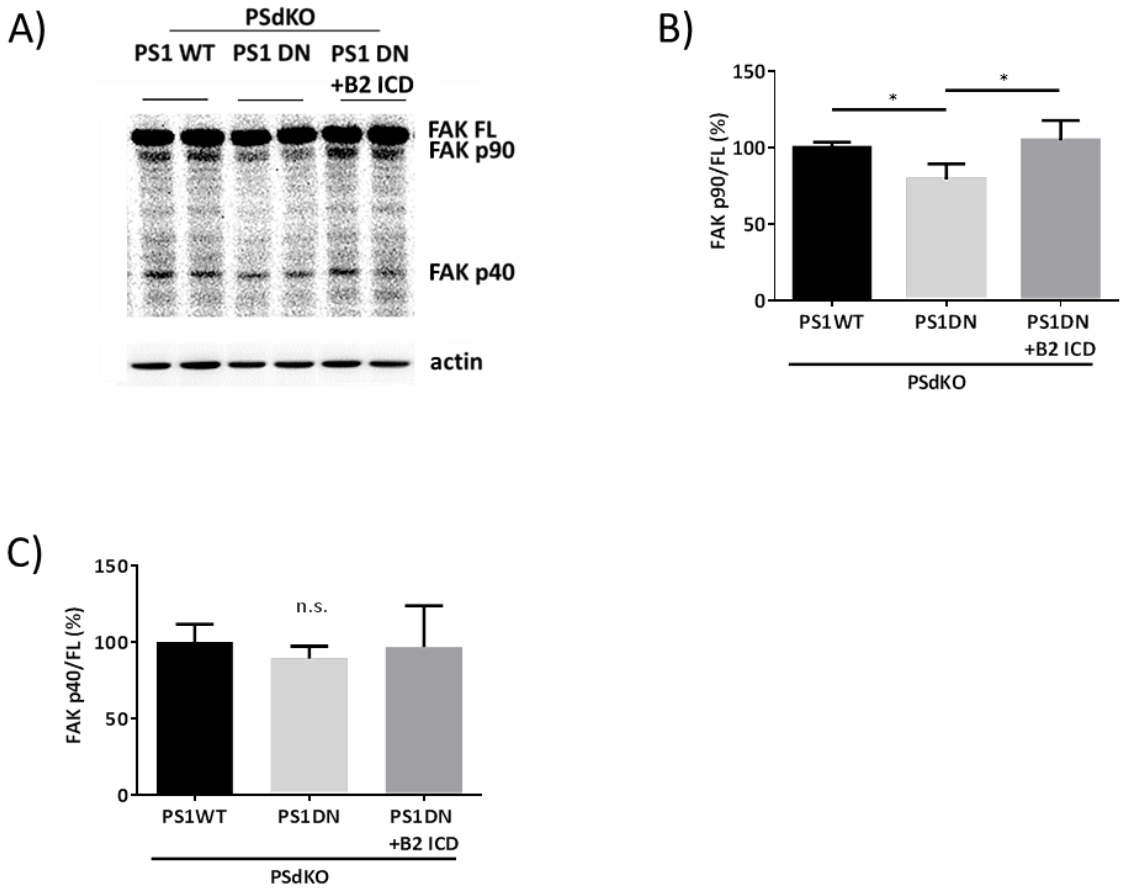

Figure 22: Role of PS1 and ephrin-B2 ICD in the cleavage of FAK.
A) Detection of FAK by Western immunoblot using an antibody against the N-terminal (binding residue AA103 to 553) in ESdM with different PS1 variants and ephrin-B2 ICD **B)** Quantification shows significant decrease of the FAK p90 fragment in cells expressing non-functional PS1 as compared to PS1 WT expressing cells. After re-expression of ephrin-B2 ICD in PS1 DN cells FAK cleavage is normalized (n=3, One-way ANOVA with Tukey post hoc). **C)** Quantification of the FAK p40 fragment shows a trend similar to the p90 fragment in all three cell lines. However, no significant differences could be detected (n=3, One-way ANOVA with Tukey post hoc). All values are represented as means ± SD.

FAK functions as a FAS adaptor molecule that transmits integrin and Src derived signals to proteins like the PI3K and the extracellular signal regulated kinase (ERK). FAK and other FAS associated proteins, are substrates for proteases of the calpain family (Carragher et al., 1999; Cooray et al., 1996; Glading et al., 2002). Calpains are calcium-dependent cysteine proteases, which play an important role in cellular motility and disassembly of FAS and podosomes (Dourdin et al., 2001; Huttenlocher et al., 1997; Palecek et al., 1998). Calpain mediated cleavage of FAK was reported to initially result in the generation of a 95 kDa and 30 kDa fragment.

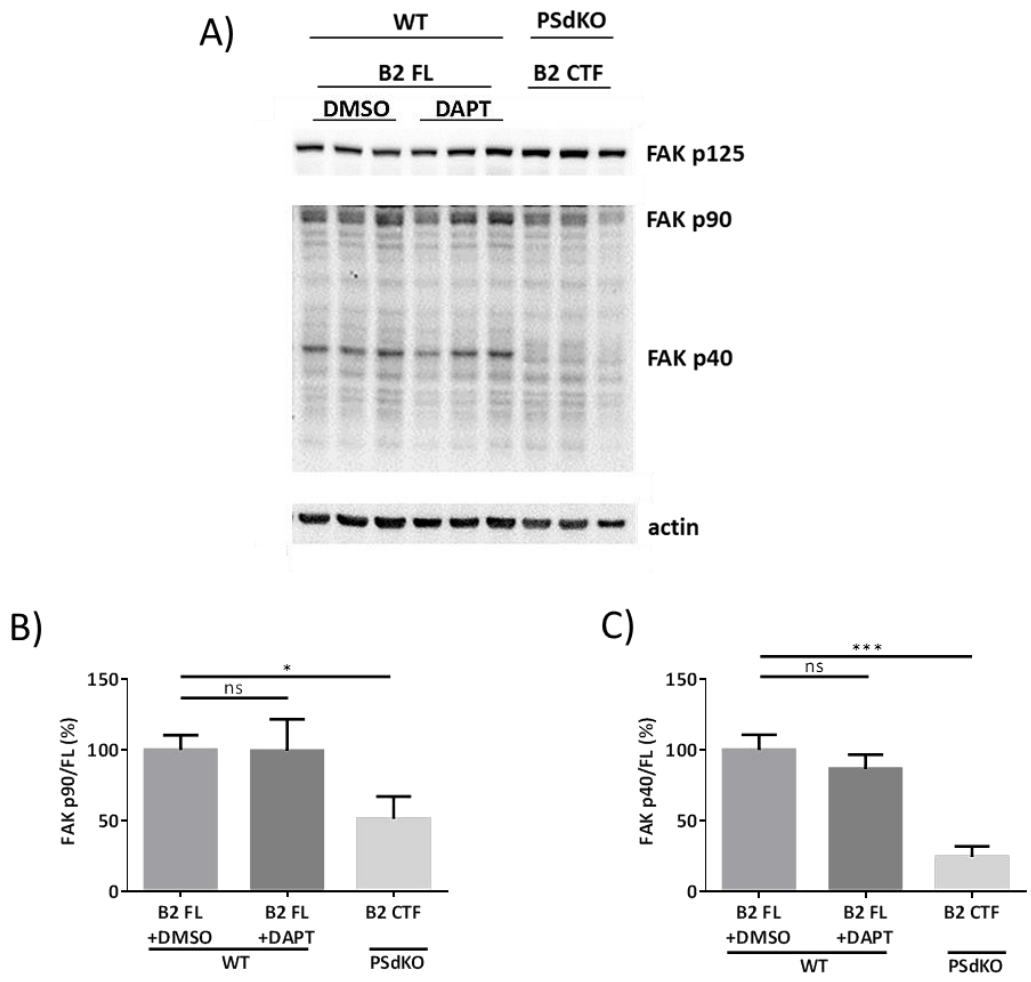

Figure 23: Impaired FAK cleavage in PSdKO cells.
A) Comparison of FAK cleavage in ESdM overexpressing ephrin-B2 FL and treated with either DAPT or DMSO, with PSdKO ephrin-B2 CTF overexpressing cells. For better visualization the FAK p90/p40 panel displays a longer exposure time than FAK FL. **B)** Densitometric analysis of FAK fragment p90 shows a significant difference between ephrin-B2 FL and PSdKO overexpressing ephrin-B2 CTF cells. **C)** Analysis shows significant decrease of FAK p40 generation between ephrin-B2 FL and PSdKO ephrin-B2 CTF overexpressing cells.
All data are represented as means ± SD.

The 95 kDa fragment has been shown to translocate from the cytoskeletal to the cytoplasmic fraction, where it is further cleaved into a 50 kDa and a 40 kDa fragment (Carragher et al., 2001; Carragher et al., 1999; Cooray et al., 1996). To investigate whether FAK cleavage is impaired in the previously described cell lines, generation of different FAK fragments was analyzed (Figure 22A). Using an antibody that binds to an N-terminal residue of FAK, the FAK FL (p125), FAK p95 and the FAK p40 could be detected. Levels of FAK p95 were significantly decreased in cells with non-functional y-secretase. When the ephrin-B2 ICD is overexpressed in those cells, FAK p95 levels normalized (Figure 22B). Although a trend to lower levels of the FAK p40 fragment could be observed in PSdKO PS1 DN cells, changes were not statistically significant (Figure 22C).

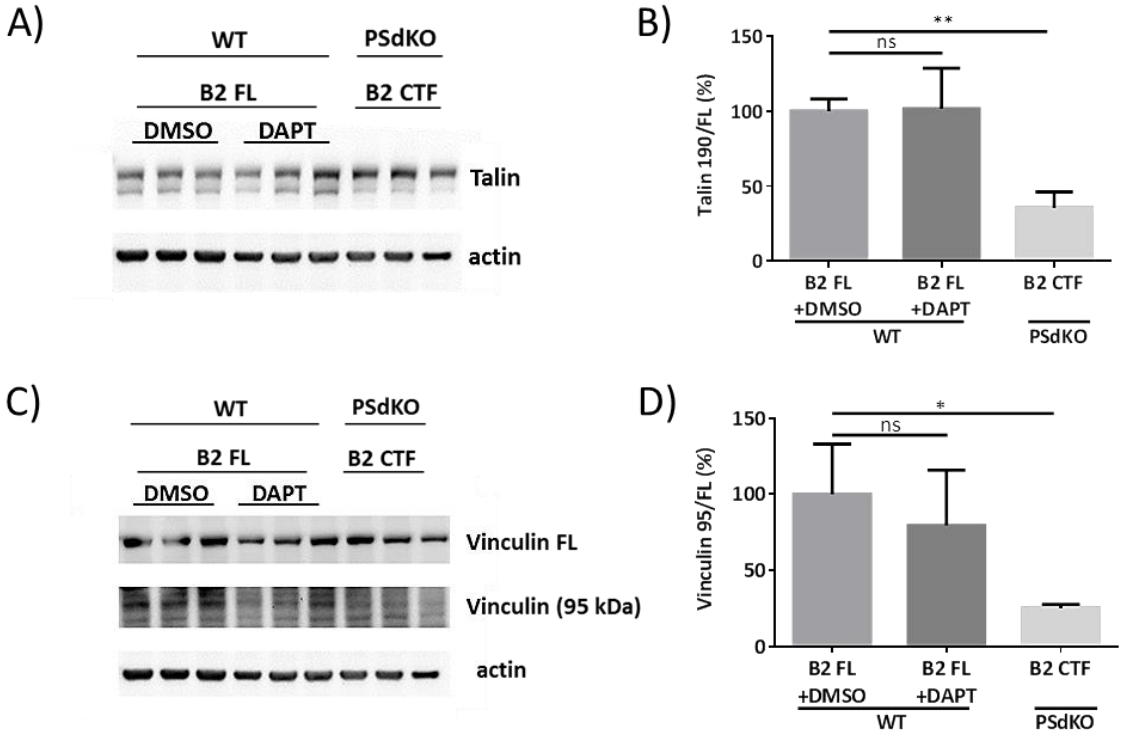

Figure 24: Processing of talin and vinculin in WT and PSdKO ESdM.
A) Detection of talin in ESdM WT after incubation with DAPT or DMSO, with PSdKO ESdM. **B)** Quantification shows no difference in talin cleavage between cells treated with DAPT or DMSO. Talin cleavage differs significantly between PSdKO ephrin-B2 CTF and WT ephrin-B2 FL cells. **C)** Comparison of vinculin cleavage in previously described cell lines. The vinculin fragment, which was revealed at ~95 kDa, is displayed after a longer exposure time than vinculin FL. D) Analysis demonstrates significant decrease of vinculin fragment 95 in PSdKO ephrin-B2 CTF cells.

In addition to FAK cleavage on a PSdKO background, processing of FAK was also investigated in ephrin-B2 FL overexpressing ESdM, which express endogenous γ-secretase. These cells were treated with the γ-secretase inhibitor DAPT or with a control solvent (DMSO) (Figure 23A). DAPT treatment did not affect FAK cleavage. Since PSdKO ephrin-B2 FL cells were not available, PSdKO overexpressing ephrin-B2 CTF cells were used in this preliminary experiment. When PSdKO overexpressing ephrin-B2 CTF cells, henceforth called PSdKO cells, were compared to the WT cells expressing ephrin-B2 FL, henceforth called WT cells (Figure 23A), a significant difference in the levels of p95 as well as the p40 fragment was measured (Figure 23B, C). Talin and vinculin are both important proteins in focal adhesion assembly and the rate of their cleavage has been shown to correlate to podosomal turnover. Like FAK, talin and vinculin are known to be cleaved by calpain (Franco et al., 2004; Schoenwaelder et al., 1997; Serrano and Devine, 2004). Talin (FL size: 230 kDa) is cleaved by calpain at amino acid 432, between its head and rod domain, to produce a 190 kDa fragment (Schoenwaelder et al., 1997). When comparing ESdM WT cells, which had been treated with or without γ-secretase inhibitor, no difference in talin cleavage was detected. Between WT and PSdKO

cells, however, a significantly decreased cleavage was observed (Figure 24A, B). Similar results were obtained when investigating vinculin cleavage in these cells. Vinculin is cleaved into multiple fragments, a major visible fragment has a molecular weight of 95 kDa (Serrano and Devine, 2004). In the PSdKO cells, less vinculin cleavage was detected (Figure 24C, D). Although these experiments show preliminary data which needs to be verified with appropriate controls, these results indicate that the function of the γ-secretase influences cleavage of multiple podosomal proteins.

3.3.4 Ephrin-B2 ICD may act as regulator of Talin-2 expression

Figure 7C shows that the ephrin-B2 ICD is translocated into the nucleus in ESdM. Next, it was tested whether the ephrin-B2 ICD influences gene expression of podosome associated proteins. mRNA levels of cells expressing functional or non-functional PS1with or without additional ephrin-B2 ICD expression were compared via qRT-PCR. The gene expression analysis showed no significant differences in the mRNA levels of talin in PS1 WT compared to PS1 DN expressing cells. However, expression of talin-2 mRNA was significantly lower in PS1 DN cells re-expressing the ephrin-B2 ICD relative to talin-2 in PS1 WT cells (Figure 25). No differences of mRNA levels were detected for the other tested FAS proteins, although a trend of reduced gene expression was observed for proteins like calpain2, FAK and talin1 in ephrin-B2 ICD expressing cells. These results could indicate a gene regulatory function for the ephrin-B2 ICD.

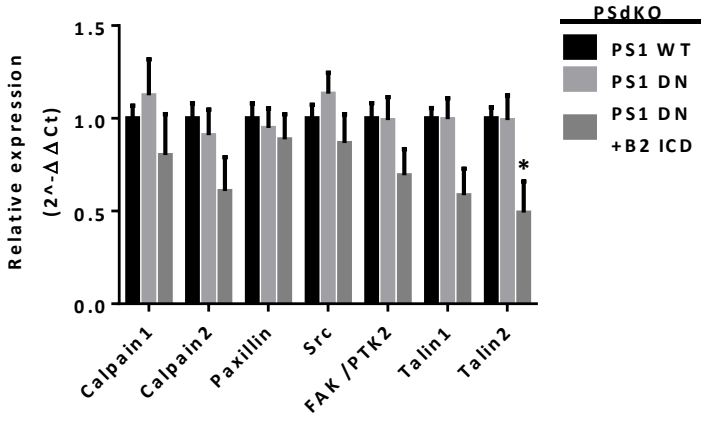

Figure 25: Ephrin-B2 ICD downregulates mRNA levels of Talin-2.
Relative gene expression analysis shows gene expression of different FAS and podosome associated proteins. The expression of the adapter protein Talin-2 is 50 % reduced in PSdKO PS1 DN ephrin-B2 ICD cells. However, PSdKO PS1 DN cells show no upregulation of Talin-2 expression (n=3). All data are represented as mean ± SD.

4. Discussion

This study shows functional involvement of the γ-secretase and ephrin-B2 in microglial physiology. In a microglial model, ephrin-B2 processing as well as stimulation of intracellular Src and FAK cascades initiated by ephrin-B2 signaling were found to be γ-secretase dependent. Importantly, ephrin-B2 processing by the γ-secretase was shown to affect podosomal dynamics as well as microglial migration.

4.1 Expression and proteolytic processing of ephrin-B2 in microglial cells

mRNA expression analysis showed that ESdM and primary microglia both endogenously express all three ephrin-B family members. Since overall mRNA expression of ephrin-Bs in microglia was low, an ESdM model was generated in which either ephrin-B2 FL, the ephrin-B2 CTF or the ephrin-B2 ICD were overexpressed. The degree of sequence homology between ephin-B1 and B2 is 56 %, while the sequence homology between ephrin-B2 and B3 is 41 %. Within the complete ICD region ephrin-B1 and B2 even show 76 % sequence homology, which may indicate similar intracellular reverse signaling cascades. Since every ephrin-B knock out displays a severe and distinctive phenotype, their presence does not seem to be redundant however. For some Eph receptors and ephrin-As on the other hand, phenotypes in knock out experiments have indicated redundancy. Three clusters of receptor genes are found on human chromosome 1 (EphA2, EphA8 and EphB2), chromosome 3 (EphA3, EphA6, EphB1 and EphB3) and on chromosome 7 (EphA1, EphB2 and EphB6) (Kullander and Klein, 2002). Mice possess similar clusters albeit not on the homologous chromosomes in humans. For ligand genes, ephrin-A1, ephrin-A3 and ephrin-A4 were found in a cluster on human chromosome 1. The arrangement of the genes suggests that these genes have evolved in a recent gene duplication process. This theory is supported by the fact that some family members possess similar functions (Table 1). Moreover, distant organisms like the fruit fly *drosophila melanogaster* and the nematode *Caenorhabditis elegans* possess a low number of Eph and ephrin genes (respectively, one Eph and one ephrin gene (Scully et al., 1999), one Eph and four ephrin genes (Chin-Sang et al., 1999; George et al., 1998; Wang et al., 1999)).

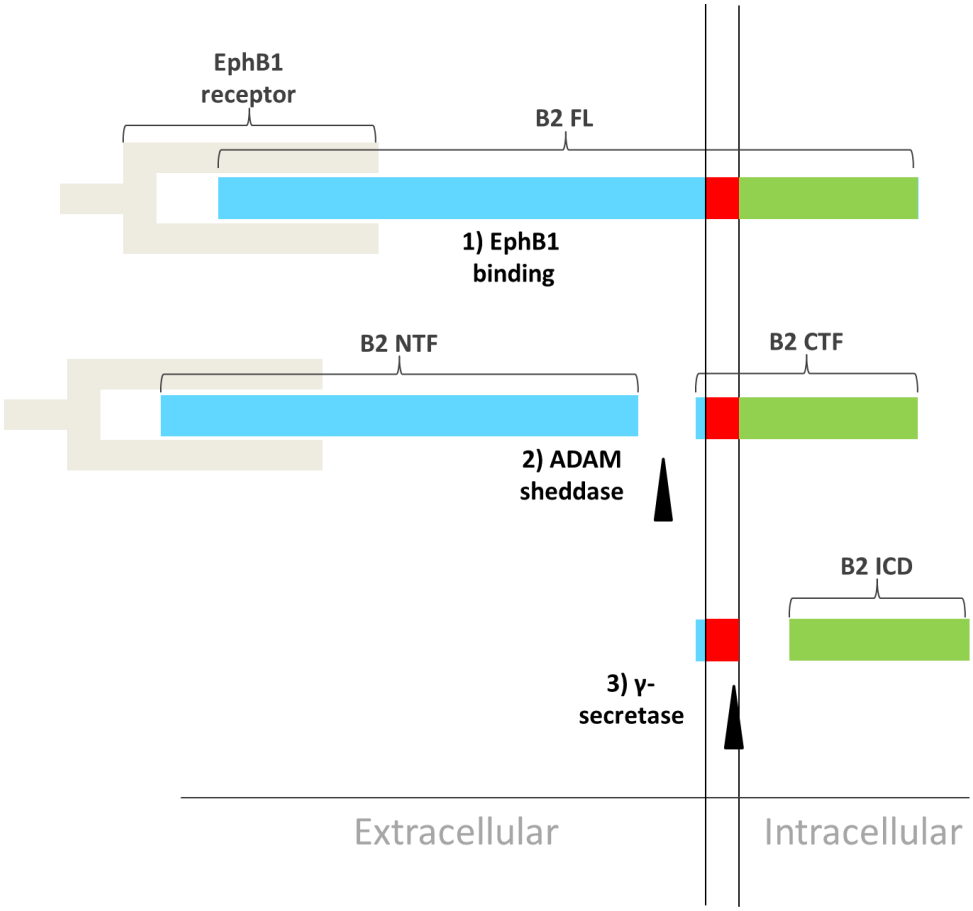

Figure 26 Ephrin-B processing in microglia.
Scheme shows **1)** extracellular EphB1 receptor binding to ephrin-B2 FL, **2)** subsequent ADAM shedding and **3)** intramembranous γ-secretase cleavage of the resultant ephrin-B CTF, thereby generating the ICD.

Endogenous ephrin-B protein in ESdM was detected as two FL bands of 50 kDa and 55 kDa after SDS-PAGE, likely caused by the divergent sizes and glycosylation of the ephrin-B family members. Ephrin-B CTFs of 20 kDa were also readily detectable, while ephrin-B ICD levels were very low. Ephrin-B2 FL was furthermore investigated regarding potential glycosylation sites. The molecular weight of ephrin-B decreased by ~5 kDa after deglycosylation, suggesting that the size deviation between predicted and apparent molecular weight was caused by post-translational modifications.

It was shown that binding of an EphB receptor caused ectodomain shedding of endogenous as well as overexpressed ephrin-B2. This mechanism has previously been described to take place in a similar fashion in fibroblasts and other cell models (Georgakopoulos et al., 2006; Tomita et al., 2006) (Figure 26). Subcellular fractionation of ESdM and BV-2 showed that ephrin-B2 FL and CTF are present in the membrane fraction. The ephrin-B2 ICD was found in the cytosol and in the nucleus, suggesting a gene regulatory function of this ephrin-B2

fragment and further supporting that after intramembranous cleavage the ICD is released from the membrane. Ephrin-B2 shedding and cleavage upon treatment with the EphB1 receptor with or without the γ-secretase inhibitor DAPT showed that ephrin-B2 cleavage, but not shedding is γ-secretase dependent. Moreover, in presenilin knock out cells, no ephrin-B2 ICD was detectable, suggesting that intramembranous processing of ephrin-B2 occurs solely by γ-secretase activity in microglial cells.

4.2 γ-secretase dependent reverse signaling of ephrin-B2

4.2.1 Ephrin-B2 ICD dependent regulation of kinases involved in cell adhesion

Others have previously revealed that Eph-ephrin signaling involves clustering of Eph-ephrin complexes (Himanen et al., 2010; Seiradake et al., 2010). It was suggested that *in trans* contact between Ephs and ephrins, initially leads to the formation of heterotetramers, followed by formation of large clusters that facilitate the transmission of forward and reverse signals. In this study it was found that when ephrin-B2 FL overexpressing ESdM were stimulated with soluble EphB1 receptor, levels of Y418 phosphorylated Src strongly increased in a time dependent manner. This shows effective EphB induced ephrin-B2 reverse signaling, potentially involving ephrin-B2 clustering. Additionally, levels of Y397 phosphorylated FAK also increased with similar kinetics after EphB1 receptor treatment in ephrin-B2 FL overexpressing cells. FAK Y397 autophosphorylation creates SH2 binding sites to which Src and other SH2 containing proteins can bind. When Src binds to Y397 phosphorylated FAK, it can further phosphorylate FAK at Y576 and Y577 to promote maximal FAK activity (Hanks et al., 2003; Mitra et al., 2005). Overall the data indicate signal transduction by ephrin-B2 in a microglial model.

Src phosphorylation of FAK SH2 domains is also associated with increased binding of SH3 domain containing podosomal proteins, such as p130 Cas, to the proline rich regions of FAK (Lim et al., 2004). It has been shown that expression of a kinase-deficient Src variant in fibroblasts decreased FAK phosphorylation. Since in our study, cells expressing non-functional PS1 also showed low Src phosphorylation, this might also be the cause for the decreased pFAK levels in these cells (Timpson et al., 2001). However, activation of FAK could also involve other ephrin-B binding proteins, which have not been investigated in this study, as for instance previously shown for Grb4 (Cowan and Henkemeyer, 2001).

Our findings show that Eph induced signaling of ephrin-B2 led to almost simultaneous activation of Src and FAK, indicating cross-activation and complex formation of both kinases. It was furthermore demonstrated that EphB receptor induced stimulation of Src is γ-secretase

dependent in microglia. It is important to note that these findings could be verified in primary microglia, supporting the physiological relevance of γ-secretase in Eph-ephrin signaling in authentic microglia and also of the ESdM as a microglial cell model. The C-terminal Src kinase (Csk) and phosphoprotein associated with GEMs (PAG)/Csk binding protein (Cbp) complex usually keeps Src bound and thereby inactive (Davidson et al., 2003; Horejsi et al., 2004; Yasuda et al., 2002). Georgakopoulos et al. demonstrated that EphB receptor binding to ephrin-B induces intramembranous cleavage of ephrin-B by the γ-secretase. This led to the release of the ephrin-B ICD from the membrane, to dissociation of Src from its inhibitory complex consisting of the Csk and PAG/Cbp. Moreover, the ephrin-B ICD was found to bind to Src, to induce autophosphorylation and thereby activation of Src (Georgakopoulos et al., 2011).

In order to investigate Src stimulation by the γ-secretase product ephrin-B2 ICD, a new cell model was established. For this purpose, presenilin double knock out ESdM cells were transduced with functional and non-functional PS 1. The homogenous genetic background of these cells allowed to exclude impacts caused by using cells from different mice. To specifically investigate effects of γ-secretase mediated cleavage of ephrin-B2, cells expressing non-functional PS1 were transduced with the ephrin-B2 ICD. PS1 WT overexpression restored Src phosphorylation levels, which overexpression of non-functional PS 1 did not, confirming γ-secretase dependence of Src phosphorylation.

Remarkably, overexpression of the ephrin-B2 ICD in the non-functional PS1 background caused a significant increase in Src phosphorylation, identifying ephrin-B2 reverse signaling as powerful regulator of Src activity. In these cells, FAK phosphorylation was similarly affected within the same time span. Our results show γ-secretase dependent phosphorylation of FAK and a rescue of FAK phosphorylation in PSdKO PS1 DN cells by ephrin-B2 ICD overexpression. This supports the postulation of simultaneous activation of Src and FAK by γ-secretase dependent ephrin-B2 reverse signaling.

The phosphoinositide-3-kinase (PI3K)/Akt cascade is known to play an important role in migration and can be activated by Src and FAK (Larsen et al., 2003; Sonoda et al., 1999; Thamilselvan et al., 2007). PI3K phosphorylates phosphatidylinositol (4,5)-bisphosphate (PtdIns(4,5)P2) to generate phosphatidylinositol (3,4,5)-trisphosphate (PtdIns(3,4,5)P3) (Chen et al., 2007). Immune cells like neutrophils, but also other cell types form sharp PtdIns(3,4,5)P3 gradients in the membrane that specify the direction of migration (Kolsch et al., 2008; Nishio et al., 2007; Servant et al., 2000). Akt can bind to PtdIns(3,4,5)P3 with its pleckstrin homology domain and thus becomes activated to initiate downstream signaling in cellular migration (Arboleda et al., 2003; Zhou et al., 2006).

To investigate whether the PI3K/Akt pathway is affected in cells expressing non-functional PS1, Akt phosphorylation levels were compared between the previously described cell lines. However, no significant differences in phosphoAkt levels were found. In order to test phosphoAkt levels upon stimulation, cells were treated with insulin, which is not only a potent activator of the PI3K/Akt pathway but has also previously been shown to activate FAK (Baron et al., 1998).

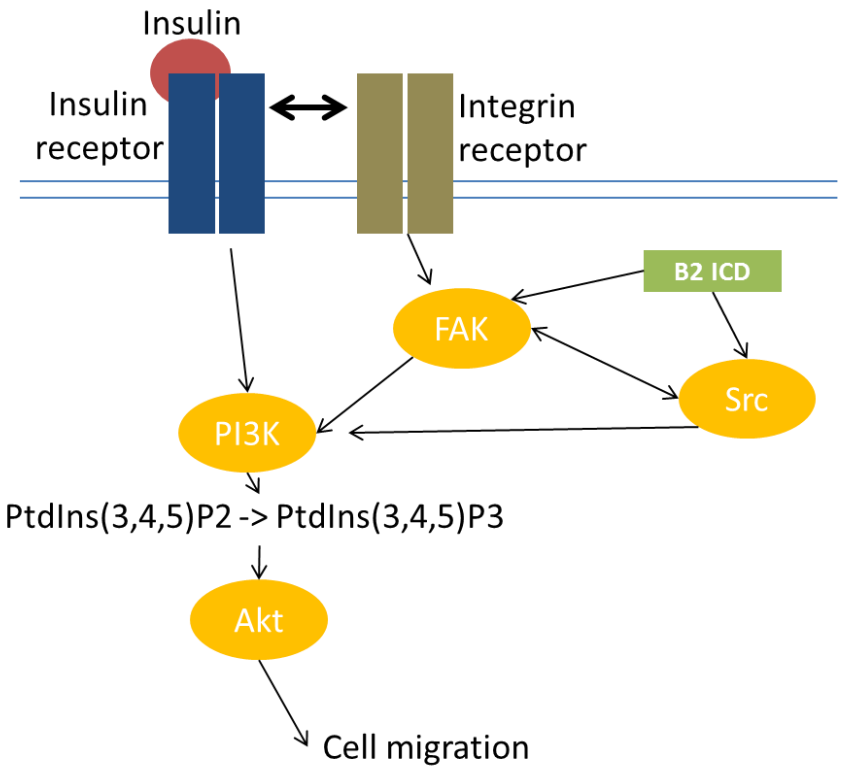

Figure 27: Akt stimulation by the insulin receptor (IR) is γ-secretase dependent.
The insulin receptor is a potent activator of the PI3K/Akt pathway. Crosstalk between the IR and an integrin receptor can additionally cause activation of FAK and Src, which in turn can activate PI3K. In the presence of ephrin-B2 ICD IR signaling may be enhanced due to high levels of phosphorylated FAK and Src.

In the insulin stimulated PSdKO PS1 DN cells, significantly decreased levels of S473 phosphorylated Akt were found, suggesting that insulin induced Akt activation is γ-secretase dependent in ESdM. In cells with non-functional PS1 re-expressing the ephrin-B2 ICD cells, however, insulin could stimulate Akt phosphorylation. The γ-secretase was proposed to control insulin signaling by controlling insulin receptor (IR) expression levels (Maesako et al., 2011). Furthermore, two studies revealed that insulin treatment stimulates migration of

hepatocytes and vascular smooth muscle cells (Benoliel et al., 1997; Wang et al., 2003). In an *in vitro* study performed in Chinese hamster ovary (CHO) cells, it was additionally demonstrated that insulin treatment increases adhesion via crosstalk between the insulin receptor (IR) and the integrin receptors, which then activates the PI3K/Akt pathway (Guilherme et al., 1998). Our findings indicate that IR signaling is affected by the γ-secretase. Since the ephrin-B2 ICD is involved in the activation of Src and FAK, it may indirectly facilitate a snowball effect of FAK and Src activation and thereby potentiate even weak signal transmission from the IR to downstream targets by PI3K/Src/FAK crosstalk (Figure 27).

4.2.2 Ephrin-B2 in the regulation of podosomes and microglial migration

Cellular migration can be subdivided into the following steps: 1) protrusion of the leading edge, determined by polarized intracellular signaling, 2)adhesion to the ECM by transmembrane receptors such as integrins, 3) contraction of the cell body and detachment of the cell rear (Petrie et al., 2009). Directional cell migration can be caused by two sources. The first source is 'intrinsic cell directionality' which is caused by a so called 'motogenic' signal (Stoker and Gherardi, 1991; Woodham and Machesky, 2014). This means, that the stimulus, such as a growth factor (Seppa et al., 1982), induces motility without providing directional information. The second source of directional cell migration is 'external regulation' (Arrieumerlou and Meyer, 2005), which mostly happens by a gradient formed for instance by chemokines (Bourne and Weiner, 2002) or ECM molecules (Carter, 1965). Random migration occurs when cells have low intrinsic cell directionality. The present data show that γ-secretase modulates reverse signaling of ephrin-B2 by intramembranous cleavage of the ephrin-B2 CTF. Interestingly, the resulting ephrin-B2 ICD regulates the phosphorylation of Src, FAK and Akt. All three kinases are known to be involved in FAS and podosome assembly and disassembly, thereby also regulating migration. As previously described, cell types that rely on a high motility, like macrophages, invasive cancer cells and dendritic cells, often form podosomes instead of FAS (Burns et al., 2001; Lehto et al., 1982; Linder et al., 1999). Both, podosomes and FAS form in a polarized manner in the cell. They are recruited to the leading edge, and thereby predetermine the direction of cellular migration. Many cells of our ESdM model displayed a clear leading edge with a single lamellipodium even without stimulation, rather than multiple lamellipodia. A single lamellipodium at the leading edge of ESdM indicates persistent intrinsic migration or in the case of gradient induced stimulation, externally regulated migration. Multiple lamellipodia indicate random migration. ESdM in culture therefore probably secrete enough growth factors to induce persistent intrinsic migration. In the adult CNS microglia usually show little migration, indicating a strong interaction with the ECM. In order to start migration they transform into an amoeboid phenotype, which likely involves cell detachment from the ECM (Eyo and Dailey, 2013).

Besides us, others also found that microglia express podosomes rather than FAS. It was demonstrated that microglia can degrade ECM molecules with proteases contained in their podosomes, similar to invading cancer cells (Siddiqui et al., 2012; Vincent et al., 2012). In the presence of the fractalkine CX3CL1, we noticed only about 10 % of motile cells in culture. This resembles findings of an *in vivo* study in which Nimmerjahn et al. observed that only 5% of microglial somata travel through the adult CNS, while processes of sessile cells are remodelled continuously. Even after local injury of the adult cortex in vivo microglia did not move for up to 5 hours (Nimmerjahn et al., 2005).

Pharmacological inhibition of the γ-secretase was previously shown to impair migration of the immortalized microglial cell line N9 after chemotactic CCL2 stimulation (Farfara et al., 2011). Downregulation of migration upon pharmacological inhibition of the γ-secretase was furthermore observed in the neuronal cell line SH-SY5Y and two breast cancer cell lines (Kim et al., 2005; Villa et al., 2014). The underlying mechanisms by which the γ-secretase regulates cellular migration have not been investigated, however.

Our results suggest that γ-secretase mediated ephrin-B2 cleavage is involved in the regulation of microglial migration by downstream Src and FAK stimulation. Remarkably, assessment of microglial motility in the previously described cell types during time lapse experiments showed significantly impaired migration in cells with inactive γ-secretase. Consistent with an important role of γ-secretase dependent cleavage of ephrin-B2 in intracellular signaling cascades, expression of the soluble ICD fully restored microglial migration. Interestingly, these results resemble findings in kinase-deficient Src, as well as FAK knock out cells, in which low Src and FAK activity were associated with reduced motility (Ilic et al., 1995; Kaplan et al., 1994).

Furthermore, ephrin-Bs have previously been shown to be involved in the regulation of neuronal migration during development (Santiago and Erickson, 2002; Senturk et al., 2011; Wang and Anderson, 1997). The homology of the three human ephrin-B family members within the signaling domain, suggests a similar function in the regulation of microglial migration between family members. To further investigate compensational mechanisms between ephrin-B family members regarding migration, a migration assay using ephrin-B2 knock down cells was performed. This preliminary experiment indicated that ephrin-B2 is not required to stimulate ESdM migration, strengthening the earlier made suggestion that the three human ephrin-B family members play similar roles in microglial migration due to the homology within their signaling sequence. However, since this experiment was only performed once, these findings will have to be verified.

Reverse signaling of ephrin-B proteins has been found to induce cell repulsion, cytoskeletal reorganization and disassembly of FAS in many cell types (Foo et al., 2006; Rudolph et al.,

2014; Tanaka et al., 2003). In this study we found that impairment of γ-secretase decreases podosomal turn-over. Notably, staining intensity of podosomal F-actin and phosphotyrosine in the leading edge was found to be increased in cells expressing non-functional PS1. Strikingly, re-expression of the ICD, led to normalization of leading edge proteins levels. These findings suggest that the podosomal leading edge surface increases when the γ- secretase complex is impaired and that the ephrin-B2 ICD is a potent regulator of podosomal assembly, disassembly or both.

The increased podosomal surface in the leading edge of cells without γ-secretase activity resembles the previously described phenotype of a Src mutant lacking its catalytic domain (Fincham et al., 2000; Kaplan et al., 1994; Timpson et al., 2001). This Src variant, which only contains the SH2 and SH3 domains (AA 1-251), translocated to and caused enlargement of FAS, which were extensively phosphorylated despite lack of Src kinase activity (Kaplan et al., 1994). These findings suggest that activation of Src promotes the turn-over of FAS by stimulating FAS disassembly rather than FAS assembly. Furthermore, Ilic et al. showed that cells from FAK knock out mice displayed a larger number of FAS (Ilic et al., 1995), indicating a similar function for FAK in the disassembly of FAS. Together with the finding that Src as well as FAK kinase activity was impaired in the absence of γ-secretase activity, the combined data indicate that γ-secretase mediated processing of ephrin-B2 and liberation of its ICD from cellular membranes regulates podosomal turn-over via phosphorylation of Src and FAK kinase.

Despite structural differences between podosomes and FAS, they consist of similar proteins (Schachtner et al., 2013). The formation of focal adhesions is induced by attachment of a cell to the ECM and subsequent clustering of integrin receptors (Vicente-Manzanares et al., 2009). Upon clustering, adaptor proteins, like talin, are recruited to the intracellular integrin domain, which in turn can bind actin-binding proteins like vinculin and a-actinin (Nagano et al., 2012). By this process, the ECM is functionally connected to the cytoskeleton. During migration these complexes undergo remodelling, thereby dis- and reconnecting from and to the ECM. Y397 phosphorylated FAK binds to Grb2 and recruits regulators of endocytosis, like dynamin, into FAS and the extension of microtubules to FAS initiates integrin internalization (Ezratty et al., 2009; Ezratty et al., 2005; Mitra et al., 2005; Mitra and Schlaepfer, 2006). Endocytic vesicles with internalized integrins are transported from the rear of the cell to the leading edge to allow establishment of new cytoskeleton-ECM interactions (Mai et al., 2011; Margadant et al., 2011; Simpson et al., 2004). Impaired FAK-Grb2 interaction due to less FAK phosphorylation and hindered integrin receptor endocytosis, may be a reason for the enlarged podosomal surface found in our microglial cell model.

Disassembly of FAS is also promoted by calpain. Pharmacological inhibition of calpain impairs retraction at the rear of the cell and cellular motility (Huttenlocher et al., 1997;

Palecek et al., 1998) and the phenotype of calpain knock out cells confirms these findings (Dourdin et al., 2001). M-Calpain (a.k.a. Calpain 2) is considered to be one of the main calpain family members implicated in cleavage of FAS and podosomal proteins, such as talin, FAK and paxillin (Chan et al., 2010; Cortesio et al., 2011; Franco and Huttenlocher, 2005; Franco et al., 2004). Calpain2 mediated cleavage of talin and vinculin has, corresponding to studies on FAK, been associated with focal adhesion turn over (Franco et al., 2004; Schoenwaelder et al., 1997; Serrano and Devine, 2004). Since we found that cells with non-functional PS1 display less Src and FAK phosphorylation together with decreased motility, it was of high interest whether calpain cleavage of FAK may be reduced. Notably, our data indicate that cleavage of FAK is, at least partially impaired in cells expressing non-functional PS1 and can be rescued by re-expression of the ephrin-B2 ICD in microglial cells. Decreased cleavage of FAK was confirmed in WT and PSdKO ESdM overexpressing ephrin-B2.

In a study by Westhoff et al, FAK phosphorylation by Src was found to be necessary to increase binding between Calpain2 and FAK (Westhoff et al., 2004). Moreover, FAK binding to calpain 2 has been shown to be important for FAK proteolysis by calpain 2 (Carragher et al., 2003). Confirming these findings, Westhoff et al. found that mutant FAK, which cannot be phosphorylated by Src, also undergoes less degradation (Westhoff et al., 2004). These results suggest that the increase in podosomal structures, observed in cells expressing non-functional PS1, may involve decreased FAK phosphorylation. This would result in lower binding between FAK and calpain, further leading to less FAK cleavage and therefore reduced podosomal turnover.

Comparison of WT and PSdKO cells overexpressing ephrin-B2 also indicated impaired cleavage of another FAS/podosomal protein, i.e. talin. Talin-1 and -2 are large cytoskeletal proteins that have been found to be crucial for focal adhesion assembly (Goksoy et al., 2008; Nayal et al., 2004). The two talin genes (tln1 and tln2) (Monkley et al., 2001; Senetar and McCann, 2005) are 74 % identical (Critchley, 2009). While talin-1 was studied in more detail, talin-2 shares the same domain structure, similar functions and binds many of the same proteins (Zhang et al., 2008). As previously mentioned, talin contains a head or FERM domain and a rod domain, both important for binding multiple FAS/podosomal proteins. The FERM domain for instance contains an F-actin binding site (Lee et al., 2004a). It binds the cytoplasmic tails of β1, β2, β3 and β7 integrin (Calderwood et al., 1999; Horwitz et al., 1986; Pfaff et al., 1998) and can also bind FAK (Chen et al., 1995). The talin head also binds acidic phospholipids (Goldmann et al., 1992; Heise et al., 1991). In two independent studies it was found that talin binds PtdIns (4,5)P2 (Di Paolo et al., 2002; Ling et al., 2002). The facts that PtdIns(4,5)P2 is the precursor for PtdIns(3,4,5)P3 and PtdIns(3,4,5)P3 levels are associated with directional migration (Kolsch et al., 2008; Nishio et al., 2007; Servant et al., 2000), link talin signaling to directional migration. The talin rod contains an additional binding site for integrins

(Moes et al., 2007; Rodius et al., 2008), at least two actin binding sites (Hemmings et al., 1996)and multiple binding sites for vinculin (Gingras et al., 2005). Accumulation of talin is an early step in the formation of FAS (Calderwood et al., 2013). Its importance was demonstrated in talin knock out embryonic stem cells, which exhibited defects in cell adhesion and spreading and lacked FAS or stress fibers (Priddle et al., 1998). FAS turnover involves talin cleavage between head and rod, and at a second site in the C-terminal dimerization domain by calpain 2 (Bate et al., 2012; Franco et al., 2004). Our findings show an increased podosomal surface as well as impaired cleavage of podosomal proteins like FAK, talin and vinculin in cells without functional PS. This suggests an involvement of γ-secretase and ephrin-B2 signaling in the regulation of calpain activity. This regulation may occur indirectly, by modulating phosphorylation states of calpain substrates.

Furthermore, after cell fractionation the ephrin-B2 ICD was localized in the nucleus, indicating a gene regulatory function. We found significant transcriptional downregulation of talin-2 upon overexpression of the ephrin-B2 ICD during gene expression analysis, indicating that the ephrin-B2 ICD acts as gene suppressor. Also, a trend to a decrease of talin-1 expression was also observed. Gene expression analysis showed no transcriptional upregulation of talin-2 in cells expressing non-functional PS1, however. These findings may result from much higher numbers of ephrin-B2 ICD molecules in overexpressing cells in comparison to the amount of endogenous molecules which are lacking in the cells expressing non-functional PS1. Alternatively, lacking ephrin-B2 ICD generation could be compensated by the ephrin–B3 ICD, since the signaling domain (AA 322-361) contained in the ICD is 100 % homologous between the ephrin-Bs. Ephrin-B3, for instance, has been reported to be cleaved in a γ-secretase independent manner, by the human rhomboid family protease 2 (RHBDL2) (Pascall and Brown, 2004). In conclusion, it is possible that by ephrin-B2 ICD mediated regulation of talin-2 expression, podosomal turnover may be stimulated or inhibited. It would be interesting to investigate whether ephrin-B family ICDs, besides the ephrin-B2 ICD also participate in the regulation of gene transcription.

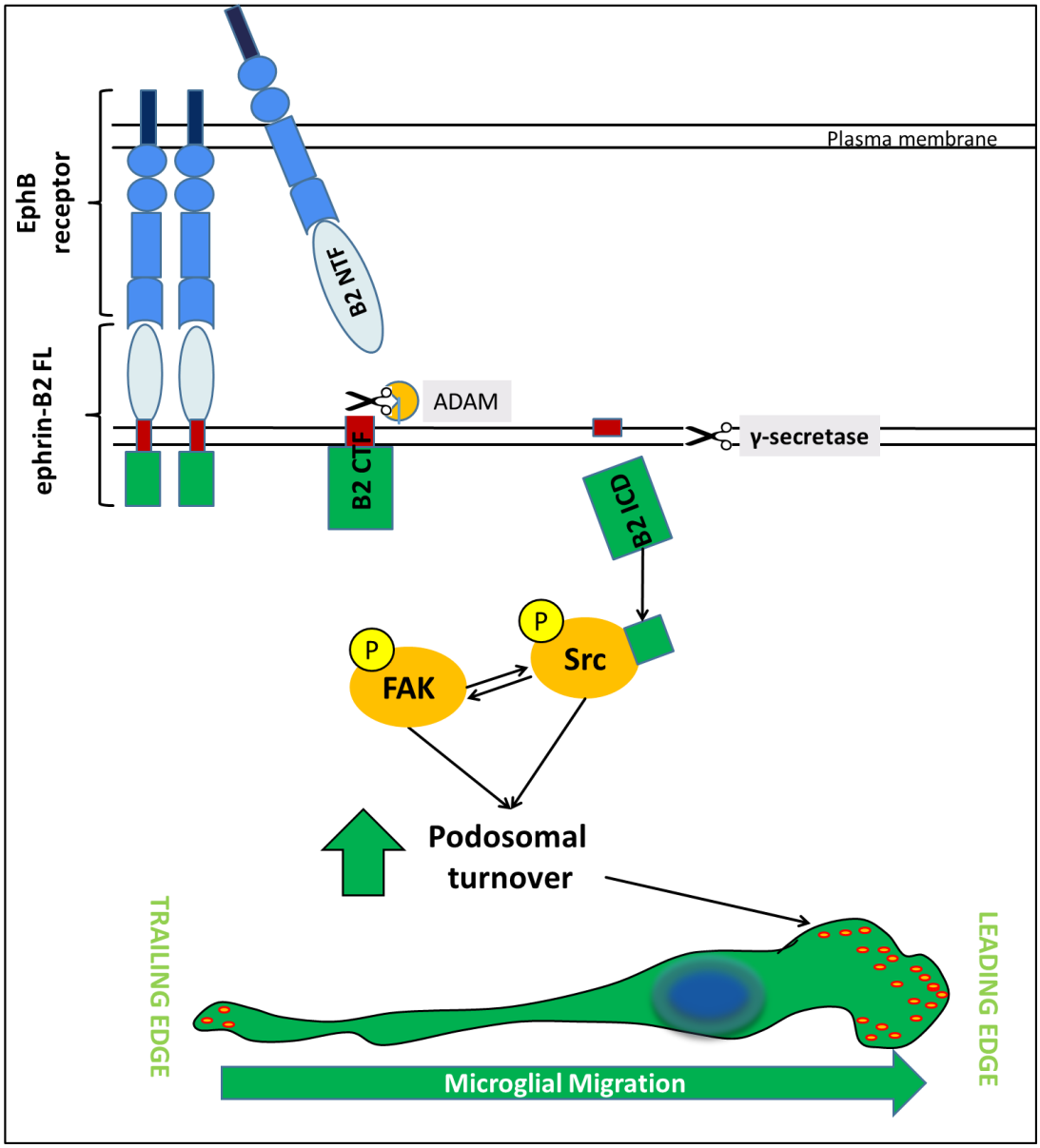

Figure 28: Model of the regulation of microglial migration by γ-secretase mediated ephrin-B2 reverse signaling.
Upon binding of the EphB1 receptor, ephrin-B2 is shed by ADAMs and subsequently intramembranously cleaved by the γ-secretase. Release of the ephrin-B2 ICD from the membrane causes Src activation, which in turn activates FAK. Increased FAK and Src activity results in higher podosomal turn over, possibly due to more calpain cleavage of podosomal proteins, and thereby to higher microglial motility.

4.3 γ-secretase mediated ephrin-B2 cleavage in the CNS

4.3.1 Potential implications for microglia with impaired motility

Our findings indicate a functional role of γ-secretase and ephrin-B2 for microglia in physiology. Since most microglia are from monocytic origin and have to migrate into the brain during development, potential stimulation by the γ-secretase and ephrin-B2 may be of great importance during this process. Furthermore, microglial migration may play a role in synaptic remodelling and efficient phagocytosis of apoptotic cells and cells debris.

Microglia, which are the first line immune defence of the CNS, show decreased immune surveillance in aged CNS tissue, demonstrated by reduced process motility and cellular migration (Damani et al., 2011; Hefendehl et al., 2014). Microglia isolated from aged mice furthermore seem to express less genes related to motility than those isolated from young mice, including genes of integrin a 4 and 6, family G (with RhoGef domain) member 5, Heparin-binding EGF-like growth factor, C-X-C chemokine receptor 4, selectin P ligand and platelet factor 4 (Orre et al., 2014). It has also been found that human brains with high amyloid loads contain a higher number of senescent microglia than non-demented with only few amyloid plaques (Flanary et al., 2007). The strongest known risk factor for AD remains progressing age. In recent years, microglia related genes have also been linked to AD. GWAS identified gene variants of the HLA-DRB4-DRB1 region (encoding for major histocompatibility complex, class II, DRβ4 and DRβ1, respectively), cluster of differentiation 33 (CD33)/Singlec-3 and the Triggering receptor on myeloid cells 2 (TREM2) that increased the risk for LOAD (Griciuc et al., 2013; Guerreiro et al., 2013; Jonsson et al., 2013; Lambert et al., 2013). These studies suggest that dysregulation of immune related pathways could influence the pathogenesis of AD. This is further supported by epidemiological studies, which showed that prolonged use of non-steroidal anti-inflammatory drugs (NSAIDs) decreased the risk for the development of AD (Imbimbo et al., 2010). Stimulation of immune related pathways might however also be a promising AD treatment. In some studies first successes with antibodies targeted against Aβ have become apparent. In passive immunization approaches with mice, antibodies were found to cross the blood brain barrier. This was associated with a reduction of the plaque burden in these mice (Schenk et al., 1999). Active immunization approaches in mice reached similar reductions of the amyloid levels in the brain and a reduction of cognitive dysfunction (Janus et al., 2000; Morgan et al., 2000). *Ex vivo* assays furthermore showed that antibody binding to Aβ plaques successfully induced microglia to phagocytose and degrade the peptides in plaques (Bard et al., 2000). These data suggest that microglia could contribute to the removal of amyloid and other harmful peptides in the brain by phagocytosis. In clinical studies, in which patients underwent active amyloid immunization, some were found to have a reduced amyloid plaque burden,

indicating that amyloid immunotherapy may be a promising treatment, at least when started at an early stage in AD progression. However, in these studies other patients developed severe meningoencephalitis (Gilman et al., 2005; Holmes et al., 2008). While it is not clear whether any of the effects seen were mediated by microglia it is likely that they at least contributed to this state. Our outcomes suggest that microglial migration may be decreased in FAD patients. This in turn might be a cause for decreased phagocytosis of amyloid in the FAD brain. It would be therefore be interesting to investigate a treatment which stimulates microglial migration but not neuroinflammation, for instance by administration of a specific ephrin-B agonist.

Strikingly, a mutation of EphA4, a receptor that binds to ephrin-As as well as to ephrin-Bs, has recently been associated with an increased risk for AD (Hollingworth et al., 2011), suggesting an involvement of the Eph-ephrin system in AD. The EphA4 receptor is expressed on glial cells within the white matter (Martone et al., 1997). Additionally, EphA and EphB receptors are associated with immunological functions (Pasquale, 2008). EphA4 receptors have been found to display an altered distribution in hippocampi of AD patients at early stages of the disease and colocalize with neuritic plaques (Rosenberger et al., 2014). This indicates that EphA4 signaling impacts memory decline in AD. It is possible that the EphA4 mutation, which was found to be linked to the occurrence of AD, also influences ephrin-A or ephrin-B reverse signaling, leading to less microglial migration.

Decreased microglial motility could not only result in a decreased clearing rate of pathogens and cell debris. As mentioned earlier, microglia probably contribute to synaptic plasticity by phagocytosing neuronal synapses (Paolicelli et al., 2011; Tremblay et al., 2010; Wake et al., 2009) and could therefore additionally affect the remodelling of neuronal circuits in AD. Interestingly, decreased EphA4 expression in a transgenic AD mouse model was associated with cognitive impairment (Simon et al., 2009), which could be a further link between EphA4 and microglial malfunctioning.

Our data demonstrate a role of the Eph-ephrin system in the regulation of microglial migration and hence indicate a potential involvement of Eph-ephrin signaling and γ-secretase in inflammation during neurodegeneration. Early onset Alzheimer's disease is often caused by loss of function mutations of the presenilins, which probably also leads to less cleavage of many γ-secretase products. This needs to be kept in mind during development of AD drugs, specifically γ-secretase inhibitors. Moreover, γ-secretase mediated ephrin-B cleavage and its regulatory effects on the migration of microglia could play important roles in chronic neuroinflammatory processes associated with several neurodegenerative diseases (Cameron and Landreth, 2010; Heneka et al., 2015).

4.3.2 Impaired γ-secretase mediated ephrin-B2 cleavage in AD

The discovery that FAD mutations in the presenilins influence the functioning of ephrin-B2 reverse signaling could have implications in many processes in which ephrin-B signaling is involved. Deduced from the fact that ephrin-B2 knock out mice die prenatally from defective early angio-and vasculogenesis and from the finding that mice which lack the ephrin-B2 ICD resemble this defective angiogenesis, it can be assumed that ephrin-B2 reverse signaling is crucial for blood vessel development (Adams et al., 2001; Gerety et al., 1999; Wang et al., 1998).

Interestingly, presenilin knock out mice also display dramatic vascular defects (Nakajima et al., 2003). Vascular pathology has been discovered in human PS1 and PS2 associated FAD cases, which mimic the pathology found in sporadic AD cases (Lleo et al., 2004). It is likely that FAD mutations affect ephrin-B1 and –B2 cleavage, which could at least contribute to the vasculo- and angiogenic defects observed in FAD patients. Besides the vascular pathology, called cerebral amyloid angiopathy (CAA), in which amyloid is deposited in the vascular walls, defects in the microvasculature have been found to be characteristic for patients suffering from familial Alzheimer's disease. In these patients, the microvasculature is less dense and shows decreased branching in the basal forebrain and the hippocampus, while other vasculature is looped and kinked (Buee et al., 1994; Fischer et al., 1990). Down syndrome patients, which are known to express large amounts of APP, display similar vascular defects at a young age preceding amyloid plaque formation, indicating the potential importance of vascular pathology for the development of Alzheimer's disease (Buee et al., 1994).

While defective ephrin-B cleavage in endothelial cells might contribute to defects in vasculo- and angiogenesis, impaired ephrin-B cleavage and/or signaling in neuronal cells could contribute to a decreased post-synaptic signal transmission in FAD. In cellular *in vitro* studies, additional complementary findings in ephrin-B defective as well as FAD mutated cells relate to defective post-synaptic transmission and LTP (Calo et al., 2006; Dalva et al., 2000). Loss of presenilin is associated with memory impairments preceding age-dependent neurodegeneration (Saura et al., 2004). Presenilin was found to associate with post-synaptic NMDA receptors and was suggested to support the synaptic delivery and localization of NMDA receptors. Interestingly, EphB binding to ephrin-B was shown to induce formation of large NMDA receptor patches (Calo et al., 2006; Dalva et al., 2000), indicating synergistic actions of γ-secretase dependent ephrin-B reverse signaling in NMDA functioning. Cisse et. al furthermore found that overexpression of hippocampal EphB2, which regulates NMDA receptor function, could reverse long term potentiation and memory deficits in amyloid precursor protein transgenic mice (Cisse et al., 2011). Like in conditional presenilin knock out mice, impaired ephrin-B function also results in memory impairments. Ephrin-B3 mutant mice

display impaired hippocampal LTP and less proficiency in hippocampal-based learning tasks (Rodenas-Ruano et al., 2006), whereas ephrin-B2 conditional knockout mice exhibited severe deficits in both LTP and in long-term depression(Bouzioukh et al., 2007; Grunwald et al., 2004). Lastly, ephrin-B1 impairment has been found to be detrimental in non-spatial learning and memory (Arvanitis et al., 2014).

Besides their function in memory and learning, ephrin-B molecules were also found to be essential for neuronal migration during development. In a study by Senturk et al. ephrin-B2, and/or –B3 overexpression resulted in a full rescue of the severe developmental disorder lissencephaly, in which the brain displays an inside-out order of the neuronal layers in the cortex (a.k.a. reeler phenotype in mice). The glycoprotein reelin binds to two lipoprotein receptors, namely the very low density lipoprotein receptor (VLDLR) and the apolipoprotein E receptor 2 (ApoER2). The study suggests that ephrin-B acts as a co-receptor for VLDLR and ApoER2, thereby activating downstream effectors like Dab1 and stimulating neuronal migration during development (Senturk et al., 2011).

5. Outlook

The present study revealed the importance of γ-secretase in the regulation of ephrin-B2 reverse signaling in microglia. Our results show the release of soluble ephrin-B2 ICD and the activation of downstream targets upon ephrin-B2 reverse signaling, like Src and FAK in a microglial model. Since knock out of the three ephrin-Bs demonstrates three different phenotypes and henceforth no redundancy between them, it would be interesting to investigate different and common effects of all ephrin-B family members, regarding intracellular pathways and their effect on microglial migration.

One could also investigate microglial migration defects in FAD and different ephrin-B knock out mouse models and, more specifically investigate by conditional knock outs of the ephrin-Bs in microglia how this influences cognitive functions of the test animals. It has previously been shown that chemotaxis of cells can be strongly affected by ephrin-B reverse signaling, which regulates PDZ-RGS and thereby mediates SDF-1 stimulation (Lu et al., 2001). As mentioned above, this could also indicate further regulation of G-protein coupled receptor, like chemokine receptors, by ephrin-B reverse signaling. *In vivo* experiments in which the motility of microglia generated in this study could be assessed in cortical tissue could give information about the reliability of our *in vitro* findings. In these experiments could also be tested whether chemotaxis of PSdKO cells towards typical stimuli present in the AD brain is impaired.

Furthermore, the finding that an EphA4 mutation correlates to the occurrence of LOAD indicates an involvement of the Eph-ephrin system in AD. Since abnormal EphA4 expression in murine hippocampi has been associated with a cognitive decline, it would be interesting to also test ephrin-B expression patterns in the AD brain.

This study strongly suggests an important role of the γ-secretase in the brain, beyond APP cleavage. Therefore general γ-secretase inhibition would likely have detrimental immunological consequences in the CNS. One of the most interesting therapeutic AD approaches is the investigation of immunotherapies. There have already been several clinical trials, which investigated the effects of immunotherapy on the amyloid plaque load in AD patients. A problem in these trials has been the occurrence of meningoencephalitis. Another major problem in some studies was that a decreased plaque load was not always associated with improved cognitive functions. Our data indicate an involvement of γ-secretase mediated ephrin-B2 cleavage in the regulation of microglial migration. Therefore, an interesting approach for an AD therapy would be specific stimulation of microglia by an ephrin-B agonist, and additional NSAID treatment, as the first would stimulate migration, while

the latter suppresses inflammatory cytokine production. It is possible that a higher degree of motility not only increases phagocytosis of cell debris, but also stimulates synaptic remodelling.

6. Abstract

The Eph-ephrin system plays pivotal roles during development and adulthood in cell-cell interaction, cell adhesion and migration. It has previously been shown that ephrin-B1 and 2 can be cleaved intramembranously by the γ-secretase. γ-Secretase mediated processing of ephrin-B has furthermore been linked to activation of Src, a kinase crucial for focal adhesion and podosome phosphorylation. Due to the finding that many familial Alzheimer's disease (FAD) mutations are located in the catalytic subunit of the γ-secretase, i.e. presenilin, the γ-secretase has in the past decades mainly been subject of investigation in early Alzheimer's disease (EOAD) studies. Additionally, the positive correlation between occurrence of late onset Alzheimer's disease (LOAD) and mutations in genes mainly expressed by microglia has drawn attention to these cells.

In this study, the role of γ-secretase and ephrin signaling on downstream effectors, podosomal turnover and the migration of embryonic stem cell derived microglia (ESdM) was tested. We demonstrate extracellular shedding and subsequent intramembranous ephin-B2 cleavage by the γ-secretase upon EphB1 receptor binding in a microglial cell model. It was furthermore found that proteolytic release of the ephrin-B2 intracellular domain (ICD) stimulates Src and FAK activity.

ESdM from presenilin double knock out (PSdKO) and wild type (WT) mice were transduced with either WT presenilin 1 (PS1 WT) or with non-functional presenilin containing an inactivating mutation (PS1 DN). A rescue cell type of the PSdKO PS1 DN cells was generated, which additionally expressed the ephrin-B2 ICD. Expression of non-functional presenilin 1 could not rescue phosphorylation of Src and FAK. Cell motility and podosomal morphology were also changed in these cells. More specifically, this genotype was associated with decreased motility and an enlargement of podosomal surface. Also, the present results indicate impaired cleavage of podosomal proteins like FAK, talin and vinculin in cells with inactive γ-secretase.

Interestingly, ephrin-B2 ICD expression could fully rescue this phenotype, indicating that ephrin-B2 ICD mediated activation of Src and FAK modulates podosomal dynamics in microglial cells. Together, these results identify γ-secretase as well as ephrin-B2 as important regulators of microglial migration.

7. References

Adams, R. H., Diella, F., Hennig, S., Helmbacher, F., Deutsch, U. and Klein, R. (2001). The cytoplasmic domain of the ligand ephrinB2 is required for vascular morphogenesis but not cranial neural crest migration. *Cell* **104**, 57-69.

Akiyama, H., Barger, S., Barnum, S., Bradt, B., Bauer, J., Cole, G. M., Cooper, N. R., Eikelenboom, P., Emmerling, M., Fiebich, B. L. et al. (2000). Inflammation and Alzheimer's disease. *Neurobiol Aging* **21**, 383-421.

Anders, L., Mertins, P., Lammich, S., Murgia, M., Hartmann, D., Saftig, P., Haass, C. and Ullrich, A. (2006). Furin-, ADAM 10-, and gamma-secretase-mediated cleavage of a receptor tyrosine phosphatase and regulation of beta-catenin's transcriptional activity. *Mol Cell Biol* **26**, 3917-34.

Andersson, C. X., Fernandez-Rodriguez, J., Laos, S., Baeckstrom, D., Haass, C. and Hansson, G. C. (2005). Shedding and gamma-secretase-mediated intramembrane proteolysis of the mucin-type molecule CD43. *Biochem J* **387**, 377-84.

Andersson, E. R., Sandberg, R. and Lendahl, U. (2011). Notch signaling: simplicity in design, versatility in function. *Development* **138**, 3593-612.

Arboleda, M. J., Lyons, J. F., Kabbinavar, F. F., Bray, M. R., Snow, B. E., Ayala, R., Danino, M., Karlan, B. Y. and Slamon, D. J. (2003). Overexpression of AKT2/protein kinase Bbeta leads to up-regulation of beta1 integrins, increased invasion, and metastasis of human breast and ovarian cancer cells. *Cancer Res* **63**, 196-206.

Arrieumerlou, C. and Meyer, T. (2005). A local coupling model and compass parameter for eukaryotic chemotaxis. *Dev Cell* **8**, 215-27.

Arvanitis, D. and Davy, A. (2008). Eph/ephrin signaling: networks. *Genes Dev* **22**, 416-29.

Arvanitis, D. N., Behar, A., Drougard, A., Roullet, P. and Davy, A. (2014). Cortical abnormalities and non-spatial learning deficits in a mouse model of CranioFrontoNasal syndrome. *PLoS One* **9**, e88325.

Asundi, V. K. and Carey, D. J. (1995). Self-association of N-syndecan (syndecan-3) core protein is mediated by a novel structural motif in the transmembrane domain and ectodomain flanking region. *J Biol Chem* **270**, 26404-10.

Balcaitis, S., Weinstein, J. R., Li, S., Chamberlain, J. S. and Moller, T. (2005). Lentiviral transduction of microglial cells. *Glia* **50**, 48-55.

Barcia, C., Ros, C. M., Annese, V., Carrillo-de Sauvage, M. A., Ros-Bernal, F., Gomez, A., Yuste, J. E., Campuzano, C. M., de Pablos, V., Fernandez-Villalba, E. et al. (2012). ROCK/Cdc42-mediated microglial motility and gliapse formation lead to phagocytosis of degenerating dopaminergic neurons in vivo. *Sci Rep* **2**, 809.

Bard, F., Cannon, C., Barbour, R., Burke, R. L., Games, D., Grajeda, H., Guido, T., Hu, K., Huang, J., Johnson-Wood, K. et al. (2000). Peripherally administered antibodies against amyloid beta-peptide enter the central nervous system and reduce pathology in a mouse model of Alzheimer disease. *Nat Med* **6**, 916-9.

Baron, V., Calleja, V., Ferrari, P., Alengrin, F. and Van Obberghen, E. (1998). p125Fak focal adhesion kinase is a substrate for the insulin and insulin-like growth factor-I tyrosine kinase receptors. *J Biol Chem* **273**, 7162-8.

Bate, N., Gingras, A. R., Bachir, A., Horwitz, R., Ye, F., Patel, B., Goult, B. T. and Critchley, D. R. (2012). Talin contains a C-terminal calpain2 cleavage site important in focal adhesion dynamics. *PLoS One* **7**, e34461.

Beauchamp, A., Lively, M. O., Mintz, A., Gibo, D., Wykosky, J. and Debinski, W. (2012). EphrinA1 is released in three forms from cancer cells by matrix metalloproteases. *Mol Cell Biol* **32**, 3253-64.

Becker-Herman, S., Arie, G., Medvedovsky, H., Kerem, A. and Shachar, I. (2005). CD74 is a member of the regulated intramembrane proteolysis-processed protein family. *Mol Biol Cell* **16**, 5061-9.

Beitz, J. M. (2014). Parkinson's disease: a review. *Front Biosci (Schol Ed)* **6**, 65-74.

Benilova, I., Karran, E. and De Strooper, B. (2012). The toxic Abeta oligomer and Alzheimer's disease: an emperor in need of clothes. *Nat Neurosci* **15**, 349-57.

Benoliel, A. M., Kahn-Perles, B., Imbert, J. and Verrando, P. (1997). Insulin stimulates haptotactic migration of human epidermal keratinocytes through activation of NF-kappa B transcription factor. *J Cell Sci* **110 (Pt 17)**, 2089-97.

Benson, M. D., Romero, M. I., Lush, M. E., Lu, Q. R., Henkemeyer, M. and Parada, L. F. (2005). Ephrin-B3 is a myelin-based inhibitor of neurite outgrowth. *Proc Natl Acad Sci U S A* **102**, 10694-9.

Bergman, A., Laudon, H., Winblad, B., Lundkvist, J. and Naslund, J. (2004). The extreme C terminus of presenilin 1 is essential for gamma-secretase complex assembly and activity. *J Biol Chem* **279**, 45564-72.

Bertout, J. A., Patel, S. A., Fryer, B. H., Durham, A. C., Covello, K. L., Olive, K. P., Goldschmidt, M. H. and Simon, M. C. (2009). Heterozygosity for hypoxia inducible factor 1alpha decreases the incidence of thymic lymphomas in a p53 mutant mouse model. *Cancer Res* **69**, 3213-20.

Beutner, C., Linnartz-Gerlach, B., Schmidt, S. V., Beyer, M., Mallmann, M. R., Staratschek-Jox, A., Schultze, J. L. and Neumann, H. (2013). Unique transcriptome signature of mouse microglia. *Glia* **61**, 1429-42.

Bianchin, M. M., Capella, H. M., Chaves, D. L., Steindel, M., Grisard, E. C., Ganev, G. G., da Silva Junior, J. P., Neto Evaldo, S., Poffo, M. A., Walz, R. et al. (2004). Nasu-Hakola disease (polycystic lipomembranous osteodysplasia with sclerosing leukoencephalopathy--PLOSL): a dementia associated with bone cystic lesions. From clinical to genetic and molecular aspects. *Cell Mol Neurobiol* **24**, 1-24.

Bird, T. D., Lampe, T. H., Nemens, E. J., Miner, G. W., Sumi, S. M. and Schellenberg, G. D. (1988). Familial Alzheimer's disease in American descendants of the Volga Germans: probable genetic founder effect. *Ann Neurol* **23**, 25-31.

Blasi, E., Barluzzi, R., Bocchini, V., Mazzolla, R. and Bistoni, F. (1990). Immortalization of murine microglial cells by a v-raf/v-myc carrying retrovirus. *J Neuroimmunol* **27**, 229-37.

Block, M. R., Badowski, C., Millon-Fremillon, A., Bouvard, D., Bouin, A. P., Faurobert, E., Gerber-Scokaert, D., Planus, E. and Albiges-Rizo, C. (2008). Podosome-type adhesions and focal adhesions, so alike yet so different. *Eur J Cell Biol* **87**, 491-506.

Boche, D., Perry, V. H. and Nicoll, J. A. (2013). Review: activation patterns of microglia and their identification in the human brain. *Neuropathol Appl Neurobiol* **39**, 3-18.

Bonn, S., Seeburg, P. H. and Schwarz, M. K. (2007). Combinatorial expression of alpha- and gamma-protocadherins alters their presenilin-dependent processing. *Mol Cell Biol* **27**, 4121-32.

Borg, J. P., Yang, Y., De Taddeo-Borg, M., Margolis, B. and Turner, R. S. (1998). The X11alpha protein slows cellular amyloid precursor protein processing and reduces Abeta40 and Abeta42 secretion. *J Biol Chem* **273**, 14761-6.

Bourne, H. R. and Weiner, O. (2002). A chemical compass. *Nature* **419**, 21.

Bouzioukh, F., Wilkinson, G. A., Adelmann, G., Frotscher, M., Stein, V. and Klein, R. (2007). Tyrosine phosphorylation sites in ephrinB2 are required for hippocampal long-term potentiation but not long-term depression. *J Neurosci* **27**, 11279-88.

Boyd, A. W., Bartlett, P. F. and Lackmann, M. (2014). Therapeutic targeting of EPH receptors and their ligands. *Nat Rev Drug Discov* **13**, 39-62.

Brantley-Sieders, D. M. and Chen, J. (2004). Eph receptor tyrosine kinases in angiogenesis: from development to disease. *Angiogenesis* **7**, 17-28.

Brochard, V., Combadiere, B., Prigent, A., Laouar, Y., Perrin, A., Beray-Berthat, V., Bonduelle, O., Alvarez-Fischer, D., Callebert, J., Launay, J. M. et al. (2009). Infiltration of CD4+ lymphocytes into the brain contributes to neurodegeneration in a mouse model of Parkinson disease. *J Clin Invest* **119**, 182-92.

Brown, G. C. and Neher, J. J. (2014). Microglial phagocytosis of live neurons. *Nat Rev Neurosci* **15**, 209-16.

Bruce Alberts, A. J., Julian Lewis, Martin Raff, Keith Roberts, Peter Walter. (2002). Intracellular vesicular transport. In *The Cell*, pp. 735-736.

Bruckner, K., Pablo Labrador, J., Scheiffele, P., Herb, A., Seeburg, P. H. and Klein, R. (1999). EphrinB ligands recruit GRIP family PDZ adaptor proteins into raft membrane microdomains. *Neuron* **22**, 511-24.

Bruckner, K., Pasquale, E. B. and Klein, R. (1997). Tyrosine phosphorylation of transmembrane ligands for Eph receptors. *Science* **275**, 1640-3.

Buckner, R. L., Snyder, A. Z., Shannon, B. J., LaRossa, G., Sachs, R., Fotenos, A. F., Sheline, Y. I., Klunk, W. E., Mathis, C. A., Morris, J. C. et al. (2005). Molecular, structural, and functional characterization of Alzheimer's disease: evidence for a relationship between default activity, amyloid, and memory. *J Neurosci* **25**, 7709-17.

Buee, L., Hof, P. R., Bouras, C., Delacourte, A., Perl, D. P., Morrison, J. H. and Fillit, H. M. (1994). Pathological alterations of the cerebral microvasculature in Alzheimer's disease and related dementing disorders. *Acta Neuropathol* **87**, 469-80.

Burgstaller, G. and Gimona, M. (2005). Podosome-mediated matrix resorption and cell motility in vascular smooth muscle cells. *Am J Physiol Heart Circ Physiol* **288**, H3001-5.

Burns, S., Thrasher, A. J., Blundell, M. P., Machesky, L. and Jones, G. E. (2001). Configuration of human dendritic cell cytoskeleton by Rho GTPases, the WAS protein, and differentiation. *Blood* **98**, 1142-9.

Buxbaum, J. D., Choi, E. K., Luo, Y., Lilliehook, C., Crowley, A. C., Merriam, D. E. and Wasco, W. (1998). Calsenilin: a calcium-binding protein that interacts with the presenilins and regulates the levels of a presenilin fragment. *Nat Med* **4**, 1177-81.

Cagnin, A., Brooks, D. J., Kennedy, A. M., Gunn, R. N., Myers, R., Turkheimer, F. E., Jones, T. and Banati, R. B. (2001). In-vivo measurement of activated microglia in dementia. *Lancet* **358**, 461-7.

Calalb, M. B., Polte, T. R. and Hanks, S. K. (1995). Tyrosine phosphorylation of focal adhesion kinase at sites in the catalytic domain regulates kinase activity: a role for Src family kinases. *Mol Cell Biol* **15**, 954-63.

Calalb, M. B., Zhang, X., Polte, T. R. and Hanks, S. K. (1996). Focal adhesion kinase tyrosine-861 is a major site of phosphorylation by Src. *Biochem Biophys Res Commun* **228**, 662-8.

Calderwood, D. A., Campbell, I. D. and Critchley, D. R. (2013). Talins and kindlins: partners in integrin-mediated adhesion. *Nat Rev Mol Cell Biol* **14**, 503-17.

Calderwood, D. A., Zent, R., Grant, R., Rees, D. J., Hynes, R. O. and Ginsberg, M. H. (1999). The Talin head domain binds to integrin beta subunit cytoplasmic tails and regulates integrin activation. *J Biol Chem* **274**, 28071-4.

Calle, Y., Carragher, N. O., Thrasher, A. J. and Jones, G. E. (2006). Inhibition of calpain stabilises podosomes and impairs dendritic cell motility. *J Cell Sci* **119**, 2375-85.

Calo, L., Cinque, C., Patane, M., Schillaci, D., Battaglia, G., Melchiorri, D., Nicoletti, F. and Bruno, V. (2006). Interaction between ephrins/Eph receptors and excitatory amino acid receptors: possible relevance in the regulation of synaptic plasticity and in the pathophysiology of neuronal degeneration. *J Neurochem* **98**, 1-10.

Cameron, B. and Landreth, G. E. (2010). Inflammation, microglia, and Alzheimer's disease. *Neurobiol Dis* **37**, 503-9.

Campbell, T. N., Attwell, S., Arcellana-Panlilio, M. and Robbins, S. M. (2006). Ephrin A5 expression promotes invasion and transformation of murine fibroblasts. *Biochem Biophys Res Commun* **350**, 623-8.

Campion, D., Dumanchin, C., Hannequin, D., Dubois, B., Belliard, S., Puel, M., Thomas-Anterion, C., Michon, A., Martin, C., Charbonnier, F. et al. (1999). Early-onset autosomal dominant Alzheimer disease: prevalence, genetic heterogeneity, and mutation spectrum. *Am J Hum Genet* **65**, 664-70.

Capell, A., Kaether, C., Edbauer, D., Shirotani, K., Merkl, S., Steiner, H. and Haass, C. (2003). Nicastrin interacts with gamma-secretase complex components via the N-terminal part of its transmembrane domain. *J Biol Chem* **278**, 52519-23.

Cardona, A. E., Pioro, E. P., Sasse, M. E., Kostenko, V., Cardona, S. M., Dijkstra, I. M., Huang, D., Kidd, G., Dombrowski, S., Dutta, R. et al. (2006). Control of microglial neurotoxicity by the fractalkine receptor. *Nat Neurosci* **9**, 917-24.

Carmona, M. A., Murai, K. K., Wang, L., Roberts, A. J. and Pasquale, E. B. (2009). Glial ephrin-A3 regulates hippocampal dendritic spine morphology and glutamate transport. *Proc Natl Acad Sci U S A* **106**, 12524-9.

Carragher, N. O., Fincham, V. J., Riley, D. and Frame, M. C. (2001). Cleavage of focal adhesion kinase by different proteases during SRC-regulated transformation and apoptosis. Distinct roles for calpain and caspases. *J Biol Chem* **276**, 4270-5.

Carragher, N. O., Levkau, B., Ross, R. and Raines, E. W. (1999). Degraded collagen fragments promote rapid disassembly of smooth muscle focal adhesions that correlates with cleavage of pp125(FAK), paxillin, and talin. *J Cell Biol* **147**, 619-30.

Carragher, N. O., Westhoff, M. A., Fincham, V. J., Schaller, M. D. and Frame, M. C. (2003). A novel role for FAK as a protease-targeting adaptor protein: regulation by p42 ERK and Src. *Curr Biol* **13**, 1442-50.

Carter, N., Nakamoto, T., Hirai, H. and Hunter, T. (2002). EphrinA1-induced cytoskeletal re-organization requires FAK and p130(cas). *Nat Cell Biol* **4**, 565-73.

Carter, S. B. (1965). Principles of cell motility: the direction of cell movement and cancer invasion. *Nature* **208**, 1183-7.

Cary, L. A., Han, D. C., Polte, T. R., Hanks, S. K. and Guan, J. L. (1998). Identification of p130Cas as a mediator of focal adhesion kinase-promoted cell migration. *J Cell Biol* **140**, 211-21.

Chan, K. T., Bennin, D. A. and Huttenlocher, A. (2010). Regulation of adhesion dynamics by calpain-mediated proteolysis of focal adhesion kinase (FAK). *J Biol Chem* **285**, 11418-26.

Chandu, D., Huppert, S. S. and Kopan, R. (2006). Analysis of transmembrane domain mutants is consistent with sequential cleavage of Notch by gamma-secretase. *J Neurochem* **96**, 228-35.

Chavez-Gutierrez, L., Tolia, A., Maes, E., Li, T., Wong, P. C. and de Strooper, B. (2008). Glu(332) in the Nicastrin ectodomain is essential for gamma-secretase complex maturation but not for its activity. *J Biol Chem* **283**, 20096-105.

Chen, F., Hasegawa, H., Schmitt-Ulms, G., Kawarai, T., Bohm, C., Katayama, T., Gu, Y., Sanjo, N., Glista, M., Rogaeva, E. et al. (2006). TMP21 is a presenilin complex component that modulates gamma-secretase but not epsilon-secretase activity. *Nature* **440**, 1208-12.

Chen, H. C., Appeddu, P. A., Parsons, J. T., Hildebrand, J. D., Schaller, M. D. and Guan, J. L. (1995). Interaction of focal adhesion kinase with cytoskeletal protein talin. *J Biol Chem* **270**, 16995-9.

Chen, L., Iijima, M., Tang, M., Landree, M. A., Huang, Y. E., Xiong, Y., Iglesias, P. A. and Devreotes, P. N. (2007). PLA2 and PI3K/PTEN pathways act in parallel to mediate chemotaxis. *Dev Cell* **12**, 603-14.

Cherry, J. D., Olschowka, J. A. and O'Banion, M. K. (2014). Neuroinflammation and M2 microglia: the good, the bad, and the inflamed. *J Neuroinflammation* **11**, 98.

Chin-Sang, I. D., George, S. E., Ding, M., Moseley, S. L., Lynch, A. S. and Chisholm, A. D. (1999). The ephrin VAB-2/EFN-1 functions in neuronal signaling to regulate epidermal morphogenesis in C. elegans. *Cell* **99**, 781-90.

Chong, L. D., Park, E. K., Latimer, E., Friesel, R. and Daar, I. O. (2000). Fibroblast growth factor receptor-mediated rescue of x-ephrin B1-induced cell dissociation in Xenopus embryos. *Mol Cell Biol* **20**, 724-34.

Chu, J., Lauretti, E., Craige, C. P. and Pratico, D. (2014). Pharmacological modulation of GSAP reduces amyloid-beta levels and tau phosphorylation in a mouse model of Alzheimer's disease with plaques and tangles. *J Alzheimers Dis* **41**, 729-37.

Chyung, J. H., Raper, D. M. and Selkoe, D. J. (2005). Gamma-secretase exists on the plasma membrane as an intact complex that accepts substrates and effects intramembrane cleavage. *J Biol Chem* **280**, 4383-92.

Cisse, M., Halabisky, B., Harris, J., Devidze, N., Dubal, D. B., Sun, B., Orr, A., Lotz, G., Kim, D. H., Hamto, P. et al. (2011). Reversing EphB2 depletion rescues cognitive functions in Alzheimer model. *Nature* **469**, 47-52.

Cohen-Cory, S. and Fraser, S. E. (1995). Effects of brain-derived neurotrophic factor on optic axon branching and remodelling in vivo. *Nature* **378**, 192-6.

Colton, C. and Wilcock, D. M. (2010). Assessing activation states in microglia. *CNS Neurol Disord Drug Targets* **9**, 174-91.

Compagni, A., Logan, M., Klein, R. and Adams, R. H. (2003). Control of skeletal patterning by ephrinB1-EphB interactions. *Dev Cell* **5**, 217-30.

Cooke, J. E. and Moens, C. B. (2002). Boundary formation in the hindbrain: Eph only it were simple. *Trends Neurosci* **25**, 260-7.

Cooray, P., Yuan, Y., Schoenwaelder, S. M., Mitchell, C. A., Salem, H. H. and Jackson, S. P. (1996). Focal adhesion kinase (pp125FAK) cleavage and regulation by calpain. *Biochem J* **318 (Pt 1)**, 41-7.

Cortesio, C. L., Boateng, L. R., Piazza, T. M., Bennin, D. A. and Huttenlocher, A. (2011). Calpain-mediated proteolysis of paxillin negatively regulates focal adhesion dynamics and cell migration. *J Biol Chem* **286**, 9998-10006.

Cowan, C. A. and Henkemeyer, M. (2001). The SH2/SH3 adaptor Grb4 transduces B-ephrin reverse signals. *Nature* **413**, 174-9.

Cowan, C. W., Shao, Y. R., Sahin, M., Shamah, S. M., Lin, M. Z., Greer, P. L., Gao, S., Griffith, E. C., Brugge, J. S. and Greenberg, M. E. (2005). Vav family GEFs link activated Ephs to endocytosis and axon guidance. *Neuron* **46**, 205-17.

Critchley, D. R. (2009). Biochemical and structural properties of the integrin-associated cytoskeletal protein talin. *Annu Rev Biophys* **38**, 235-54.

Cruts, M. and Van Broeckhoven, C. (1998). Presenilin mutations in Alzheimer's disease. *Hum Mutat* **11**, 183-90.

Cui, W., Ke, J. Z., Zhang, Q., Ke, H. Z., Chalouni, C. and Vignery, A. (2006). The intracellular domain of CD44 promotes the fusion of macrophages. *Blood* **107**, 796-805.

Cutforth, T., Moring, L., Mendelsohn, M., Nemes, A., Shah, N. M., Kim, M. M., Frisen, J. and Axel, R. (2003). Axonal ephrin-As and odorant receptors: coordinate determination of the olfactory sensory map. *Cell* **114**, 311-22.

Dailey, M. E. and Waite, M. (1999). Confocal imaging of microglial cell dynamics in hippocampal slice cultures. *Methods* **18**, 222-30, 177.

Dalmau, I., Vela, J. M., Gonzalez, B., Finsen, B. and Castellano, B. (2003). Dynamics of microglia in the developing rat brain. *J Comp Neurol* **458**, 144-57.

Dalva, M. B., Takasu, M. A., Lin, M. Z., Shamah, S. M., Hu, L., Gale, N. W. and Greenberg, M. E. (2000). EphB receptors interact with NMDA receptors and regulate excitatory synapse formation. *Cell* **103**, 945-56.

Damani, M. R., Zhao, L., Fontainhas, A. M., Amaral, J., Fariss, R. N. and Wong, W. T. (2011). Age-related alterations in the dynamic behavior of microglia. *Aging Cell* **10**, 263-76.

Darie, C. C., Deinhardt, K., Zhang, G., Cardasis, H. S., Chao, M. V. and Neubert, T. A. (2011). Identifying transient protein-protein interactions in EphB2 signaling by blue native PAGE and mass spectrometry. *Proteomics* **11**, 4514-28.

Davidson, D., Bakinowski, M., Thomas, M. L., Horejsi, V. and Veillette, A. (2003). Phosphorylation-dependent regulation of T-cell activation by PAG/Cbp, a lipid raft-associated transmembrane adaptor. *Mol Cell Biol* **23**, 2017-28.

Davy, A., Aubin, J. and Soriano, P. (2004). Ephrin-B1 forward and reverse signaling are required during mouse development. *Genes Dev* **18**, 572-83.

Davy, A., Bush, J. O. and Soriano, P. (2006). Inhibition of gap junction communication at ectopic Eph/ephrin boundaries underlies craniofrontonasal syndrome. *PLoS Biol* **4**, e315.

Davy, A., Gale, N. W., Murray, E. W., Klinghoffer, R. A., Soriano, P., Feuerstein, C. and Robbins, S. M. (1999). Compartmentalized signaling by GPI-anchored ephrin-A5 requires the Fyn tyrosine kinase to regulate cellular adhesion. *Genes Dev* **13**, 3125-35.

Davy, A. and Robbins, S. M. (2000). Ephrin-A5 modulates cell adhesion and morphology in an integrin-dependent manner. *EMBO J* **19**, 5396-405.

Di Paolo, G., Pellegrini, L., Letinic, K., Cestra, G., Zoncu, R., Voronov, S., Chang, S., Guo, J., Wenk, M. R. and De Camilli, P. (2002). Recruitment and regulation of phosphatidylinositol phosphate kinase type 1 gamma by the FERM domain of talin. *Nature* **420**, 85-9.

Donoviel, D. B., Hadjantonakis, A. K., Ikeda, M., Zheng, H., Hyslop, P. S. and Bernstein, A. (1999). Mice lacking both presenilin genes exhibit early embryonic patterning defects. *Genes Dev* **13**, 2801-10.

Dourdin, N., Bhatt, A. K., Dutt, P., Greer, P. A., Arthur, J. S., Elce, J. S. and Huttenlocher, A. (2001). Reduced cell migration and disruption of the actin cytoskeleton in calpain-deficient embryonic fibroblasts. *J Biol Chem* **276**, 48382-8.

Dries, D. R. and Yu, G. (2008). Assembly, maturation, and trafficking of the gamma-secretase complex in Alzheimer's disease. *Curr Alzheimer Res* **5**, 132-46.

Duffy, S. L., Coulthard, M. G., Spanevello, M. D., Herath, N. I., Yeadon, T. M., McCarron, J. K., Carter, J. C., Tonks, I. D., Kay, G. F., Phillips, G. E. et al. (2008). Generation and characterization of EphA1 receptor tyrosine kinase reporter knockout mice. *Genesis* **46**, 553-61.

Dufour, A., Seibt, J., Passante, L., Depaepe, V., Ciossek, T., Frisen, J., Kullander, K., Flanagan, J. G., Polleux, F. and Vanderhaeghen, P. (2003). Area specificity and topography of thalamocortical projections are controlled by ephrin/Eph genes. *Neuron* **39**, 453-65.

Durbin, L., Brennan, C., Shiomi, K., Cooke, J., Barrios, A., Shanmugalingam, S., Guthrie, B., Lindberg, R. and Holder, N. (1998). Eph signaling is required for segmentation and differentiation of the somites. *Genes Dev* **12**, 3096-109.

Edbauer, D., Kaether, C., Steiner, H. and Haass, C. (2004). Co-expression of nicastrin and presenilin rescues a loss of function mutant of APH-1. *J Biol Chem* **279**, 37311-5.

Edbauer, D., Winkler, E., Haass, C. and Steiner, H. (2002). Presenilin and nicastrin regulate each other and determine amyloid beta-peptide production via complex formation. *Proc Natl Acad Sci U S A* **99**, 8666-71.

Edbauer, D., Winkler, E., Regula, J. T., Pesold, B., Steiner, H. and Haass, C. (2003). Reconstitution of gamma-secretase activity. *Nat Cell Biol* **5**, 486-8.

Elliott, M. R., Chekeni, F. B., Trampont, P. C., Lazarowski, E. R., Kadl, A., Walk, S. F., Park, D., Woodson, R. I., Ostankovich, M., Sharma, P. et al. (2009). Nucleotides released by apoptotic cells act as a find-me signal to promote phagocytic clearance. *Nature* **461**, 282-6.

Elowe, S., Holland, S. J., Kulkarni, S. and Pawson, T. (2001). Downregulation of the Ras-mitogen-activated protein kinase pathway by the EphB2 receptor tyrosine kinase is required for ephrin-induced neurite retraction. *Mol Cell Biol* **21**, 7429-41.

Eyo, U. B. and Dailey, M. E. (2013). Microglia: key elements in neural development, plasticity, and pathology. *J Neuroimmune Pharmacol* **8**, 494-509.

Ezratty, E. J., Bertaux, C., Marcantonio, E. E. and Gundersen, G. G. (2009). Clathrin mediates integrin endocytosis for focal adhesion disassembly in migrating cells. *J Cell Biol* **187**, 733-47.

Ezratty, E. J., Partridge, M. A. and Gundersen, G. G. (2005). Microtubule-induced focal adhesion disassembly is mediated by dynamin and focal adhesion kinase. *Nat Cell Biol* **7**, 581-90.

Fantl, W. J., Johnson, D. E. and Williams, L. T. (1993). Signalling by receptor tyrosine kinases. *Annu Rev Biochem* **62**, 453-81.

Farfara, D., Trudler, D., Segev-Amzaleg, N., Galron, R., Stein, R. and Frenkel, D. (2011). gamma-Secretase component presenilin is important for microglia beta-amyloid clearance. *Ann Neurol* **69**, 170-80.

Feldheim, D. A., Kim, Y. I., Bergemann, A. D., Frisen, J., Barbacid, M. and Flanagan, J. G. (2000). Genetic analysis of ephrin-A2 and ephrin-A5 shows their requirement in multiple aspects of retinocollicular mapping. *Neuron* **25**, 563-74.

Feldheim, D. A., Nakamoto, M., Osterfield, M., Gale, N. W., DeChiara, T. M., Rohatgi, R., Yancopoulos, G. D. and Flanagan, J. G. (2004). Loss-of-function analysis of EphA receptors in retinotectal mapping. *J Neurosci* **24**, 2542-50.

Fincham, V. J., Brunton, V. G. and Frame, M. C. (2000). The SH3 domain directs acto-myosin-dependent targeting of v-Src to focal adhesions via phosphatidylinositol 3-kinase. *Mol Cell Biol* **20**, 6518-36.

Finckh, U., Alberici, A., Antoniazzi, M., Benussi, L., Fedi, V., Giannini, C., Gal, A., Nitsch, R. M. and Binetti, G. (2000). Variable expression of familial Alzheimer disease associated with presenilin 2 mutation M239I. *Neurology* **54**, 2006-8.

Fischer, V. W., Siddiqi, A. and Yusufaly, Y. (1990). Altered angioarchitecture in selected areas of brains with Alzheimer's disease. *Acta Neuropathol* **79**, 672-9.

Flanary, B. E., Sammons, N. W., Nguyen, C., Walker, D. and Streit, W. J. (2007). Evidence that aging and amyloid promote microglial cell senescence. *Rejuvenation Res* **10**, 61-74.

Foo, S. S., Turner, C. J., Adams, S., Compagni, A., Aubyn, D., Kogata, N., Lindblom, P., Shani, M., Zicha, D. and Adams, R. H. (2006). Ephrin-B2 controls cell motility and adhesion during blood-vessel-wall assembly. *Cell* **124**, 161-73.

Forcet, C., Stein, E., Pays, L., Corset, V., Llambi, F., Tessier-Lavigne, M. and Mehlen, P. (2002). Netrin-1-mediated axon outgrowth requires deleted in colorectal cancer-dependent MAPK activation. *Nature* **417**, 443-7.

Frame, M. C., Patel, H., Serrels, B., Lietha, D. and Eck, M. J. (2010). The FERM domain: organizing the structure and function of FAK. *Nat Rev Mol Cell Biol* **11**, 802-14.

Francis, R., McGrath, G., Zhang, J., Ruddy, D. A., Sym, M., Apfeld, J., Nicoll, M., Maxwell, M., Hai, B., Ellis, M. C. et al. (2002). aph-1 and pen-2 are required for Notch pathway signaling, gamma-secretase cleavage of betaAPP, and presenilin protein accumulation. *Dev Cell* **3**, 85-97.

Franco, S. J. and Huttenlocher, A. (2005). Regulating cell migration: calpains make the cut. *J Cell Sci* **118**, 3829-38.

Franco, S. J., Rodgers, M. A., Perrin, B. J., Han, J., Bennin, D. A., Critchley, D. R. and Huttenlocher, A. (2004). Calpain-mediated proteolysis of talin regulates adhesion dynamics. *Nat Cell Biol* **6**, 977-83.

Fricker, M., Neher, J. J., Zhao, J. W., Thery, C., Tolkovsky, A. M. and Brown, G. C. (2012). MFG-E8 mediates primary phagocytosis of viable neurons during neuroinflammation. *J Neurosci* **32**, 2657-66.

Frieden, L. A., Townsend, T. A., Vaught, D. B., Delaughter, D. M., Hwang, Y., Barnett, J. V. and Chen, J. (2010). Regulation of heart valve morphogenesis by Eph receptor ligand, ephrin-A1. *Dev Dyn* **239**, 3226-34.

Frisen, J., Yates, P. A., McLaughlin, T., Friedman, G. C., O'Leary, D. D. and Barbacid, M. (1998). Ephrin-A5 (AL-1/RAGS) is essential for proper retinal axon guidance and topographic mapping in the mammalian visual system. *Neuron* **20**, 235-43.

Fu, A. K., Hung, K. W., Huang, H., Gu, S., Shen, Y., Cheng, E. Y., Ip, F. C., Huang, X., Fu, W. Y. and Ip, N. Y. (2014). Blockade of EphA4 signaling ameliorates hippocampal synaptic dysfunctions in mouse models of Alzheimer's disease. *Proc Natl Acad Sci U S A* **111**, 9959-64.

Georgakopoulos, A., Litterst, C., Ghersi, E., Baki, L., Xu, C., Serban, G. and Robakis, N. K. (2006). Metalloproteinase/Presenilin1 processing of ephrinB regulates EphB-induced Src phosphorylation and signaling. *EMBO J* **25**, 1242-52.

Georgakopoulos, A., Xu, J., Xu, C., Mauger, G., Barthet, G. and Robakis, N. K. (2011). Presenilin1/gamma-secretase promotes the EphB2-induced phosphorylation of ephrinB2 by regulating phosphoprotein associated with glycosphingolipid-enriched microdomains/Csk binding protein. *FASEB J* **25**, 3594-604.

George, S. E., Simokat, K., Hardin, J. and Chisholm, A. D. (1998). The VAB-1 Eph receptor tyrosine kinase functions in neural and epithelial morphogenesis in C. elegans. *Cell* **92**, 633-43.

Gerety, S. S., Wang, H. U., Chen, Z. F. and Anderson, D. J. (1999). Symmetrical mutant phenotypes of the receptor EphB4 and its specific transmembrane ligand ephrin-B2 in cardiovascular development. *Mol Cell* **4**, 403-14.

Gilman, S., Koller, M., Black, R. S., Jenkins, L., Griffith, S. G., Fox, N. C., Eisner, L., Kirby, L., Rovira, M. B., Forette, F. et al. (2005). Clinical effects of Abeta immunization (AN1792) in patients with AD in an interrupted trial. *Neurology* **64**, 1553-62.

Gimona, M., Buccione, R., Courtneidge, S. A. and Linder, S. (2008). Assembly and biological role of podosomes and invadopodia. *Curr Opin Cell Biol* **20**, 235-41.

Gingras, A. R., Ziegler, W. H., Frank, R., Barsukov, I. L., Roberts, G. C., Critchley, D. R. and Emsley, J. (2005). Mapping and consensus sequence identification for multiple vinculin binding sites within the talin rod. *J Biol Chem* **280**, 37217-24.

Ginhoux, F., Greter, M., Leboeuf, M., Nandi, S., See, P., Gokhan, S., Mehler, M. F., Conway, S. J., Ng, L. G., Stanley, E. R. et al. (2010). Fate mapping analysis reveals that adult microglia derive from primitive macrophages. *Science* **330**, 841-5.

Glading, A., Lauffenburger, D. A. and Wells, A. (2002). Cutting to the chase: calpain proteases in cell motility. *Trends Cell Biol* **12**, 46-54.

Goksoy, E., Ma, Y. Q., Wang, X., Kong, X., Perera, D., Plow, E. F. and Qin, J. (2008). Structural basis for the autoinhibition of talin in regulating integrin activation. *Mol Cell* **31**, 124-33.

Goldmann, W. H., Niggli, V., Kaufmann, S. and Isenberg, G. (1992). Probing actin and liposome interaction of talin and talin-vinculin complexes: a kinetic, thermodynamic and lipid labeling study. *Biochemistry* **31**, 7665-71.

Goldshmit, Y., McLenachan, S. and Turnley, A. (2006). Roles of Eph receptors and ephrins in the normal and damaged adult CNS. *Brain Res Rev* **52**, 327-45.

Goutte, C., Tsunozaki, M., Hale, V. A. and Priess, J. R. (2002). APH-1 is a multipass membrane protein essential for the Notch signaling pathway in Caenorhabditis elegans embryos. *Proc Natl Acad Sci U S A* **99**, 775-9.

Griciuc, A., Serrano-Pozo, A., Parrado, A. R., Lesinski, A. N., Asselin, C. N., Mullin, K., Hooli, B., Choi, S. H., Hyman, B. T. and Tanzi, R. E. (2013). Alzheimer's disease risk gene CD33 inhibits microglial uptake of amyloid beta. *Neuron* **78**, 631-43.

Griffin, W. S., Stanley, L. C., Ling, C., White, L., MacLeod, V., Perrot, L. J., White, C. L., 3rd and Araoz, C. (1989). Brain interleukin 1 and S-100 immunoreactivity are elevated in Down syndrome and Alzheimer disease. *Proc Natl Acad Sci U S A* **86**, 7611-5.

Grunwald, I. C., Korte, M., Adelmann, G., Plueck, A., Kullander, K., Adams, R. H., Frotscher, M., Bonhoeffer, T. and Klein, R. (2004). Hippocampal plasticity requires postsynaptic ephrinBs. *Nat Neurosci* **7**, 33-40.

Gu, J., Tamura, M., Pankov, R., Danen, E. H., Takino, T., Matsumoto, K. and Yamada, K. M. (1999). Shc and FAK differentially regulate cell motility and directionality modulated by PTEN. *J Cell Biol* **146**, 389-403.

Gude, D. R., Alvarez, S. E., Paugh, S. W., Mitra, P., Yu, J., Griffiths, R., Barbour, S. E., Milstien, S. and Spiegel, S. (2008). Apoptosis induces expression of sphingosine kinase 1 to release sphingosine-1-phosphate as a "come-and-get-me" signal. *FASEB J* **22**, 2629-38.

Guerreiro, R., Wojtas, A., Bras, J., Carrasquillo, M., Rogaeva, E., Majounie, E., Cruchaga, C., Sassi, C., Kauwe, J. S., Younkin, S. et al. (2013). TREM2 variants in Alzheimer's disease. *N Engl J Med* **368**, 117-27.

Guilherme, A., Torres, K. and Czech, M. P. (1998). Cross-talk between insulin receptor and integrin alpha5 beta1 signaling pathways. *J Biol Chem* **273**, 22899-903.

Gustafsson, M. V., Zheng, X., Pereira, T., Gradin, K., Jin, S., Lundkvist, J., Ruas, J. L., Poellinger, L., Lendahl, U. and Bondesson, M. (2005). Hypoxia requires notch signaling to maintain the undifferentiated cell state. *Dev Cell* **9**, 617-28.

Haapasalo, A. and Kovacs, D. M. (2011). The many substrates of presenilin/gamma-secretase. *J Alzheimers Dis* **25**, 3-28.

Haas, I. G., Frank, M., Veron, N. and Kemler, R. (2005). Presenilin-dependent processing and nuclear function of gamma-protocadherins. *J Biol Chem* **280**, 9313-9.

Hafner, C., Schmitz, G., Meyer, S., Bataille, F., Hau, P., Langmann, T., Dietmaier, W., Landthaler, M. and Vogt, T. (2004). Differential gene expression of Eph receptors and ephrins in benign human tissues and cancers. *Clin Chem* **50**, 490-9.

Hambsch, B., Grinevich, V., Seeburg, P. H. and Schwarz, M. K. (2005). {gamma}-Protocadherins, presenilin-mediated release of C-terminal fragment promotes locus expression. *J Biol Chem* **280**, 15888-97.

Hanks, S. K., Ryzhova, L., Shin, N. Y. and Brabek, J. (2003). Focal adhesion kinase signaling activities and their implications in the control of cell survival and motility. *Front Biosci* **8**, d982-96.

Hansson, E. M., Stromberg, K., Bergstedt, S., Yu, G., Naslund, J., Lundkvist, J. and Lendahl, U. (2005). Aph-1 interacts at the cell surface with proteins in the active gamma-secretase complex and membrane-tethered Notch. *J Neurochem* **92**, 1010-20.

Hardy, J. A. and Higgins, G. A. (1992). Alzheimer's disease: the amyloid cascade hypothesis. *Science* **256**, 184-5.

Hartmann, D., de Strooper, B., Serneels, L., Craessaerts, K., Herreman, A., Annaert, W., Umans, L., Lubke, T., Lena Illert, A., von Figura, K. et al. (2002). The disintegrin/metalloprotease

ADAM 10 is essential for Notch signalling but not for alpha-secretase activity in fibroblasts. *Hum Mol Genet* **11**, 2615-24.

Hasegawa, H., Sanjo, N., Chen, F., Gu, Y. J., Shier, C., Petit, A., Kawarai, T., Katayama, T., Schmidt, S. D., Mathews, P. M. et al. (2004). Both the sequence and length of the C terminus of PEN-2 are critical for intermolecular interactions and function of presenilin complexes. *J Biol Chem* **279**, 46455-63.

Hashimoto, D., Chow, A., Noizat, C., Teo, P., Beasley, M. B., Leboeuf, M., Becker, C. D., See, P., Price, J., Lucas, D. et al. (2013). Tissue-resident macrophages self-maintain locally throughout adult life with minimal contribution from circulating monocytes. *Immunity* **38**, 792-804.

Hattori, M., Osterfield, M. and Flanagan, J. G. (2000). Regulated cleavage of a contact-mediated axon repellent. *Science* **289**, 1360-5.

He, G., Luo, W., Li, P., Remmers, C., Netzer, W. J., Hendrick, J., Bettayeb, K., Flajolet, M., Gorelick, F., Wennogle, L. P. et al. (2010). Gamma-secretase activating protein is a therapeutic target for Alzheimer's disease. *Nature* **467**, 95-8.

Hefendehl, J. K., Neher, J. J., Suhs, R. B., Kohsaka, S., Skodras, A. and Jucker, M. (2014). Homeostatic and injury-induced microglia behavior in the aging brain. *Aging Cell* **13**, 60-9.

Heise, H., Bayerl, T., Isenberg, G. and Sackmann, E. (1991). Human platelet P-235, a talin-like actin binding protein, binds selectively to mixed lipid bilayers. *Biochim Biophys Acta* **1061**, 121-31.

Hemming, M. L., Elias, J. E., Gygi, S. P. and Selkoe, D. J. (2008). Proteomic profiling of gamma-secretase substrates and mapping of substrate requirements. *PLoS Biol* **6**, e257.

Hemmings, L., Rees, D. J., Ohanian, V., Bolton, S. J., Gilmore, A. P., Patel, B., Priddle, H., Trevithick, J. E., Hynes, R. O. and Critchley, D. R. (1996). Talin contains three actin-binding sites each of which is adjacent to a vinculin-binding site. *J Cell Sci* **109 (Pt 11)**, 2715-26.

Heneka, M. T., Golenbock, D. T. and Latz, E. (2015). Innate immunity in Alzheimer's disease. *Nat Immunol* **16**, 229-36.

Heneka, M. T., Sastre, M., Dumitrescu-Ozimek, L., Dewachter, I., Walter, J., Klockgether, T. and Van Leuven, F. (2005). Focal glial activation coincides with increased BACE1 activation and precedes amyloid plaque deposition in APP[V717I] transgenic mice. *J Neuroinflammation* **2**, 22.

Henkemeyer, M., Itkis, O. S., Ngo, M., Hickmott, P. W. and Ethell, I. M. (2003). Multiple EphB receptor tyrosine kinases shape dendritic spines in the hippocampus. *J Cell Biol* **163**, 1313-26.

Henkemeyer, M., Orioli, D., Henderson, J. T., Saxton, T. M., Roder, J., Pawson, T. and Klein, R. (1996). Nuk controls pathfinding of commissural axons in the mammalian central nervous system. *Cell* **86**, 35-46.

Heroult, M., Schaffner, F. and Augustin, H. G. (2006). Eph receptor and ephrin ligand-mediated interactions during angiogenesis and tumor progression. *Exp Cell Res* **312**, 642-50.

Herreman, A., Hartmann, D., Annaert, W., Saftig, P., Craessaerts, K., Serneels, L., Umans, L., Schrijvers, V., Checler, F., Vanderstichele, H. et al. (1999). Presenilin 2 deficiency causes a mild pulmonary phenotype and no changes in amyloid precursor protein processing but enhances the embryonic lethal phenotype of presenilin 1 deficiency. *Proc Natl Acad Sci U S A* **96**, 11872-7.

Hickman, S. E., Kingery, N. D., Ohsumi, T. K., Borowsky, M. L., Wang, L. C., Means, T. K. and El Khoury, J. (2013). The microglial sensome revealed by direct RNA sequencing. *Nat Neurosci* **16**, 1896-905.

Himanen, J. P., Henkemeyer, M. and Nikolov, D. B. (1998). Crystal structure of the ligand-binding domain of the receptor tyrosine kinase EphB2. *Nature* **396**, 486-91.

Himanen, J. P., Rajashankar, K. R., Lackmann, M., Cowan, C. A., Henkemeyer, M. and Nikolov, D. B. (2001). Crystal structure of an Eph receptor-ephrin complex. *Nature* **414**, 933-8.

Himanen, J. P., Yermekbayeva, L., Janes, P. W., Walker, J. R., Xu, K., Atapattu, L., Rajashankar, K. R., Mensinga, A., Lackmann, M., Nikolov, D. B. et al. (2010). Architecture of Eph receptor clusters. *Proc Natl Acad Sci U S A* **107**, 10860-5.

Hoffmann, O., Braun, J. S., Becker, D., Halle, A., Freyer, D., Dagand, E., Lehnardt, S. and Weber, J. R. (2007). TLR2 mediates neuroinflammation and neuronal damage. *J Immunol* **178**, 6476-81.

Holland, S. J., Gale, N. W., Mbamalu, G., Yancopoulos, G. D., Henkemeyer, M. and Pawson, T. (1996). Bidirectional signalling through the EPH-family receptor Nuk and its transmembrane ligands. *Nature* **383**, 722-5.

Hollingworth, P. Harold, D. Sims, R. Gerrish, A. Lambert, J. C. Carrasquillo, M. M. Abraham, R. Hamshere, M. L. Pahwa, J. S. Moskvina, V. et al. (2011). Common variants at ABCA7, MS4A6A/MS4A4E, EPHA1, CD33 and CD2AP are associated with Alzheimer's disease. *Nat Genet* **43**, 429-35.

Holmberg, J., Armulik, A., Senti, K. A., Edoff, K., Spalding, K., Momma, S., Cassidy, R., Flanagan, J. G. and Frisen, J. (2005). Ephrin-A2 reverse signaling negatively regulates neural progenitor proliferation and neurogenesis. *Genes Dev* **19**, 462-71.

Holmes, C., Boche, D., Wilkinson, D., Yadegarfar, G., Hopkins, V., Bayer, A., Jones, R. W., Bullock, R., Love, S., Neal, J. W. et al. (2008). Long-term effects of Abeta42 immunisation in Alzheimer's disease: follow-up of a randomised, placebo-controlled phase I trial. *Lancet* **372**, 216-23.

Hong, S. E., Shugart, Y. Y., Huang, D. T., Shahwan, S. A., Grant, P. E., Hourihane, J. O., Martin, N. D. and Walsh, C. A. (2000). Autosomal recessive lissencephaly with cerebellar hypoplasia is associated with human RELN mutations. *Nat Genet* **26**, 93-6.

Horejsi, V., Zhang, W. and Schraven, B. (2004). Transmembrane adaptor proteins: organizers of immunoreceptor signalling. *Nat Rev Immunol* **4**, 603-16.

Horwitz, A., Duggan, K., Buck, C., Beckerle, M. C. and Burridge, K. (1986). Interaction of plasma membrane fibronectin receptor with talin--a transmembrane linkage. *Nature* **320**, 531-3.

Huai, J. and Drescher, U. (2001). An ephrin-A-dependent signaling pathway controls integrin function and is linked to the tyrosine phosphorylation of a 120-kDa protein. *J Biol Chem* **276**, 6689-94.

Huber, O., Kemler, R. and Langosch, D. (1999). Mutations affecting transmembrane segment interactions impair adhesiveness of E-cadherin. *J Cell Sci* **112 (Pt 23)**, 4415-23.

Huppert, S. S., Le, A., Schroeter, E. H., Mumm, J. S., Saxena, M. T., Milner, L. A. and Kopan, R. (2000). Embryonic lethality in mice homozygous for a processing-deficient allele of Notch1. *Nature* **405**, 966-70.

Huttenlocher, A., Palecek, S. P., Lu, Q., Zhang, W., Mellgren, R. L., Lauffenburger, D. A., Ginsberg, M. H. and Horwitz, A. F. (1997). Regulation of cell migration by the calcium-dependent protease calpain. *J Biol Chem* **272**, 32719-22.

Ilic, D., Furuta, Y., Kanazawa, S., Takeda, N., Sobue, K., Nakatsuji, N., Nomura, S., Fujimoto, J., Okada, M. and Yamamoto, T. (1995). Reduced cell motility and enhanced focal adhesion contact formation in cells from FAK-deficient mice. *Nature* **377**, 539-44.

Imbimbo, B. P., Solfrizzi, V. and Panza, F. (2010). Are NSAIDs useful to treat Alzheimer's disease or mild cognitive impairment? *Front Aging Neurosci* **2**.

Inoue, E., Deguchi-Tawarada, M., Togawa, A., Matsui, C., Arita, K., Katahira-Tayama, S., Sato, T., Yamauchi, E., Oda, Y. and Takai, Y. (2009). Synaptic activity prompts gamma-secretase-mediated cleavage of EphA4 and dendritic spine formation. *J Cell Biol* **185**, 551-64.

Ireton, R. C. and Chen, J. (2005). EphA2 receptor tyrosine kinase as a promising target for cancer therapeutics. *Curr Cancer Drug Targets* **5**, 149-57.

Ito, K., Okamoto, I., Araki, N., Kawano, Y., Nakao, M., Fujiyama, S., Tomita, K., Mimori, T. and Saya, H. (1999). Calcium influx triggers the sequential proteolysis of extracellular and cytoplasmic domains of E-cadherin, leading to loss of beta-catenin from cell-cell contacts. *Oncogene* **18**, 7080-90.

Janes, P. W., Saha, N., Barton, W. A., Kolev, M. V., Wimmer-Kleikamp, S. H., Nievergall, E., Blobel, C. P., Himanen, J. P., Lackmann, M. and Nikolov, D. B. (2005). Adam meets Eph: an ADAM substrate recognition module acts as a molecular switch for ephrin cleavage in trans. *Cell* **123**, 291-304.

Janus, C., Pearson, J., McLaurin, J., Mathews, P. M., Jiang, Y., Schmidt, S. D., Chishti, M. A., Horne, P., Heslin, D., French, J. et al. (2000). A beta peptide immunization reduces behavioural impairment and plaques in a model of Alzheimer's disease. *Nature* **408**, 979-82.

Jay, T. R., Miller, C. M., Cheng, P. J., Graham, L. C., Bemiller, S., Broihier, M. L., Xu, G., Margevicius, D., Karlo, J. C., Sousa, G. L. et al. (2015). TREM2 deficiency eliminates TREM2+ inflammatory macrophages and ameliorates pathology in Alzheimer's disease mouse models. *J Exp Med* **212**, 287-95.

Jayadev, S., Case, A., Eastman, A. J., Nguyen, H., Pollak, J., Wiley, J. C., Moller, T., Morrison, R. S. and Garden, G. A. (2010). Presenilin 2 is the predominant gamma-secretase in microglia and modulates cytokine release. *PLoS One* **5**, e15743.

Jonsson, T., Stefansson, H., Steinberg, S., Jonsdottir, I., Jonsson, P. V., Snaedal, J., Bjornsson, S., Huttenlocher, J., Levey, A. I., Lah, J. J. et al. (2013). Variant of TREM2 associated with the risk of Alzheimer's disease. *N Engl J Med* **368**, 107-16.

Kaether, C., Capell, A., Edbauer, D., Winkler, E., Novak, B., Steiner, H. and Haass, C. (2004). The presenilin C-terminus is required for ER-retention, nicastrin-binding and gamma-secretase activity. *EMBO J* **23**, 4738-48.

Kaether, C., Scheuermann, J., Fassler, M., Zilow, S., Shirotani, K., Valkova, C., Novak, B., Kacmar, S., Steiner, H. and Haass, C. (2007). Endoplasmic reticulum retention of the gamma-secretase complex component Pen2 by Rer1. *EMBO Rep* **8**, 743-8.

Kalo, M. S. and Pasquale, E. B. (1999). Signal transfer by eph receptors. *Cell Tissue Res* **298**, 1-9.

Kaplan, K. B., Bibbins, K. B., Swedlow, J. R., Arnaud, M., Morgan, D. O. and Varmus, H. E. (1994). Association of the amino-terminal half of c-Src with focal adhesions alters their properties and is regulated by phosphorylation of tyrosine 527. *EMBO J* **13**, 4745-56.

Kim, D. Y., Carey, B. W., Wang, H., Ingano, L. A., Binshtok, A. M., Wertz, M. H., Pettingell, W. H., He, P., Lee, V. M., Woolf, C. J. et al. (2007). BACE1 regulates voltage-gated sodium channels and neuronal activity. *Nat Cell Biol* **9**, 755-64.

Kim, D. Y., Ingano, L. A., Carey, B. W., Pettingell, W. H. and Kovacs, D. M. (2005). Presenilin/gamma-secretase-mediated cleavage of the voltage-gated sodium channel beta2-subunit regulates cell adhesion and migration. *J Biol Chem* **280**, 23251-61.

Kim, D. Y., Ingano, L. A. and Kovacs, D. M. (2002a). Nectin-1alpha, an immunoglobulin-like receptor involved in the formation of synapses, is a substrate for presenilin/gamma-secretase-like cleavage. *J Biol Chem* **277**, 49976-81.

Kim, I., Ryu, Y. S., Kwak, H. J., Ahn, S. Y., Oh, J. L., Yancopoulos, G. D., Gale, N. W. and Koh, G. Y. (2002b). EphB ligand, ephrinB2, suppresses the VEGF- and angiopoietin 1-induced Ras/mitogen-activated protein kinase pathway in venous endothelial cells. *FASEB J* **16**, 1126-8.

Kim, S. H., Yin, Y. I., Li, Y. M. and Sisodia, S. S. (2004). Evidence that assembly of an active gamma-secretase complex occurs in the early compartments of the secretory pathway. *J Biol Chem* **279**, 48615-9.

Klein, R. (2009). Bidirectional modulation of synaptic functions by Eph/ephrin signaling. *Nat Neurosci* **12**, 15-20.

Klein, R. (2012). Eph/ephrin signalling during development. *Development* **139**, 4105-9.

Klemke, R. L., Cai, S., Giannini, A. L., Gallagher, P. J., de Lanerolle, P. and Cheresh, D. A. (1997). Regulation of cell motility by mitogen-activated protein kinase. *J Cell Biol* **137**, 481-92.

Knoll, B. and Drescher, U. (2002). Ephrin-As as receptors in topographic projections. *Trends Neurosci* **25**, 145-9.

Knoll, B., Zarbalis, K., Wurst, W. and Drescher, U. (2001). A role for the EphA family in the topographic targeting of vomeronasal axons. *Development* **128**, 895-906.

Kolsch, V., Charest, P. G. and Firtel, R. A. (2008). The regulation of cell motility and chemotaxis by phospholipid signaling. *J Cell Sci* **121**, 551-9.

Kopan, R. and Ilagan, M. X. (2004). Gamma-secretase: proteasome of the membrane? *Nat Rev Mol Cell Biol* **5**, 499-504.

Kopatz, J., Beutner, C., Welle, K., Bodea, L. G., Reinhardt, J., Claude, J., Linnartz-Gerlach, B. and Neumann, H. (2013). Siglec-h on activated microglia for recognition and engulfment of glioma cells. *Glia* **61**, 1122-33.

Krull, C. E., Lansford, R., Gale, N. W., Collazo, A., Marcelle, C., Yancopoulos, G. D., Fraser, S. E. and Bronner-Fraser, M. (1997). Interactions of Eph-related receptors and ligands confer rostrocaudal pattern to trunk neural crest migration. *Curr Biol* **7**, 571-80.

Kullander, K., Croll, S. D., Zimmer, M., Pan, L., McClain, J., Hughes, V., Zabski, S., DeChiara, T. M., Klein, R., Yancopoulos, G. D. et al. (2001a). Ephrin-B3 is the midline barrier that prevents corticospinal tract axons from recrossing, allowing for unilateral motor control. *Genes Dev* **15**, 877-88.

Kullander, K. and Klein, R. (2002). Mechanisms and functions of Eph and ephrin signalling. *Nat Rev Mol Cell Biol* **3**, 475-86.

Kullander, K., Mather, N. K., Diella, F., Dottori, M., Boyd, A. W. and Klein, R. (2001b). Kinase-dependent and kinase-independent functions of EphA4 receptors in major axon tract formation in vivo. *Neuron* **29**, 73-84.

Kutner, R. H., Zhang, X. Y. and Reiser, J. (2009). Production, concentration and titration of pseudotyped HIV-1-based lentiviral vectors. *Nat Protoc* **4**, 495-505.

Lai, M. T., Chen, E., Crouthamel, M. C., DiMuzio-Mower, J., Xu, M., Huang, Q., Price, E., Register, R. B., Shi, X. P., Donoviel, D. B. et al. (2003). Presenilin-1 and presenilin-2 exhibit distinct yet overlapping gamma-secretase activities. *J Biol Chem* **278**, 22475-81.

Lambert, J. C. Ibrahim-Verbaas, C. A. Harold, D. Naj, A. C. Sims, R. Bellenguez, C. DeStafano, A. L. Bis, J. C. Beecham, G. W. Grenier-Boley, B. et al. (2013). Meta-analysis of 74,046 individuals identifies 11 new susceptibility loci for Alzheimer's disease. *Nat Genet* **45**, 1452-8.

Lammich, S., Okochi, M., Takeda, M., Kaether, C., Capell, A., Zimmer, A. K., Edbauer, D., Walter, J., Steiner, H. and Haass, C. (2002). Presenilin-dependent intramembrane proteolysis of CD44 leads to the liberation of its intracellular domain and the secretion of an Abeta-like peptide. *J Biol Chem* **277**, 44754-9.

Larsen, M., Tremblay, M. L. and Yamada, K. M. (2003). Phosphatases in cell-matrix adhesion and migration. *Nat Rev Mol Cell Biol* **4**, 700-11.

Lauber, K., Bohn, E., Krober, S. M., Xiao, Y. J., Blumenthal, S. G., Lindemann, R. K., Marini, P., Wiedig, C., Zobywalski, A., Baksh, S. et al. (2003). Apoptotic cells induce migration of phagocytes via caspase-3-mediated release of a lipid attraction signal. *Cell* **113**, 717-30.

Laudon, H., Hansson, E. M., Melen, K., Bergman, A., Farmery, M. R., Winblad, B., Lendahl, U., von Heijne, G. and Naslund, J. (2005). A nine-transmembrane domain topology for presenilin 1. *J Biol Chem* **280**, 35352-60.

Lauterbach, J. and Klein, R. (2006). Release of full-length EphB2 receptors from hippocampal neurons to cocultured glial cells. *J Neurosci* **26**, 11575-81.

Lawson, L. J., Perry, V. H., Dri, P. and Gordon, S. (1990). Heterogeneity in the distribution and morphology of microglia in the normal adult mouse brain. *Neuroscience* **39**, 151-70.

Lee, H. S., Bellin, R. M., Walker, D. L., Patel, B., Powers, P., Liu, H., Garcia-Alvarez, B., de Pereda, J. M., Liddington, R. C., Volkmann, N. et al. (2004a). Characterization of an actin-binding site within the talin FERM domain. *J Mol Biol* **343**, 771-84.

Lee, S., Varvel, N. H., Konerth, M. E., Xu, G., Cardona, A. E., Ransohoff, R. M. and Lamb, B. T. (2010). CX3CR1 deficiency alters microglial activation and reduces beta-amyloid deposition in two Alzheimer's disease mouse models. *Am J Pathol* **177**, 2549-62.

Lee, S. F., Shah, S., Li, H., Yu, C., Han, W. and Yu, G. (2002). Mammalian APH-1 interacts with presenilin and nicastrin and is required for intramembrane proteolysis of amyloid-beta precursor protein and Notch. *J Biol Chem* **277**, 45013-9.

Lee, S. F., Shah, S., Yu, C., Wigley, W. C., Li, H., Lim, M., Pedersen, K., Han, W., Thomas, P., Lundkvist, J. et al. (2004b). A conserved GXXXG motif in APH-1 is critical for assembly and activity of the gamma-secretase complex. *J Biol Chem* **279**, 4144-52.

Lehto, V. P., Hovi, T., Vartio, T., Badley, R. A. and Virtanen, I. (1982). Reorganization of cytoskeletal and contractile elements during transition of human monocytes into adherent macrophages. *Lab Invest* **47**, 391-9.

Levitan, D., Lee, J., Song, L., Manning, R., Wong, G., Parker, E. and Zhang, L. (2001). PS1 N- and C-terminal fragments form a complex that functions in APP processing and Notch signaling. *Proc Natl Acad Sci U S A* **98**, 12186-90.

Lichtenthaler, S. F., Wang, R., Grimm, H., Uljon, S. N., Masters, C. L. and Beyreuther, K. (1999). Mechanism of the cleavage specificity of Alzheimer's disease gamma-secretase identified by phenylalanine-scanning mutagenesis of the transmembrane domain of the amyloid precursor protein. *Proc Natl Acad Sci U S A* **96**, 3053-8.

Liebl, D. J., Morris, C. J., Henkemeyer, M. and Parada, L. F. (2003). mRNA expression of ephrins and Eph receptor tyrosine kinases in the neonatal and adult mouse central nervous system. *J Neurosci Res* **71**, 7-22.

Lim, Y., Han, I., Jeon, J., Park, H., Bahk, Y. Y. and Oh, E. S. (2004). Phosphorylation of focal adhesion kinase at tyrosine 861 is crucial for Ras transformation of fibroblasts. *J Biol Chem* **279**, 29060-5.

Lim, Y. S., McLaughlin, T., Sung, T. C., Santiago, A., Lee, K. F. and O'Leary, D. D. (2008). p75(NTR) mediates ephrin-A reverse signaling required for axon repulsion and mapping. *Neuron* **59**, 746-58.

Linder, S. and Aepfelbacher, M. (2003). Podosomes: adhesion hot-spots of invasive cells. *Trends Cell Biol* **13**, 376-85.

Linder, S. and Kopp, P. (2005). Podosomes at a glance. *J Cell Sci* **118**, 2079-82.

Linder, S., Nelson, D., Weiss, M. and Aepfelbacher, M. (1999). Wiskott-Aldrich syndrome protein regulates podosomes in primary human macrophages. *Proc Natl Acad Sci U S A* **96**, 9648-53.

Ling, K., Doughman, R. L., Firestone, A. J., Bunce, M. W. and Anderson, R. A. (2002). Type I gamma phosphatidylinositol phosphate kinase targets and regulates focal adhesions. *Nature* **420**, 89-93.

Litterst, C., Georgakopoulos, A., Shioi, J., Ghersi, E., Wisniewski, T., Wang, R., Ludwig, A. and Robakis, N. K. (2007). Ligand binding and calcium influx induce distinct ectodomain/gamma-secretase-processing pathways of EphB2 receptor. *J Biol Chem* **282**, 16155-63.

Liu, X., Hawkes, E., Ishimaru, T., Tran, T. and Sretavan, D. W. (2006). EphB3: an endogenous mediator of adult axonal plasticity and regrowth after CNS injury. *J Neurosci* **26**, 3087-101.

Lleo, A., Berezovska, O., Growdon, J. H. and Hyman, B. T. (2004). Clinical, pathological, and biochemical spectrum of Alzheimer disease associated with PS-1 mutations. *Am J Geriatr Psychiatry* **12**, 146-56.

Lu, Q., Sun, E. E., Klein, R. S. and Flanagan, J. G. (2001). Ephrin-B reverse signaling is mediated by a novel PDZ-RGS protein and selectively inhibits G protein-coupled chemoattraction. *Cell* **105**, 69-79.

Lue, L. F., Schmitz, C. T., Serrano, G., Sue, L. I., Beach, T. G. and Walker, D. G. (2015). TREM2 Protein Expression Changes Correlate with Alzheimer's Disease Neurodegenerative Pathologies in Post-Mortem Temporal Cortices. *Brain Pathol* **25**, 469-80.

Ly, A., Nikolaev, A., Suresh, G., Zheng, Y., Tessier-Lavigne, M. and Stein, E. (2008). DSCAM is a netrin receptor that collaborates with DCC in mediating turning responses to netrin-1. *Cell* **133**, 1241-54.

Maesako, M., Uemura, K., Kuzuya, A., Sasaki, K., Asada, M., Watanabe, K., Ando, K., Kubota, M., Kihara, T. and Kinoshita, A. (2011). Presenilin regulates insulin signaling via a gamma-secretase-independent mechanism. *J Biol Chem* **286**, 25309-16.

Maetzel, D., Denzel, S., Mack, B., Canis, M., Went, P., Benk, M., Kieu, C., Papior, P., Baeuerle, P. A., Munz, M. et al. (2009). Nuclear signalling by tumour-associated antigen EpCAM. *Nat Cell Biol* **11**, 162-71.

Mai, A., Veltel, S., Pellinen, T., Padzik, A., Coffey, E., Marjomaki, V. and Ivaska, J. (2011). Competitive binding of Rab21 and p120RasGAP to integrins regulates receptor traffic and migration. *J Cell Biol* **194**, 291-306.

Makarov, R., Steiner, B., Gucev, Z., Tasic, V., Wieacker, P. and Wieland, I. (2010). The impact of CFNS-causing EFNB1 mutations on ephrin-B1 function. *BMC Med Genet* **11**, 98.

Makinen, T., Adams, R. H., Bailey, J., Lu, Q., Ziemiecki, A., Alitalo, K., Klein, R. and Wilkinson, G. A. (2005). PDZ interaction site in ephrinB2 is required for the remodeling of lymphatic vasculature. *Genes Dev* **19**, 397-410.

Mambole, A., Baruch, D., Nusbaum, P., Bigot, S., Suzuki, M., Lesavre, P., Fukuda, M. and Halbwachs-Mecarelli, L. (2008). The cleavage of neutrophil leukosialin (CD43) by cathepsin G releases its extracellular domain and triggers its intramembrane proteolysis by presenilin/gamma-secretase. *J Biol Chem* **283**, 23627-35.

Mann, F., Miranda, E., Weinl, C., Harmer, E. and Holt, C. E. (2003). B-type Eph receptors and ephrins induce growth cone collapse through distinct intracellular pathways. *J Neurobiol* **57**, 323-36.

Marambaud, P., Shioi, J., Serban, G., Georgakopoulos, A., Sarner, S., Nagy, V., Baki, L., Wen, P., Efthimiopoulos, S., Shao, Z. et al. (2002). A presenilin-1/gamma-secretase cleavage releases the E-cadherin intracellular domain and regulates disassembly of adherens junctions. *EMBO J* **21**, 1948-56.

Marambaud, P., Wen, P. H., Dutt, A., Shioi, J., Takashima, A., Siman, R. and Robakis, N. K. (2003). A CBP binding transcriptional repressor produced by the PS1/epsilon-cleavage of N-cadherin is inhibited by PS1 FAD mutations. *Cell* **114**, 635-45.

Maretzky, T., Schulte, M., Ludwig, A., Rose-John, S., Blobel, C., Hartmann, D., Altevogt, P., Saftig, P. and Reiss, K. (2005). L1 is sequentially processed by two differently activated metalloproteases and presenilin/gamma-secretase and regulates neural cell adhesion, cell migration, and neurite outgrowth. *Mol Cell Biol* **25**, 9040-53.

Margadant, C., Monsuur, H. N., Norman, J. C. and Sonnenberg, A. (2011). Mechanisms of integrin activation and trafficking. *Curr Opin Cell Biol* **23**, 607-14.

Margolis, S. S., Salogiannis, J., Lipton, D. M., Mandel-Brehm, C., Wills, Z. P., Mardinly, A. R., Hu, L., Greer, P. L., Bikoff, J. B., Ho, H. Y. et al. (2010). EphB-mediated degradation of the RhoA GEF Ephexin5 relieves a developmental brake on excitatory synapse formation. *Cell* **143**, 442-55.

Marler, K. J., Becker-Barroso, E., Martinez, A., Llovera, M., Wentzel, C., Poopalasundaram, S., Hindges, R., Soriano, E., Comella, J. and Drescher, U. (2008). A TrkB/EphrinA interaction controls retinal axon branching and synaptogenesis. *J Neurosci* **28**, 12700-12.

Marler, K. J., Poopalasundaram, S., Broom, E. R., Wentzel, C. and Drescher, U. (2010). Pro-neurotrophins secreted from retinal ganglion cell axons are necessary for ephrinA-p75NTR-mediated axon guidance. *Neural Dev* **5**, 30.

Marquardt, T., Shirasaki, R., Ghosh, S., Andrews, S. E., Carter, N., Hunter, T. and Pfaff, S. L. (2005). Coexpressed EphA receptors and ephrin-A ligands mediate opposing actions on growth cone navigation from distinct membrane domains. *Cell* **121**, 127-39.

Marston, D. J., Dickinson, S. and Nobes, C. D. (2003). Rac-dependent trans-endocytosis of ephrinBs regulates Eph-ephrin contact repulsion. *Nat Cell Biol* **5**, 879-88.

Martinez, F. O. and Gordon, S. (2014). The M1 and M2 paradigm of macrophage activation: time for reassessment. *F1000Prime Rep* **6**, 13.

Martone, M. E., Holash, J. A., Bayardo, A., Pasquale, E. B. and Ellisman, M. H. (1997). Immunolocalization of the receptor tyrosine kinase EphA4 in the adult rat central nervous system. *Brain Res* **771**, 238-50.

McGeer, P. L., Itagaki, S., Boyes, B. E. and McGeer, E. G. (1988). Reactive microglia are positive for HLA-DR in the substantia nigra of Parkinson's and Alzheimer's disease brains. *Neurology* **38**, 1285-91.

McGeer, P. L. and McGeer, E. G. (2004). Inflammation and the degenerative diseases of aging. *Ann N Y Acad Sci* **1035**, 104-16.

Mendrola, J. M., Berger, M. B., King, M. C. and Lemmon, M. A. (2002). The single transmembrane domains of ErbB receptors self-associate in cell membranes. *J Biol Chem* **277**, 4704-12.

Meyer, E. L., Strutz, N., Gahring, L. C. and Rogers, S. W. (2003). Glutamate receptor subunit 3 is modified by site-specific limited proteolysis including cleavage by gamma-secretase. *J Biol Chem* **278**, 23786-96.

Meyer, S., Hafner, C., Guba, M., Flegel, S., Geissler, E. K., Becker, B., Koehl, G. E., Orso, E., Landthaler, M. and Vogt, T. (2005). Ephrin-B2 overexpression enhances integrin-mediated ECM-attachment and migration of B16 melanoma cells. *Int J Oncol* **27**, 1197-206.

Miao, H., Wei, B. R., Peehl, D. M., Li, Q., Alexandrou, T., Schelling, J. R., Rhim, J. S., Sedor, J. R., Burnett, E. and Wang, B. (2001). Activation of EphA receptor tyrosine kinase inhibits the Ras/MAPK pathway. *Nat Cell Biol* **3**, 527-30.

Miletti-Gonzalez, K. E., Murphy, K., Kumaran, M. N., Ravindranath, A. K., Wernyj, R. P., Kaur, S., Miles, G. D., Lim, E., Chan, R., Chekmareva, M. et al. (2012). Identification of function for CD44 intracytoplasmic domain (CD44-ICD): modulation of matrix metalloproteinase 9 (MMP-9) transcription via novel promoter response element. *J Biol Chem* **287**, 18995-9007.

Miller, K., Kolk, S. M. and Donoghue, M. J. (2006). EphA7-ephrin-A5 signaling in mouse somatosensory cortex: developmental restriction of molecular domains and postnatal maintenance of functional compartments. *J Comp Neurol* **496**, 627-42.

Minghetti, L. (2005). Role of inflammation in neurodegenerative diseases. *Curr Opin Neurol* **18**, 315-21.

Mitra, S. K., Hanson, D. A. and Schlaepfer, D. D. (2005). Focal adhesion kinase: in command and control of cell motility. *Nat Rev Mol Cell Biol* **6**, 56-68.

Mitra, S. K. and Schlaepfer, D. D. (2006). Integrin-regulated FAK-Src signaling in normal and cancer cells. *Curr Opin Cell Biol* **18**, 516-23.

Mittelbronn, M., Dietz, K., Schluesener, H. J. and Meyermann, R. (2001). Local distribution of microglia in the normal adult human central nervous system differs by up to one order of magnitude. *Acta Neuropathol* **101**, 249-55.

Mizuno, T., Doi, Y., Mizoguchi, H., Jin, S., Noda, M., Sonobe, Y., Takeuchi, H. and Suzumura, A. (2011). Interleukin-34 selectively enhances the neuroprotective effects of microglia to attenuate oligomeric amyloid-beta neurotoxicity. *Am J Pathol* **179**, 2016-27.

Moes, M., Rodius, S., Coleman, S. J., Monkley, S. J., Goormaghtigh, E., Tremuth, L., Kox, C., van der Holst, P. P., Critchley, D. R. and Kieffer, N. (2007). The integrin binding site 2 (IBS2) in the talin rod domain is essential for linking integrin beta subunits to the cytoskeleton. *J Biol Chem* **282**, 17280-8.

Monkley, S. J., Pritchard, C. A. and Critchley, D. R. (2001). Analysis of the mammalian talin2 gene TLN2. *Biochem Biophys Res Commun* **286**, 880-5.

Moore, S. W., Tessier-Lavigne, M. and Kennedy, T. E. (2007). Netrins and their receptors. *Adv Exp Med Biol* **621**, 17-31.

Morais, V. A., Crystal, A. S., Pijak, D. S., Carlin, D., Costa, J., Lee, V. M. and Doms, R. W. (2003). The transmembrane domain region of nicastrin mediates direct interactions with APH-1 and the gamma-secretase complex. *J Biol Chem* **278**, 43284-91.

Morgan, D., Diamond, D. M., Gottschall, P. E., Ugen, K. E., Dickey, C., Hardy, J., Duff, K., Jantzen, P., DiCarlo, G., Wilcock, D. et al. (2000). A beta peptide vaccination prevents memory loss in an animal model of Alzheimer's disease. *Nature* **408**, 982-5.

Mosley, R. L., Hutter-Saunders, J. A., Stone, D. K. and Gendelman, H. E. (2012). Inflammation and adaptive immunity in Parkinson's disease. *Cold Spring Harb Perspect Med* **2**, a009381.

Mukherjee, T., Kim, W. S., Mandal, L. and Banerjee, U. (2011). Interaction between Notch and Hif-alpha in development and survival of Drosophila blood cells. *Science* **332**, 1210-3.

Munter, L. M., Voigt, P., Harmeier, A., Kaden, D., Gottschalk, K. E., Weise, C., Pipkorn, R., Schaefer, M., Langosch, D. and Multhaup, G. (2007). GxxxG motifs within the amyloid precursor protein transmembrane sequence are critical for the etiology of Abeta42. *EMBO J* **26**, 1702-12.

Murai, K. K., Nguyen, L. N., Irie, F., Yamaguchi, Y. and Pasquale, E. B. (2003). Control of hippocampal dendritic spine morphology through ephrin-A3/EphA4 signaling. *Nat Neurosci* **6**, 153-60.

Murai, K. K. and Pasquale, E. B. (2005). New exchanges in eph-dependent growth cone dynamics. *Neuron* **46**, 161-3.

Murakami, D., Okamoto, I., Nagano, O., Kawano, Y., Tomita, T., Iwatsubo, T., De Strooper, B., Yumoto, E. and Saya, H. (2003). Presenilin-dependent gamma-secretase activity mediates the intramembranous cleavage of CD44. *Oncogene* **22**, 1511-6.

Murphy, M. P. and LeVine, H., 3rd. (2010). Alzheimer's disease and the amyloid-beta peptide. *J Alzheimers Dis* **19**, 311-23.

Nagano, M., Hoshino, D., Koshikawa, N., Akizawa, T. and Seiki, M. (2012). Turnover of focal adhesions and cancer cell migration. *Int J Cell Biol* **2012**, 310616.

Nakahara, S., Saito, T., Kondo, N., Moriwaki, K., Noda, K., Ihara, S., Takahashi, M., Ide, Y., Gu, J., Inohara, H. et al. (2006). A secreted type of beta1,6 N-acetylglucosaminyltransferase V (GnT-V), a novel angiogenesis inducer, is regulated by gamma-secretase. *FASEB J* **20**, 2451-9.

Nakajima, M., Yuasa, S., Ueno, M., Takakura, N., Koseki, H. and Shirasawa, T. (2003). Abnormal blood vessel development in mice lacking presenilin-1. *Mech Dev* **120**, 657-67.

Napoli, I., Kierdorf, K. and Neumann, H. (2009). Microglial precursors derived from mouse embryonic stem cells. *Glia* **57**, 1660-71.

Naruse-Nakajima, C., Asano, M. and Iwakura, Y. (2001). Involvement of EphA2 in the formation of the tail notochord via interaction with ephrinA1. *Mech Dev* **102**, 95-105.

Nayal, A., Webb, D. J. and Horwitz, A. F. (2004). Talin: an emerging focal point of adhesion dynamics. *Curr Opin Cell Biol* **16**, 94-8.

Neher, J. J., Neniskyte, U., Zhao, J. W., Bal-Price, A., Tolkovsky, A. M. and Brown, G. C. (2011). Inhibition of microglial phagocytosis is sufficient to prevent inflammatory neuronal death. *J Immunol* **186**, 4973-83.

Neukomm, L. J., Frei, A. P., Cabello, J., Kinchen, J. M., Zaidel-Bar, R., Ma, Z., Haney, L. B., Hardin, J., Ravichandran, K. S., Moreno, S. et al. (2011). Loss of the RhoGAP SRGP-1 promotes the clearance of dead and injured cells in Caenorhabditis elegans. *Nat Cell Biol* **13**, 79-86.

Neumann, J., Sauerzweig, S., Ronicke, R., Gunzer, F., Dinkel, K., Ullrich, O., Gunzer, M. and Reymann, K. G. (2008). Microglia cells protect neurons by direct engulfment of invading neutrophil granulocytes: a new mechanism of CNS immune privilege. *J Neurosci* **28**, 5965-75.

Nimmerjahn, A., Kirchhoff, F. and Helmchen, F. (2005). Resting microglial cells are highly dynamic surveillants of brain parenchyma in vivo. *Science* **308**, 1314-8.

Nishimura, T., Yamaguchi, T., Tokunaga, A., Hara, A., Hamaguchi, T., Kato, K., Iwamatsu, A., Okano, H. and Kaibuchi, K. (2006). Role of numb in dendritic spine development with a Cdc42 GEF intersectin and EphB2. *Mol Biol Cell* **17**, 1273-85.

Nishio, M., Watanabe, K., Sasaki, J., Taya, C., Takasuga, S., Iizuka, R., Balla, T., Yamazaki, M., Watanabe, H., Itoh, R. et al. (2007). Control of cell polarity and motility by the PtdIns(3,4,5)P3 phosphatase SHIP1. *Nat Cell Biol* **9**, 36-44.

Nyabi, O., Bentahir, M., Horre, K., Herreman, A., Gottardi-Littell, N., Van Broeckhoven, C., Merchiers, P., Spittaels, K., Annaert, W. and De Strooper, B. (2003). Presenilins mutated at Asp-257 or Asp-385 restore Pen-2 expression and Nicastrin glycosylation but remain catalytically inactive in the absence of wild type Presenilin. *J Biol Chem* **278**, 43430-6.

Ogita, H., Kunimoto, S., Kamioka, Y., Sawa, H., Masuda, M. and Mochizuki, N. (2003). EphA4-mediated Rho activation via Vsm-RhoGEF expressed specifically in vascular smooth muscle cells. *Circ Res* **93**, 23-31.

Oh, Y. S. and Turner, R. J. (2005). Topology of the C-terminal fragment of human presenilin 1. *Biochemistry* **44**, 11821-8.

Okamoto, I., Kawano, Y., Murakami, D., Sasayama, T., Araki, N., Miki, T., Wong, A. J. and Saya, H. (2001). Proteolytic release of CD44 intracellular domain and its role in the CD44 signaling pathway. *J Cell Biol* **155**, 755-62.

Okello, A., Edison, P., Archer, H. A., Turkheimer, F. E., Kennedy, J., Bullock, R., Walker, Z., Kennedy, A., Fox, N., Rossor, M. et al. (2009). Microglial activation and amyloid deposition in mild cognitive impairment: a PET study. *Neurology* **72**, 56-62.

Olsson, B., Legros, L., Guilhot, F., Stromberg, K., Smith, J., Livesey, F. J., Wilson, D. H., Zetterberg, H. and Blennow, K. (2014). Imatinib treatment and Abeta42 in humans. *Alzheimers Dement* **10**, S374-80.

Orioli, D., Henkemeyer, M., Lemke, G., Klein, R. and Pawson, T. (1996). Sek4 and Nuk receptors cooperate in guidance of commissural axons and in palate formation. *EMBO J* **15**, 6035-49.

Orre, M., Kamphuis, W., Osborn, L. M., Melief, J., Kooijman, L., Huitinga, I., Klooster, J., Bossers, K. and Hol, E. M. (2014). Acute isolation and transcriptome characterization of cortical astrocytes and microglia from young and aged mice. *Neurobiol Aging* **35**, 1-14.

Osiak, A. E., Zenner, G. and Linder, S. (2005). Subconfluent endothelial cells form podosomes downstream of cytokine and RhoGTPase signaling. *Exp Cell Res* **307**, 342-53.

Pabon, M. M., Bachstetter, A. D., Hudson, C. E., Gemma, C. and Bickford, P. C. (2011). CX3CL1 reduces neurotoxicity and microglial activation in a rat model of Parkinson's disease. *J Neuroinflammation* **8**, 9.

Palecek, S. P., Huttenlocher, A., Horwitz, A. F. and Lauffenburger, D. A. (1998). Physical and biochemical regulation of integrin release during rear detachment of migrating cells. *J Cell Sci* **111 (Pt 7)**, 929-40.

Palmer, A., Zimmer, M., Erdmann, K. S., Eulenburg, V., Porthin, A., Heumann, R., Deutsch, U. and Klein, R. (2002). EphrinB phosphorylation and reverse signaling: regulation by Src kinases and PTP-BL phosphatase. *Mol Cell* **9**, 725-37.

Paloneva, J., Manninen, T., Christman, G., Hovanes, K., Mandelin, J., Adolfsson, R., Bianchin, M., Bird, T., Miranda, R., Salmaggi, A. et al. (2002). Mutations in two genes encoding different subunits of a receptor signaling complex result in an identical disease phenotype. *Am J Hum Genet* **71**, 656-62.

Paolicelli, R. C., Bolasco, G., Pagani, F., Maggi, L., Scianni, M., Panzanelli, P., Giustetto, M., Ferreira, T. A., Guiducci, E., Dumas, L. et al. (2011). Synaptic pruning by microglia is necessary for normal brain development. *Science* **333**, 1456-8.

Parent, A. T., Barnes, N. Y., Taniguchi, Y., Thinakaran, G. and Sisodia, S. S. (2005). Presenilin attenuates receptor-mediated signaling and synaptic function. *J Neurosci* **25**, 1540-9.

Parisiadou, L., Fassa, A., Fotinopoulou, A., Bethani, I. and Efthimiopoulos, S. (2004). Presenilin 1 and cadherins: stabilization of cell-cell adhesion and proteolysis-dependent regulation of transcription. *Neurodegener Dis* **1**, 184-91.

Park, S., Frisen, J. and Barbacid, M. (1997). Aberrant axonal projections in mice lacking EphA8 (Eek) tyrosine protein kinase receptors. *EMBO J* **16**, 3106-14.

Pascall, J. C. and Brown, K. D. (2004). Intramembrane cleavage of ephrinB3 by the human rhomboid family protease, RHBDL2. *Biochem Biophys Res Commun* **317**, 244-52.

Pasquale, E. B. (2004). Eph-ephrin promiscuity is now crystal clear. *Nat Neurosci* **7**, 417-8.

Pasquale, E. B. (2008). Eph-ephrin bidirectional signaling in physiology and disease. *Cell* **133**, 38-52.

Pasquale, E. B. (2010). Eph receptors and ephrins in cancer: bidirectional signalling and beyond. *Nat Rev Cancer* **10**, 165-80.

Pasternak, S. H., Bagshaw, R. D., Guiral, M., Zhang, S., Ackerley, C. A., Pak, B. J., Callahan, J. W. and Mahuran, D. J. (2003). Presenilin-1, nicastrin, amyloid precursor protein, and gamma-secretase activity are co-localized in the lysosomal membrane. *J Biol Chem* **278**, 26687-94.

Pelletier, L., Guillaumot, P., Freche, B., Luquain, C., Christiansen, D., Brugiere, S., Garin, J. and Manie, S. N. (2006). Gamma-secretase-dependent proteolysis of CD44 promotes neoplastic transformation of rat fibroblastic cells. *Cancer Res* **66**, 3681-7.

Penzes, P., Beeser, A., Chernoff, J., Schiller, M. R., Eipper, B. A., Mains, R. E. and Huganir, R. L. (2003). Rapid induction of dendritic spine morphogenesis by trans-synaptic ephrinB-EphB receptor activation of the Rho-GEF kalirin. *Neuron* **37**, 263-74.

Perry, V. H. and Teeling, J. (2013). Microglia and macrophages of the central nervous system: the contribution of microglia priming and systemic inflammation to chronic neurodegeneration. *Semin Immunopathol* **35**, 601-12.

Petrie, R. J., Doyle, A. D. and Yamada, K. M. (2009). Random versus directionally persistent cell migration. *Nat Rev Mol Cell Biol* **10**, 538-49.

Pfaff, M., Liu, S., Erle, D. J. and Ginsberg, M. H. (1998). Integrin beta cytoplasmic domains differentially bind to cytoskeletal proteins. *J Biol Chem* **273**, 6104-9.

Pitulescu, M. E. and Adams, R. H. (2010). Eph/ephrin molecules--a hub for signaling and endocytosis. *Genes Dev* **24**, 2480-92.

Priddle, H., Hemmings, L., Monkley, S., Woods, A., Patel, B., Sutton, D., Dunn, G. A., Zicha, D. and Critchley, D. R. (1998). Disruption of the talin gene compromises focal adhesion assembly in undifferentiated but not differentiated embryonic stem cells. *J Cell Biol* **142**, 1121-33.

Prokop, S., Shirotani, K., Edbauer, D., Haass, C. and Steiner, H. (2004). Requirement of PEN-2 for stabilization of the presenilin N-/C-terminal fragment heterodimer within the gamma-secretase complex. *J Biol Chem* **279**, 23255-61.

Ravichandran, K. S. (2011). Beginnings of a good apoptotic meal: the find-me and eat-me signaling pathways. *Immunity* **35**, 445-55.

Reddien, P. W., Cameron, S. and Horvitz, H. R. (2001). Phagocytosis promotes programmed cell death in C. elegans. *Nature* **412**, 198-202.

Richardson, A., Malik, R. K., Hildebrand, J. D. and Parsons, J. T. (1997). Inhibition of cell spreading by expression of the C-terminal domain of focal adhesion kinase (FAK) is rescued by coexpression of Src or catalytically inactive FAK: a role for paxillin tyrosine phosphorylation. *Mol Cell Biol* **17**, 6906-14.

Rodenas-Ruano, A., Perez-Pinzon, M. A., Green, E. J., Henkemeyer, M. and Liebl, D. J. (2006). Distinct roles for ephrinB3 in the formation and function of hippocampal synapses. *Dev Biol* **292**, 34-45.

Rodius, S., Chaloin, O., Moes, M., Schaffner-Reckinger, E., Landrieu, I., Lippens, G., Lin, M., Zhang, J. and Kieffer, N. (2008). The talin rod IBS2 alpha-helix interacts with the beta3 integrin cytoplasmic tail membrane-proximal helix by establishing charge complementary salt bridges. *J Biol Chem* **283**, 24212-23.

Rogaeva, E. A., Fafel, K. C., Song, Y. Q., Medeiros, H., Sato, C., Liang, Y., Richard, E., Rogaev, E. I., Frommelt, P., Sadovnick, A. D. et al. (2001). Screening for PS1 mutations in a referral-based series of AD cases: 21 novel mutations. *Neurology* **57**, 621-5.

Rosenberger, A. F., Rozemuller, A. J., van der Flier, W. M., Scheltens, P., van der Vies, S. M. and Hoozemans, J. J. (2014). Altered distribution of the EphA4 kinase in hippocampal brain tissue of patients with Alzheimer's disease correlates with pathology. *Acta Neuropathol Commun* **2**, 79.

Rudolph, J., Gerstmann, K., Zimmer, G., Steinecke, A., Doding, A. and Bolz, J. (2014). A dual role of EphB1/ephrin-B3 reverse signaling on migrating striatal and cortical neurons originating in the preoptic area: should I stay or go away? *Front Cell Neurosci* **8**, 185.

Sahin, M., Greer, P. L., Lin, M. Z., Poucher, H., Eberhart, J., Schmidt, S., Wright, T. M., Shamah, S. M., O'Connell, S., Cowan, C. W. et al. (2005). Eph-dependent tyrosine phosphorylation of ephexin1 modulates growth cone collapse. *Neuron* **46**, 191-204.

Sahlgren, C., Gustafsson, M. V., Jin, S., Poellinger, L. and Lendahl, U. (2008). Notch signaling mediates hypoxia-induced tumor cell migration and invasion. *Proc Natl Acad Sci U S A* **105**, 6392-7.

Santiago, A. and Erickson, C. A. (2002). Ephrin-B ligands play a dual role in the control of neural crest cell migration. *Development* **129**, 3621-32.

Sato, T., del Carmen Ovejero, M., Hou, P., Heegaard, A. M., Kumegawa, M., Foged, N. T. and Delaisse, J. M. (1997). Identification of the membrane-type matrix metalloproteinase MT1-MMP in osteoclasts. *J Cell Sci* **110 (Pt 5)**, 589-96.

Saura, C. A., Choi, S. Y., Beglopoulos, V., Malkani, S., Zhang, D., Shankaranarayana Rao, B. S., Chattarji, S., Kelleher, R. J., 3rd, Kandel, E. R., Duff, K. et al. (2004). Loss of presenilin function causes impairments of memory and synaptic plasticity followed by age-dependent neurodegeneration. *Neuron* **42**, 23-36.

Savelieva, K. V., Rajan, I., Baker, K. B., Vogel, P., Jarman, W., Allen, M. and Lanthorn, T. H. (2008). Learning and memory impairment in Eph receptor A6 knockout mice. *Neurosci Lett* **438**, 205-9.

Sawamiphak, S., Seidel, S., Essmann, C. L., Wilkinson, G. A., Pitulescu, M. E., Acker, T. and Acker-Palmer, A. (2010). Ephrin-B2 regulates VEGFR2 function in developmental and tumour angiogenesis. *Nature* **465**, 487-91.

Schachtner, H., Calaminus, S. D., Thomas, S. G. and Machesky, L. M. (2013). Podosomes in adhesion, migration, mechanosensing and matrix remodeling. *Cytoskeleton (Hoboken)* **70**, 572-89.

Schafer, D. P., Lehrman, E. K., Kautzman, A. G., Koyama, R., Mardinly, A. R., Yamasaki, R., Ransohoff, R. M., Greenberg, M. E., Barres, B. A. and Stevens, B. (2012). Microglia sculpt postnatal neural circuits in an activity and complement-dependent manner. *Neuron* **74**, 691-705.

Schaller, M. D. (2010). Cellular functions of FAK kinases: insight into molecular mechanisms and novel functions. *J Cell Sci* **123**, 1007-13.

Schaller, M. D., Hildebrand, J. D., Shannon, J. D., Fox, J. W., Vines, R. R. and Parsons, J. T. (1994). Autophosphorylation of the focal adhesion kinase, pp125FAK, directs SH2-dependent binding of pp60src. *Mol Cell Biol* **14**, 1680-8.

Schenk, D., Barbour, R., Dunn, W., Gordon, G., Grajeda, H., Guido, T., Hu, K., Huang, J., Johnson-Wood, K., Khan, K. et al. (1999). Immunization with amyloid-beta attenuates Alzheimer-disease-like pathology in the PDAPP mouse. *Nature* **400**, 173-7.

Schlaepfer, D. D., Hanks, S. K., Hunter, T. and van der Geer, P. (1994). Integrin-mediated signal transduction linked to Ras pathway by GRB2 binding to focal adhesion kinase. *Nature* **372**, 786-91.

Schlaepfer, D. D. and Hunter, T. (1996). Evidence for in vivo phosphorylation of the Grb2 SH2-domain binding site on focal adhesion kinase by Src-family protein-tyrosine kinases. *Mol Cell Biol* **16**, 5623-33.

Schlaepfer, D. D., Mitra, S. K. and Ilic, D. (2004). Control of motile and invasive cell phenotypes by focal adhesion kinase. *Biochim Biophys Acta* **1692**, 77-102.

Schoenwaelder, S. M., Yuan, Y., Cooray, P., Salem, H. H. and Jackson, S. P. (1997). Calpain cleavage of focal adhesion proteins regulates the cytoskeletal attachment of integrin alphaIIbbeta3 (platelet glycoprotein IIb/IIIa) and the cellular retraction of fibrin clots. *J Biol Chem* **272**, 1694-702.

Schulte, A., Schulz, B., Andrzejewski, M. G., Hundhausen, C., Mletzko, S., Achilles, J., Reiss, K., Paliga, K., Weber, C., John, S. R. et al. (2007). Sequential processing of the transmembrane chemokines CX3CL1 and CXCL16 by alpha- and gamma-secretases. *Biochem Biophys Res Commun* **358**, 233-40.

Schulz, J. G., Annaert, W., Vandekerckhove, J., Zimmermann, P., De Strooper, B. and David, G. (2003). Syndecan 3 intramembrane proteolysis is presenilin/gamma-secretase-dependent and modulates cytosolic signaling. *J Biol Chem* **278**, 48651-7.

Scully, A. L., McKeown, M. and Thomas, J. B. (1999). Isolation and characterization of Dek, a Drosophila eph receptor protein tyrosine kinase. *Mol Cell Neurosci* **13**, 337-47.

Seeger, M., Nordstedt, C., Petanceska, S., Kovacs, D. M., Gouras, G. K., Hahne, S., Fraser, P., Levesque, L., Czernik, A. J., George-Hyslop, P. S. et al. (1997). Evidence for phosphorylation and oligomeric assembly of presenilin 1. *Proc Natl Acad Sci U S A* **94**, 5090-4.

Segura, I., Essmann, C. L., Weinges, S. and Acker-Palmer, A. (2007). Grb4 and GIT1 transduce ephrinB reverse signals modulating spine morphogenesis and synapse formation. *Nat Neurosci* **10**, 301-10.

Seiradake, E., Harlos, K., Sutton, G., Aricescu, A. R. and Jones, E. Y. (2010). An extracellular steric seeding mechanism for Eph-ephrin signaling platform assembly. *Nat Struct Mol Biol* **17**, 398-402.

Senetar, M. A. and McCann, R. O. (2005). Gene duplication and functional divergence during evolution of the cytoskeletal linker protein talin. *Gene* **362**, 141-52.

Senturk, A., Pfennig, S., Weiss, A., Burk, K. and Acker-Palmer, A. (2011). Ephrin Bs are essential components of the Reelin pathway to regulate neuronal migration. *Nature* **472**, 356-60.

Seppa, H., Grotendorst, G., Seppa, S., Schiffmann, E. and Martin, G. R. (1982). Platelet-derived growth factor in chemotactic for fibroblasts. *J Cell Biol* **92**, 584-8.

Serneels, L., Van Biervliet, J., Craessaerts, K., Dejaegere, T., Horre, K., Van Houtvin, T., Esselmann, H., Paul, S., Schafer, M. K., Berezovska, O. et al. (2009). gamma-Secretase heterogeneity in the Aph1 subunit: relevance for Alzheimer's disease. *Science* **324**, 639-42.

Serrano, K. and Devine, D. V. (2004). Vinculin is proteolyzed by calpain during platelet aggregation: 95 kDa cleavage fragment associates with the platelet cytoskeleton. *Cell Motil Cytoskeleton* **58**, 242-52.

Servant, G., Weiner, O. D., Herzmark, P., Balla, T., Sedat, J. W. and Bourne, H. R. (2000). Polarization of chemoattractant receptor signaling during neutrophil chemotaxis. *Science* **287**, 1037-40.

Sessa, G., Podini, P., Mariani, M., Meroni, A., Spreafico, R., Sinigaglia, F., Colonna, M., Panina, P. and Meldolesi, J. (2004). Distribution and signaling of TREM2/DAP12, the receptor system mutated in human polycystic lipomembraneous osteodysplasia with sclerosing leukoencephalopathy dementia. *Eur J Neurosci* **20**, 2617-28.

Shah, S., Lee, S. F., Tabuchi, K., Hao, Y. H., Yu, C., LaPlant, Q., Ball, H., Dann, C. E., 3rd, Sudhof, T. and Yu, G. (2005). Nicastrin functions as a gamma-secretase-substrate receptor. *Cell* **122**, 435-47.

Shamah, S. M., Lin, M. Z., Goldberg, J. L., Estrach, S., Sahin, M., Hu, L., Bazalakova, M., Neve, R. L., Corfas, G., Debant, A. et al. (2001). EphA receptors regulate growth cone dynamics through the novel guanine nucleotide exchange factor ephexin. *Cell* **105**, 233-44.

Sharaf, A., Krieglstein, K. and Spittau, B. (2013). Distribution of microglia in the postnatal murine nigrostriatal system. *Cell Tissue Res* **351**, 373-82.

Shi, Y., Pontrello, C. G., DeFea, K. A., Reichardt, L. F. and Ethell, I. M. (2009). Focal adhesion kinase acts downstream of EphB receptors to maintain mature dendritic spines by regulating cofilin activity. *J Neurosci* **29**, 8129-42.

Shimoyama, M., Matsuoka, H., Nagata, A., Iwata, N., Tamekane, A., Okamura, A., Gomyo, H., Ito, M., Jishage, K., Kamada, N. et al. (2002). Developmental expression of EphB6 in the thymus: lessons from EphB6 knockout mice. *Biochem Biophys Res Commun* **298**, 87-94.

Shin, H. M., Minter, L. M., Cho, O. H., Gottipati, S., Fauq, A. H., Golde, T. E., Sonenshein, G. E. and Osborne, B. A. (2006). Notch1 augments NF-kappaB activity by facilitating its nuclear retention. *EMBO J* **25**, 129-38.

Shirotani, K., Edbauer, D., Kostka, M., Steiner, H. and Haass, C. (2004a). Immature nicastrin stabilizes APH-1 independent of PEN-2 and presenilin: identification of nicastrin mutants that selectively interact with APH-1. *J Neurochem* **89**, 1520-7.

Shirotani, K., Edbauer, D., Prokop, S., Haass, C. and Steiner, H. (2004b). Identification of distinct gamma-secretase complexes with different APH-1 variants. *J Biol Chem* **279**, 41340-5.

Siddiqui, T. A., Lively, S., Vincent, C. and Schlichter, L. C. (2012). Regulation of podosome formation, microglial migration and invasion by Ca(2+)-signaling molecules expressed in podosomes. *J Neuroinflammation* **9**, 250.

Sieg, D. J., Hauck, C. R., Ilic, D., Klingbeil, C. K., Schaefer, E., Damsky, C. H. and Schlaepfer, D. D. (2000). FAK integrates growth-factor and integrin signals to promote cell migration. *Nat Cell Biol* **2**, 249-56.

Sierra, A., Encinas, J. M., Deudero, J. J., Chancey, J. H., Enikolopov, G., Overstreet-Wadiche, L. S., Tsirka, S. E. and Maletic-Savatic, M. (2010). Microglia shape adult hippocampal neurogenesis through apoptosis-coupled phagocytosis. *Cell Stem Cell* **7**, 483-95.

Simon, A. M., de Maturana, R. L., Ricobaraza, A., Escribano, L., Schiapparelli, L., Cuadrado-Tejedor, M., Perez-Mediavilla, A., Avila, J., Del Rio, J. and Frechilla, D. (2009). Early changes in hippocampal Eph receptors precede the onset of memory decline in mouse models of Alzheimer's disease. *J Alzheimers Dis* **17**, 773-86.

Simpson, J. C., Griffiths, G., Wessling-Resnick, M., Fransen, J. A., Bennett, H. and Jones, A. T. (2004). A role for the small GTPase Rab21 in the early endocytic pathway. *J Cell Sci* **117**, 6297-311.

Smolny, M., Rogers, M. L., Shafton, A., Rush, R. A. and Stebbing, M. J. (2014). Development of non-viral vehicles for targeted gene transfer into microglia via the integrin receptor CD11b. *Front Mol Neurosci* **7**, 79.

Sonoda, Y., Watanabe, S., Matsumoto, Y., Aizu-Yokota, E. and Kasahara, T. (1999). FAK is the upstream signal protein of the phosphatidylinositol 3-kinase-Akt survival pathway in hydrogen peroxide-induced apoptosis of a human glioblastoma cell line. *J Biol Chem* **274**, 10566-70.

Spacek, J. and Harris, K. M. (2004). Trans-endocytosis via spinules in adult rat hippocampus. *J Neurosci* **24**, 4233-41.

Spasic, D., Raemaekers, T., Dillen, K., Declerck, I., Baert, V., Serneels, L., Fullekrug, J. and Annaert, W. (2007). Rer1p competes with APH-1 for binding to nicastrin and regulates gamma-secretase complex assembly in the early secretory pathway. *J Cell Biol* **176**, 629-40.

Spasic, D., Tolia, A., Dillen, K., Baert, V., De Strooper, B., Vrijens, S. and Annaert, W. (2006). Presenilin-1 maintains a nine-transmembrane topology throughout the secretory pathway. *J Biol Chem* **281**, 26569-77.

Stefanova, N., Fellner, L., Reindl, M., Masliah, E., Poewe, W. and Wenning, G. K. (2011). Toll-like receptor 4 promotes alpha-synuclein clearance and survival of nigral dopaminergic neurons. *Am J Pathol* **179**, 954-63.

Steiner, H., Capell, A., Pesold, B., Citron, M., Kloetzel, P. M., Selkoe, D. J., Romig, H., Mendla, K. and Haass, C. (1998). Expression of Alzheimer's disease-associated presenilin-1 is controlled by proteolytic degradation and complex formation. *J Biol Chem* **273**, 32322-31.

Steiner, H., Fluhrer, R. and Haass, C. (2008). Intramembrane proteolysis by gamma-secretase. *J Biol Chem* **283**, 29627-31.

Stence, N., Waite, M. and Dailey, M. E. (2001). Dynamics of microglial activation: a confocal time-lapse analysis in hippocampal slices. *Glia* **33**, 256-66.

Stephen, L. J., Fawkes, A. L., Verhoeve, A., Lemke, G. and Brown, A. (2007). A critical role for the EphA3 receptor tyrosine kinase in heart development. *Dev Biol* **302**, 66-79.

Stoker, M. and Gherardi, E. (1991). Regulation of cell movement: the motogenic cytokines. *Biochim Biophys Acta* **1072**, 81-102.

Streit, W. J. (2004). Microglia and Alzheimer's disease pathogenesis. *J Neurosci Res* **77**, 1-8.

Streit, W. J., Miller, K. R., Lopes, K. O. and Njie, E. (2008). Microglial degeneration in the aging brain--bad news for neurons? *Front Biosci* **13**, 3423-38.

Struhl, G. and Adachi, A. (2000). Requirements for presenilin-dependent cleavage of notch and other transmembrane proteins. *Mol Cell* **6**, 625-36.

Tanaka, M., Kamo, T., Ota, S. and Sugimura, H. (2003). Association of Dishevelled with Eph tyrosine kinase receptor and ephrin mediates cell repulsion. *EMBO J* **22**, 847-58.

Tanaka, M., Ohashi, R., Nakamura, R., Shinmura, K., Kamo, T., Sakai, R. and Sugimura, H. (2004). Tiam1 mediates neurite outgrowth induced by ephrin-B1 and EphA2. *EMBO J* **23**, 1075-88.

Tanaka, M., Sasaki, K., Kamata, R. and Sakai, R. (2007). The C-terminus of ephrin-B1 regulates metalloproteinase secretion and invasion of cancer cells. *J Cell Sci* **120**, 2179-89.

Taniguchi, Y., Kim, S. H. and Sisodia, S. S. (2003). Presenilin-dependent "gamma-secretase" processing of deleted in colorectal cancer (DCC). *J Biol Chem* **278**, 30425-8.

Tepass, U., Godt, D. and Winklbauer, R. (2002). Cell sorting in animal development: signalling and adhesive mechanisms in the formation of tissue boundaries. *Curr Opin Genet Dev* **12**, 572-82.

Thamilselvan, V., Craig, D. H. and Basson, M. D. (2007). FAK association with multiple signal proteins mediates pressure-induced colon cancer cell adhesion via a Src-dependent PI3K/Akt pathway. *FASEB J* **21**, 1730-41.

Thomas, W. E. (1990). Characterization of the dynamic nature of microglial cells. *Brain Res Bull* **25**, 351-4.

Thrash, J. C., Torbett, B. E. and Carson, M. J. (2009). Developmental regulation of TREM2 and DAP12 expression in the murine CNS: implications for Nasu-Hakola disease. *Neurochem Res* **34**, 38-45.

Timpson, P., Jones, G. E., Frame, M. C. and Brunton, V. G. (2001). Coordination of cell polarization and migration by the Rho family GTPases requires Src tyrosine kinase activity. *Curr Biol* **11**, 1836-46.

Tomita, T., Tanaka, S., Morohashi, Y. and Iwatsubo, T. (2006). Presenilin-dependent intramembrane cleavage of ephrin-B1. *Mol Neurodegener* **1**, 2.

Tong, J., Elowe, S., Nash, P. and Pawson, T. (2003). Manipulation of EphB2 regulatory motifs and SH2 binding sites switches MAPK signaling and biological activity. *J Biol Chem* **278**, 6111-9.

Tremblay, M. E., Lowery, R. L. and Majewska, A. K. (2010). Microglial interactions with synapses are modulated by visual experience. *PLoS Biol* **8**, e1000527.

Truman, L. A., Ford, C. A., Pasikowska, M., Pound, J. D., Wilkinson, S. J., Dumitriu, I. E., Melville, L., Melrose, L. A., Ogden, C. A., Nibbs, R. et al. (2008). CX3CL1/fractalkine is released from apoptotic lymphocytes to stimulate macrophage chemotaxis. *Blood* **112**, 5026-36.

Uemura, K., Kihara, T., Kuzuya, A., Okawa, K., Nishimoto, T., Ninomiya, H., Sugimoto, H., Kinoshita, A. and Shimohama, S. (2006). Characterization of sequential N-cadherin cleavage by ADAM10 and PS1. *Neurosci Lett* **402**, 278-83.

Uziel, D., Muhlfriedel, S., Zarbalis, K., Wurst, W., Levitt, P. and Bolz, J. (2002). Miswiring of limbic thalamocortical projections in the absence of ephrin-A5. *J Neurosci* **22**, 9352-7.

van den Dries, K., Meddens, M. B., de Keijzer, S., Shekhar, S., Subramaniam, V., Figdor, C. G. and Cambi, A. (2013). Interplay between myosin IIA-mediated contractility and actin network integrity orchestrates podosome composition and oscillations. *Nat Commun* **4**, 1412.

Vargas, L. M., Leal, N., Estrada, L. D., Gonzalez, A., Serrano, F., Araya, K., Gysling, K., Inestrosa, N. C., Pasquale, E. B. and Alvarez, A. R. (2014). EphA4 activation of c-Abl mediates synaptic loss and LTP blockade caused by amyloid-beta oligomers. *PLoS One* **9**, e92309.

Vicente-Manzanares, M., Choi, C. K. and Horwitz, A. R. (2009). Integrins in cell migration--the actin connection. *J Cell Sci* **122**, 199-206.

Vidal, G. A., Naresh, A., Marrero, L. and Jones, F. E. (2005). Presenilin-dependent gamma-secretase processing regulates multiple ERBB4/HER4 activities. *J Biol Chem* **280**, 19777-83.

Vihanto, M. M., Vindis, C., Djonov, V., Cerretti, D. P. and Huynh-Do, U. (2006). Caveolin-1 is required for signaling and membrane targeting of EphB1 receptor tyrosine kinase. *J Cell Sci* **119**, 2299-309.

Villa, J. C., Chiu, D., Brandes, A. H., Escorcia, F. E., Villa, C. H., Maguire, W. F., Hu, C. J., de Stanchina, E., Simon, M. C., Sisodia, S. S. et al. (2014). Nontranscriptional role of Hif-1alpha in activation of gamma-secretase and notch signaling in breast cancer. *Cell Rep* **8**, 1077-92.

Villemagne, V. L. and Masters, C. L. (2014). Alzheimer disease: the landscape of ageing--insights from AD imaging markers. *Nat Rev Neurol* **10**, 678-9.

Vincent, C., Siddiqui, T. A. and Schlichter, L. C. (2012). Podosomes in migrating microglia: components and matrix degradation. *J Neuroinflammation* **9**, 190.

Wake, H., Moorhouse, A. J., Jinno, S., Kohsaka, S. and Nabekura, J. (2009). Resting microglia directly monitor the functional state of synapses in vivo and determine the fate of ischemic terminals. *J Neurosci* **29**, 3974-80.

Wang, C. C., Gurevich, I. and Draznin, B. (2003). Insulin affects vascular smooth muscle cell phenotype and migration via distinct signaling pathways. *Diabetes* **52**, 2562-9.

Wang, H. U. and Anderson, D. J. (1997). Eph family transmembrane ligands can mediate repulsive guidance of trunk neural crest migration and motor axon outgrowth. *Neuron* **18**, 383-96.

Wang, H. U., Chen, Z. F. and Anderson, D. J. (1998). Molecular distinction and angiogenic interaction between embryonic arteries and veins revealed by ephrin-B2 and its receptor Eph-B4. *Cell* **93**, 741-53.

Wang, X., Roy, P. J., Holland, S. J., Zhang, L. W., Culotti, J. G. and Pawson, T. (1999). Multiple ephrins control cell organization in C. elegans using kinase-dependent and -independent functions of the VAB-1 Eph receptor. *Mol Cell* **4**, 903-13.

Waschbusch, D., Born, S., Niediek, V., Kirchgessner, N., Tamboli, I. Y., Walter, J., Merkel, R. and Hoffmann, B. (2009). Presenilin 1 affects focal adhesion site formation and cell force generation via c-Src transcriptional and posttranslational regulation. *J Biol Chem* **284**, 10138-49.

Wernimont, S. A., Cortesio, C. L., Simonson, W. T. and Huttenlocher, A. (2008). Adhesions ring: a structural comparison between podosomes and the immune synapse. *Eur J Cell Biol* **87**, 507-15.

Westhoff, M. A., Serrels, B., Fincham, V. J., Frame, M. C. and Carragher, N. O. (2004). SRC-mediated phosphorylation of focal adhesion kinase couples actin and adhesion dynamics to survival signaling. *Mol Cell Biol* **24**, 8113-33.

Wieland, I., Jakubiczka, S., Muschke, P., Cohen, M., Thiele, H., Gerlach, K. L., Adams, R. H. and Wieacker, P. (2004). Mutations of the ephrin-B1 gene cause craniofrontonasal syndrome. *Am J Hum Genet* **74**, 1209-15.

Wilkinson, D. G. (2000). Topographic mapping: organising by repulsion and competition? *Curr Biol* **10**, R447-51.

Wong, H. K., Sakurai, T., Oyama, F., Kaneko, K., Wada, K., Miyazaki, H., Kurosawa, M., De Strooper, B., Saftig, P. and Nukina, N. (2005). beta Subunits of voltage-gated sodium channels are novel substrates of beta-site amyloid precursor protein-cleaving enzyme (BACE1) and gamma-secretase. *J Biol Chem* **280**, 23009-17.

Woodham, E. F. and Machesky, L. M. (2014). Polarised cell migration: intrinsic and extrinsic drivers. *Curr Opin Cell Biol* **30**, 25-32.

Wu, Z., Ghosh-Roy, A., Yanik, M. F., Zhang, J. Z., Jin, Y. and Chisholm, A. D. (2007). Caenorhabditis elegans neuronal regeneration is influenced by life stage, ephrin signaling, and synaptic branching. *Proc Natl Acad Sci U S A* **104**, 15132-7.

Wybenga-Groot, L. E., Baskin, B., Ong, S. H., Tong, J., Pawson, T. and Sicheri, F. (2001). Structural basis for autoinhibition of the Ephb2 receptor tyrosine kinase by the unphosphorylated juxtamembrane region. *Cell* **106**, 745-57.

Yasuda, K., Nagafuku, M., Shima, T., Okada, M., Yagi, T., Yamada, T., Minaki, Y., Kato, A., Tani-Ichi, S., Hamaoka, T. et al. (2002). Cutting edge: Fyn is essential for tyrosine phosphorylation of Csk-binding protein/phosphoprotein associated with glycolipid-enriched microdomains in lipid rafts in resting T cells. *J Immunol* **169**, 2813-7.

Yokote, H., Fujita, K., Jing, X., Sawada, T., Liang, S., Yao, L., Yan, X., Zhang, Y., Schlessinger, J. and Sakaguchi, K. (2005). Trans-activation of EphA4 and FGF receptors mediated by direct interactions between their cytoplasmic domains. *Proc Natl Acad Sci U S A* **102**, 18866-71.

Yokoyama, N., Romero, M. I., Cowan, C. A., Galvan, P., Helmbacher, F., Charnay, P., Parada, L. F. and Henkemeyer, M. (2001). Forward signaling mediated by ephrin-B3 prevents contralateral corticospinal axons from recrossing the spinal cord midline. *Neuron* **29**, 85-97.

Yonekura, S., Ting, C. Y., Neves, G., Hung, K., Hsu, S. N., Chiba, A., Chess, A. and Lee, C. H. (2006). The variable transmembrane domain of Drosophila N-cadherin regulates adhesive activity. *Mol Cell Biol* **26**, 6598-608.

Yu, G., Chen, F., Levesque, G., Nishimura, M., Zhang, D. M., Levesque, L., Rogaeva, E., Xu, D., Liang, Y., Duthie, M. et al. (1998). The presenilin 1 protein is a component of a high molecular weight intracellular complex that contains beta-catenin. *J Biol Chem* **273**, 16470-5.

Yu, G., Nishimura, M., Arawaka, S., Levitan, D., Zhang, L., Tandon, A., Song, Y. Q., Rogaeva, E., Chen, F., Kawarai, T. et al. (2000). Nicastrin modulates presenilin-mediated notch/glp-1 signal transduction and betaAPP processing. *Nature* **407**, 48-54.

Yue, Y., Su, J., Cerretti, D. P., Fox, G. M., Jing, S. and Zhou, R. (1999). Selective inhibition of spinal cord neurite outgrowth and cell survival by the Eph family ligand ephrin-A5. *J Neurosci* **19**, 10026-35.

Zambonin-Zallone, A., Teti, A., Carano, A. and Marchisio, P. C. (1988). The distribution of podosomes in osteoclasts cultured on bone laminae: effect of retinol. *J Bone Miner Res* **3**, 517-23.

Zamir, E. and Geiger, B. (2001). Molecular complexity and dynamics of cell-matrix adhesions. *J Cell Sci* **114**, 3583-90.

Zhang, X., Jiang, G., Cai, Y., Monkley, S. J., Critchley, D. R. and Sheetz, M. P. (2008). Talin depletion reveals independence of initial cell spreading from integrin activation and traction. *Nat Cell Biol* **10**, 1062-8.

Zhao, G., Tan, J., Mao, G., Cui, M. Z. and Xu, X. (2007). The same gamma-secretase accounts for the multiple intramembrane cleavages of APP. *J Neurochem* **100**, 1234-46.

Zhou, G. L., Tucker, D. F., Bae, S. S., Bhatheja, K., Birnbaum, M. J. and Field, J. (2006). Opposing roles for Akt1 and Akt2 in Rac/Pak signaling and cell migration. *J Biol Chem* **281**, 36443-53.

Zhou, S., Zhou, H., Walian, P. J. and Jap, B. K. (2005). CD147 is a regulatory subunit of the gamma-secretase complex in Alzheimer's disease amyloid beta-peptide production. *Proc Natl Acad Sci U S A* **102**, 7499-504.

Zhu, M., Tao, Y., He, Q., Gao, H., Song, F., Sun, Y. M., Li, H. L., Wu, Z. Y. and Saffen, D. (2014). A common GSAP promoter variant contributes to Alzheimer's disease liability. *Neurobiol Aging* **35**, 2656 e1-7.

Zimmer, M., Palmer, A., Kohler, J. and Klein, R. (2003). EphB-ephrinB bi-directional endocytosis terminates adhesion allowing contact mediated repulsion. *Nat Cell Biol* **5**, 869-78.

8. Acknowledgements

I express my deep gratitude to my supervisor Prof. Dr. Jochen Walter for giving me the opportunity to do my PhD in his lab. His calm, pragmatic and encouraging personality and his guidance helped me to acquire the knowledge that is needed to design and carry out scientific experiments independently.

I am grateful to Prof. Dr. Sven Burgdorf that he kindly agreed to act as the second reviewer for this dissertation. I am also thankful to Prof. Dr. Höhfeld and Prof. Dr. Kemna for their valuable time.

Furthermore, I thank Prof. Dr. Harald Neumann and his colleagues, especially Dr. Clara Beutner and Dr. Bettina Linnartz-Gerlach, for providing me with the ES derived microglia cells which were the basis for my experiments. Also I would like to thank Dr. Jerome Mertens and Kathrin Stüber for providing me with the lentiviral constructs and teaching me how generate viral particles. I also thank Dr. Dagmar Wachten for the allocation of her microscope and Houssein Hamzehs great help teaching me how to use it.

Thanks also to my former supervisor Dr. Patrick Wunderlich and the rest of my colleagues who gave me so much professional and personal advice. It was so much fun working with you, I couldn't have done it without you: Dr. Ilker Karaca, Dr. Constanin Glebov, Dr. Sathish Kumar, Dr. Tien Nguyien, Dr. Naoto Oikawa, Sandra Theil, Janina Gerth, Marie Löchner, Esteban Gutierrez, Anna-Lena Bepple, Christina Schütz, Josefine Richter and the members of the neurobiology lab.

I especially would like to thank my mother Margarete Kemmerling and my grandparents Carl and Marianne Kemmerling who never left my side, always nurtured my curiosity and made me the pragmatic and optimistic person I am.

Finally, I would like to thank Dennis de Coninck who was the greatest personal support one could wish for during the past four years. His social intelligence, his (sometimes annoying) nit-picker personality and his contagious passion for science make him one of the best researchers I have ever met.